UNIVERSITY OF TURKU

ENDOGENOUS REGULATION OF BROWN ADIPOSE TISSUE IN HUMANS

Minna Lahesmaa

TURUN YLIOPISTON JULKAISUJA – ANNALES UNIVERSITATIS TURKUENSIS
SARJA - SER. D OSA - TOM. 1391 | MEDICA – ODONTOLOGICA | TURKU 2018

UNIVERSITY OF TURKU

ENDOGENOUS REGULATION OF BROWN ADIPOSE TISSUE IN HUMANS

Minna Lahesmaa

TURUN YLIOPISTON JULKAISUJA – ANNALES UNIVERSITATIS TURKUENSIS
SARJA - SER. D OSA - TOM. 1391 | MEDICA – ODONTOLOGICA | TURKU 2018

University of Turku

Faculty of Medicine
Department of Internal Medicine
Doctoral Programme in Clinical Research
Turku PET Centre
Turku University Hospital

Supervised by

Docent Kirsi A. Virtanen, MD, PhD
Turku PET Centre, University of Turku
Turku, Finland

Professor Pirjo Nuutila, MD, PhD
Turku PET Centre, University of Turku
Department of Endocrinology,
Turku University Hospital
Turku, Finland

Reviewed by

Docent Niina Matikainen, MD, PhD
Department of Endocrinology
Helsinki University Hospital
Helsinki, Finland

Professor Uberto Pagotto, MD, PhD
Endocrinology Unit
Department of Medical and Surgical Sciences
Alma Mater Studiorum University of Bologna
Bologna, Italy

Opponent

Professor Patrick Schrauwen, MSc, PhD
NUTRIM School for Nutrition and Translational Research in Metabolism
Maastricht University Medical Center
Maastricht, Netherlands

ISBN 978-951-29-7430-6 (PRINT)
ISBN 978-951-29-7431-3 (PDF)
ISSN 0355-9483 (Print)
ISSN 2343-3213 (Online)
Grano Oy - Turku, Finland, 2018

“The world is full of great and wonderful things for those who are ready for them.”
– Moominpappa

ABSTRACT

Minna Lahesmaa

Endogenous Regulation of Brown Adipose Tissue in Humans

University of Turku, Faculty of Medicine, Department of Internal Medicine, Doctoral Programme of Clinical Investigation, Turku PET Centre

Annales Universitatis Turkuensis, Turku, 2018

Brown adipose tissue (BAT) is a functional and metabolically active tissue found in humans. Instead of storing energy like white adipose tissue (WAT), BAT dissipates energy in the form of heat in a process called thermogenesis. Enhanced BAT metabolism can increase metabolic rate and help regulate systemic glucose and lipid levels, hence stimulating BAT could provide a potential approach for the treatment and prevention of obesity, type 2 diabetes and metabolic disease in humans. It is well known that human BAT can be activated by cold exposure, and BAT function is also controlled by many endogenous factors, which currently are poorly understood. Pre-clinical studies have provided important insights about BAT regulation, but human studies are also essential to translate novel findings into innovative treatments for improving human health and metabolism.

The aim of this thesis was to investigate endogenous factors that regulate human BAT function by using positron emission tomography (PET). This work focused on three endogenous systems, thyroid hormones, the adenosinergic system, and the endocannabinoid system.

The results showed that thyroid hormones modulate human BAT function. Patients with hyperthyroidism exhibit increased metabolism of BAT, which can be restored to a normal level after treatment of the condition. This work showed for the first time in humans that adenosine A_{2A} receptors and cannabinoid type 1 receptors regulate the cold-induced activation of BAT. Furthermore, overweight subjects have blunted cold activation of BAT and impaired regulation of the endocannabinoid system. These endogenous mechanisms of BAT regulation provide potential new therapeutic targets for human BAT activation and management of obesity.

Keywords: Brown adipose tissue, regulation, thyroid hormone, adenosine, endocannabinoid system, obesity, positron emission tomography, PET

TIIVISTELMÄ

Minna Lahesmaa
Ihmisen ruskean rasvan endogeeninen säätely

Turun yliopisto, Lääketieteellinen tiedekunta, Sisätautioppi,
Turun kliininen tohtoriohjelma (TKT), Valtakunnallinen PET-keskus

Annales Universitatis Turkuensis, Turku, 2018

Ihmisellä on elimistössään aineenvaihdunnallisesti aktiivista ruskeaa rasvaa. Toisin kuin energiaa varastoiva valkoinen rasva, ruskea rasva aktivoituu kylmässä ympäristössä ja kuluttaa energiaa lämmön muodossa. Aktiivinen ruskea rasva lisää perusaineenvaihduntaa ja voi parantaa elimistön sokeri- ja rasva-arvoja. Ruskean rasvan toimintaa voitaisiinkin hyödyntää lihavuuden ja sen oheissairauksien kuten tyypin 2 diabeteksen ennaltaehkäisyssä ja hoidossa. Kudoksen toiminnan säätelyyn osallistuvat useat tekijät, joita tunnetaan vielä huonosti. Koe-eläimillä tehdyt tutkimukset ovat tuottaneet paljon tietoa ruskean rasvan säätelystä, mutta alalla tarvitaan myös tutkimuksia ihmisillä, jotta innovatiiviset löydökset voidaan soveltaa ihmisen terveyden ja aineenvaihdunnan parantamiseksi.

Tämän väitöskirjatyön tavoitteena oli tutkia positroniemissiotomografiaa eli PET-kuvantamista käyttäen elimistön endogeenisiä eli sisäisiä tekijöitä, jotka säätelevät ruskean rasvan toimintaa. Tutkimuksessa tarkasteltiin kolmea endogeenistä säätelytekijää: kilpirauhashormoneita, adenosiinijärjestelmää ja endokannabinoidijärjestelmää. Tulokset osoittavat että kilpirauhashormonit säätelevät ruskean rasvan toimintaa. Kudoksen aktiivisuus oli lisääntynyttä potilailla, joilla oli diagnosoitu kilpirauhasen liikatoiminta, ja aktiivisuus palautui terveiden verrokkien tasolle liikatoiminnan hoidon jälkeen. Lisäksi todettiin ensimmäistä kertaa ihmisillä, että adenosiini A_{2A}-reseptorit sekä tyypin 1 kannabinoidireseptorit (CB1-reseptorit) säätelevät ruskean rasvan toimintaa kylmäaltistuksen aikana. Ruskean rasvan toiminta on heikentynyttä ylipainoisilla tutkittavilla ja heillä endokannabinoidijärjestelmän säätely on häiriintynyttä. Näitä endogeenisiä säätelymekanismeja voitaisiin hyödyntää uusien ruskean rasvan toimintaa lisäävien lääkkeiden kehittämiseksi ja tulevaisuudessa lihavuuden hoitoon.

Avainsanat: Ruskea rasva, säätely, kilpirauhashormoni, adenosiini, endokannabinoidijärjestelmä, lihavuus, positroniemissiotomografia, PET

TABLE OF CONTENTS

ABBREVIATIONS

[^{11}C]HED	[^{11}C]-meta-hydroxyephedrin
[^{11}C]TMSX	[7-methyl-^{11}C]-(E)-8-(3,4,5-Trimethoxystyryl)-1,3,7-trimethylxanthine
[^{15}O]H_2O	Radiowater
[^{18}F]FDG	[^{18}F]fluorodeoxyglucose
[^{18}F]FMPEP-d_2	(3R,5R)-5-(3-[^{18}F]Fluoromethoxy-d2)phenyl)-3-((R)-1-phenyl-ethylamino)-1-(4-trifluoromethyl-phenyl)-pyrrolidin-2-one
[^{18}F]FTHA	14(R,S)-[^{18}F]fluoro-6-thia-heptadecanoic acid
A_1, A_{2A}, A_{2B}, A_3	The four G protein-coupled adenosine receptor subtypes
A2AR	Adenosine A_{2A} receptor
AC	Adenylyl cyclase
ADP	Adenosine diphosphate
AMP	Adenosine monophosphate
AMPK	Activated protein kinase
ATP	Adenosine triphosphate
β3-AR	Beta-3 adrenergic receptor
BAT	Brown adipose tissue
BMI	Body mass index
BMP	Bone morphogenic protein
cAMP	Cyclic adenosine monophosphate
CB1R	Cannabinoid type 1 receptor
CB2R	Cannabinoid type 2 receptor
CD36	Cluster of differentiation 36
CT	Computed tomography
D2	Type 2 deiodinase
ECS	Endocannabinoid system
EE	Energy expenditure
FFA	Free fatty acid
FGF21	Fibroblast growth factor 21
FUR	Fractional uptake rate
GLUT1	Glucose transporter protein 1
GLUT4	Glucose transporter protein 4
GU	Glucose uptake
H&E	Hematoxylin and eosin (staining)
HbA1c	Glycosylated hemoglobin A1c
HDL	High density lipoprotein
hMADS	Human multipotent adipose-derived stem cells
HPLC	High-performance liquid chromatography
HU	Hounsfield unit
i.v.	Intravenous

IL-4	Interleukin-4
IP WAT	Intraperitoneal WAT
kBq	Kilobecquerel
kcal	Kilocalorie
kg	Kilogram
LC	Lumped constant
LDL	Low density lipoprotein
LPL	Lipoprotein lipase
MBq	Megabecquerel
MRI	Magnetic resonance imaging
mRNA	messenger RNA (Ribonucleic acid)
PET	Positron emission tomography
PGC-1α	PPARγ co-activator 1 alpha
pKA	Protein kinase A
PPARγ	Peroxisome proliferator-activated receptor gamma
PRDM16	PR domain containing 16
ROI	Region of interest
RT	Room temperature
SC WAT	Subcutaneous WAT
SNS	Sympathetic nervous system
SUV	Standardized uptake value
T_3	Triiodothyronine
T_4	Thyroxine
TAC	Time-activity curve
TGRF	Transmembrane G protein-coupled receptor 5
TRα	Thyroid hormone receptor alpha
TRβ	Thyroid hormone receptor beta
TRH	Thyrotropin releasing hormone
TSH	Thyroid stimulating hormone
UCP1	Uncoupling protein-1
UCP3	Uncoupling protein-3
WAT	White adipose tissue
VEGFA	Vascular endothelial growth factor A
VLDL	Very low density lipoprotein
V_T	Volume distribution

LIST OF ORIGINAL PUBLICATIONS

This thesis is based on the following original publications, which are referred to in the text by the Roman numerals I-III:

I. **Lahesmaa M.**, Orava J., Schalin-Jäntti C., Soinio M., Hannukainen J. C., Noponen T., Kirjavainen A., Iida H., Kudomi N., Enerbäck S., Virtanen K. A., Nuutila P.
Hyperthyroidism Increases Brown Fat Metabolism in Humans.
J. Clin. Endocrinol. Metab. 2014; 99(1):E28-35. doi: 10.1210/jc.2013-2312.

II. **Lahesmaa M.**, Oikonen V., Helin S., Luoto P., U Din M., Pfeifer A., Nuutila P., Virtanen K. A.
Regulation of Human Brown Adipose Tissue by Adenosine and A_{2A} receptors – Studies with [^{15}O]H_2O and [^{11}C]TMSX PET/CT.
Eur. J. Nucl. Med. Mol. Imaging. 2018. doi: 10.1007/s00259-018-4120-2.

III. **Lahesmaa M.**, Eriksson O., Gnad T., Oikonen V., Bucci M., Hirvonen J., Koskensalo K., Teuho J., Niemi T., Taittonen M., Lahdenpohja S., U Din M., Haaparanta-Solin M., Pfeifer A., Virtanen K. A., Nuutila P.
Cannabinoid Type 1 Receptors are Upregulated during Acute Activation of Brown Adipose Tissue
Diabetes. 2018; 67(7):1226-1236. doi: 10.2337/db17-1366.

1 INTRODUCTION

Brown adipose tissue (BAT) is involved in the metabolism and energy expenditure of humans. White adipose tissue (WAT) stores excess energy in the body, whereas BAT is able to dissipate energy in the form of heat in a phenomenon called thermogenesis. After the recent re-discovery of metabolically active BAT depots in adults, (Saito et al., 2009; van Marken Lichtenbelt et al., 2009; Virtanen et al., 2009) much ongoing research is being conducted to understand the role and significance of BAT for human metabolism. There is increasing evidence that enhanced BAT function can improve systemic health in humans by utilizing glucose and lipids from the circulation and by increasing metabolic rate in individuals. Therefore, augmenting BAT activation could provide a potential strategy to combat the increasing epidemic of obesity and type 2 diabetes (Bhatt et al., 2017).

The function of BAT is considered to be controlled by various endogenous factors (Broeders et al., 2014), many of which are still unknown or largely unexplored. Information from the environment, such as ambient temperature is received and processed in the central nervous system, and a response is sent via the sympathetic nervous system to the BAT in the form of increased noradrenaline levels which increases BAT metabolism (Cannon and Nedergaard, 2004). This process is controlled by many signaling molecules and hormones, including the thyroid hormones, the endocannabinoid system (ECS) and the adenosinergic system (Cannon and Nedergaard, 2010; Gnad et al., 2014; Krott et al., 2016; Verty et al., 2009; Villarroya et al., 2017). In healthy individuals, BAT can be activated by certain stimuli, including cold exposure, and during such activation excess energy is liberated as heat in a process called thermogenesis. However, in a disease state or conditions of abnormal metabolism such as hyperthyroidism or obesity, the regulatory systems of BAT may become impaired. Understanding the mechanisms of BAT regulation are important for understanding human physiology, and targeting these regulatory factors with therapeutic molecules or other treatments could provide new ways to activate BAT and improve metabolism (Pfeifer and Hoffmann, 2015).

Positron emission tomography (PET) provides a non-invasive method to investigate BAT function in humans *in vivo*. However, the potential of this imaging technique has not been fully utilized. Many previous PET studies have focused on studying the glucose metabolism of BAT, and have often presented merely semi-quantitative data (Cypess et al., 2014). The aim of this doctoral work is to utilize a variety of different PET radioligands to investigate BAT in humans, and to provide new information about the regulation and physiology of BAT.

2 REVIEW OF LITERATURE

2.1 Brown Adipose Tissue in Humans

BAT has been recognized in rodents and human infants for centuries. Autopsy studies from the early 1900's, described BAT as a separate anatomical organ or endocrine gland, found in the shoulder, neck, perivertebral and perirenal areas. The dense vasculature of the organ and its close location to the main vessels of the neck were considered important for its function (Bonnot, 1908; Cramer, 1920). Later autopsy studies done in the 1970's and 1980's also demonstrated the presence of brown fat depots in humans. One study showed that during childhood the depots were widely distributed in the body, but in the human adult BAT depots decreased and became anatomically concentrated around deeper organs of the body such as the kidneys, aorta, neck and mediastinum (Heaton, 1972). It was also reported that outdoor workers exposed to a cold environment had more brown-like adipose tissue compared to indoor workers (Huttunen et al., 1981). These early studies provided the first anatomical evidence of BAT in humans, but the function of BAT and any possible significance it had were still speculative.

Functional imaging using PET combined with anatomical computed tomography (CT) provided a new tool to investigate functions of the body *in vivo*. The development of hybrid scanners advanced in the 1990's, and especially their use with the radiotracer [^{18}F]fluorodeoxyglucose ([^{18}F]FDG) increased for cancer imaging. High glucose uptake visualized using PET could localize a metabolically active malignant tumor in the body. However, many [^{18}F]FDG scans also showed small, bilateral hotspots in the shoulder areas of patients, which were considered to be benign artefacts of muscular tension. Later, large retrospective studies with carcinoma patients showed that these supraclavicular hotspots were in fact situated in adipose tissue, they were also found to be more prevalent in women, children and lean patients (i. e. normal weight patients), and their prevalence was closely linked to the cold outdoor temperature during the time of the scans (Cohade et al., 2003b, 2003a; Hany et al., 2002). It was clear that these "artefacts" indeed indicated the presence of BAT.

In 2009 three independent research groups confirmed the existence of metabolically active, *bona fide* BAT in human adults (Saito et al., 2009; van Marken Lichtenbelt et al., 2009; Virtanen et al., 2009). Morphological and biochemical analyses of tissue samples acquired from PET image-guided biopsies of supraclavicular BAT showed gene expression and proteins unique for brown adipocytes (Virtanen et al., 2009). These same three studies also confirmed that

cold exposure can markedly increase BAT activation, and that obesity, higher body mass index (BMI) and body fat are associated with less active BAT.

Human infants have an interscapular BAT depot, which regresses with time and is absent in adults (Heaton, 1972; Lidell et al., 2013). BAT develops in the prenatal stage from myoblast precursors, and is established in fetuses by the fifth gestational month (Merklin, 1974). BAT abundance is highest at birth, as it comprises up to 5% of body weight, and has a very high thermogenic capacity. The rapid heat production is essential for survival, because newborn humans lack the ability to shiver. (Rogers, 2015) The amount of BAT declines over the next 6 months (Ponrartana et al., 2016) and even further during childhood and adolescence, while the skeletal musculature develops. Interestingly, there is evidence of a transient increase in BAT volume during puberty, which may be linked to changes in sex hormones (Rogers, 2015). Aging further seems to decrease detectable BAT. Findings obtained from PET studies estimate that cold-activated BAT can be detected in approximately 50% of young adults (aged 20–35 years) compared to less than 10% of older subjects (aged 40–50 years and older) (Saito et al., 2009; Yoneshiro et al., 2011) and that active BAT seems to be more prevalent in women than in men (Cypess et al., 2009; Pfannenberg et al., 2010). It has recently been confirmed that the principal sites for BAT in adults are the cervical and supraclavicular fat depots, with smaller amounts found in the paraspinal, periaortic, perirenal, perihepatic and perisplenic areas (Cypess et al., 2015). Due to their thermogenic capacity, it is thought that BAT depots around core blood vessels of the neck and organs may function to ensure adequate warm blood flow to the brain and other essential organs, which is similar to what scientists hypothesized in the beginning of the 20th century. Over the years much research with animal models and humans has given important insights to the function of BAT, but there are still many unanswered questions about the regulation, metabolic significance and potential of BAT in humans.

2.2 Physiology of Brown Adipose Tissue

2.2.1 Brown, White and Beige Adipocytes

BAT differs from WAT structurally and functionally. White adipocytes have a single large lipid droplet filled with stored triglycerides. Brown adipocytes consist of several smaller lipid droplets and have numerous mitochondria. The mitochondria in brown adipocytes resemble those found in muscle and support energy consumption, whereas the mitochondria in WAT support more anabolic

and protective functions (Forner et al., 2009). BAT is densely vascularized and innervated by terminal nerve fibers of the sympathetic nervous system (SNS) (Cannon and Nedergaard, 2004). WAT mainly functions as an energy storage, whereas BAT has the ability to dissipate energy in the form of heat when it is activated. BAT functions as an essential thermoregulatory organ in small mammals with a relatively large surface area to volume ratio. Maintaining a stable core temperature is necessary for survival in cold environments and during hibernation. (Jakus et al., 2008) Although this purpose is less relevant in adult humans, there is some evidence of seasonal variation in BAT activation, suggesting that BAT is metabolically more active in cold winters than in summer seasons (Au-Yong et al., 2009; Saito et al., 2009; Yoneshiro et al., 2016).

In addition to classical brown and white adipocytes, another type named “beige” or “brite” (brown-in-white) adipocytes are found in human adults. There is evidence that much of the BAT identified by PET imaging in supraclavicular depots consists of beige adipocytes, interspersed among large white-like, unilocular adipocytes (Wu et al., 2012), and this cell type is also found in the periadrenal depots of BAT (Lidell et al., 2013). Both brown and beige cells express the proteins that facilitate thermogenesis in the cell. These include uncoupling protein 1 (UCP1), the thyroid hormone converting enzyme deiodinase type 2 (D2), and transcription factors PR domain containing 16 (PRDM16) and PPARγ co-activator 1 alpha (PGC-1α). However, beige and brown adipocytes also have distinct characteristics and differ by origin. Brown adipocytes develop prenatally and originate from the precursor cells of the dermomyotome. These precursors express the genes *Myf5* (encoding Myogenic factor-5), *Pax7* (encoding Paired box protein Pax-7) and *En1* (encoding Engrailed 1) similar to the skeletal muscle cells. (Sepa-Kishi and Ceddia, 2018) The origin of beige cells, however, is still under investigation. It seems beige adipocytes emerge postnatally and they may either develop by converting from mature (white) adipocytes or develop *de novo* from different populations of precursor cells, including mural cells, vascular smooth muscle cells and preadipose cells. This can occur in response to a variety of different stimuli, such as cold exposure, PPARγ agonism, exercise or hormonal signals, and the process involves the action of many proteins, including EBF2 (early B-cell factor 2), ZFP516 (zinc finger protein 516), PRDM16 and PGC-1α. (Wang and Seale, 2016) It is also noteworthy that beige adipocytes require constant stimulus for active thermogenesis, otherwise they transform into a white-like phenotype (Harms and Seale, 2013; Hoeke et al., 2016).

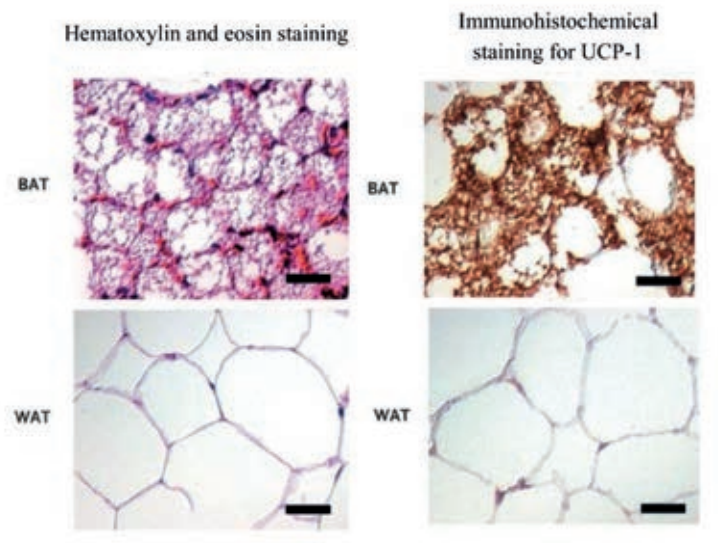

Figure 1. Microscopic images of brown (BAT) and white adipose (WAT) tissue samples. Modified from Virtanen et al., 2009.

2.2.2 BAT Thermogenesis and Substrate Utilization

Temperature regulation of the body is controlled by the central nervous system. In a cold environment, ambient temperature is sensed on the skin by thermoreceptors, which relay information via afferent peripheral nerves to the spinal cord and further to the brain. The ventromedial hypothalamus is especially important in processing this information. (Contreras et al., 2015) A response is sent via the efferent sympathetic nerves to the periphery and to the BAT, which is densely innervated with sympathetic nerves. Noradrenaline is released at the nerve endings and this subsequently binds to the β3-adrenoreceptors (ß3-ARs) on the brown adipocytes, which causes a cascade of intracellular reactions that in turn trigger thermogenesis (Morrison et al., 2012).

Upon ß3-AR stimulus, adenylyl cyclase (AC) is activated, which produces cyclic adenosine monophosphate (cAMP). The cAMP then activates protein kinase A (pKA). This enzyme then triggers many pathways, including the transcriptional activation of thermogenic genes and the hydrolysis of intracellular triglyceride stores into free fatty acids (FFAs). The FFAs produced by this hydrolysis subsequently undergo β-oxidation forming acetyl coenzyme A, which is transferred to Kreb's cycle and further for oxidative phosphorylation, which yields adenosine triphosphate molecules (ATP) under normal conditions. Brown adipocytes, however, express UCP1, which causes uncoupling of the electron

transport chain, and results in the leakage of protons down the electron gradient. Consequently, chemical energy is converted into heat. This process is called non-shivering or facultative thermogenesis. (Cannon and Nedergaard, 2004)

When thermogenesis is activated, brown adipocytes take in nutrients from the systemic blood circulation. Glucose is taken up via the glucose transporter proteins 1 (GLUT1) and 4 (GLUT4), which are stimulated by insulin. The glucose molecule is quickly phosphorylated to glucose-6-phosphate, and under high energy demand it is converted to two molecules of pyruvate via glycolysis, and then further oxidized in the mitochondria in Kreb's cycle. This pathway provides energy for and supports the general functions of the adipocyte. Alternatively, glucose-6-phophate can be stored as glycogen or converted to lactate by anaerobic glycolysis. Glucose can also be converted directly to fatty acids via *de novo* lipogenesis or converted to glycerol-3-phosphate and used to synthesize triglycerides. BAT may therefore act as an important glucose sink and may also improve insulin sensitivity during cold exposure. (Townsend and Tseng, 2014)

Fatty acid metabolism in brown adipocytes is still being actively investigated. During the sympathetic activation of BAT, FFAs are produced from intracellular lipid droplets by three consecutive lipases; adipose triglyceride lipase (ATGL), hormone sensitive lipase (HSL) and monoglyceride lipase (MGL). The FFAs function as activators of UCP1 in addition to being metabolic substrates for thermogenesis (Cannon and Nedergaard, 2004; Festuccia et al., 2011). Studies with nicotinic acid have shown that fully blocking intracellular lipolysis suppresses thermogenesis and the oxidative metabolism in both rats and humans (Blondin et al., 2017a; Labbé et al., 2015). Interestingly, other recent studies have shown that intracellular lipolysis by ATGL in BAT is not required for thermogenesis when lipolysis still occurs in WAT, or when glucose and FFAs can be utilized by BAT from the circulation (Schreiber et al., 2017; Shin et al., 2017). As the intracellular triglyceride stores become depleted, *de novo* lipogenesis and the uptake of fatty acids from the circulation are increased. Triglycerides are transported in the blood stream in chylomicrons and very low density lipoproteins (VLDL). It seems that the uptake of fatty acids occurs mainly after lipolysis of these triglycerides by lipoprotein lipase (LPL) with the transporter cluster of differentiation 36 (CD36), similar to that which occur in the heart, skeletal muscle tissue and WAT (Hoeke et al., 2016). However, recent data have shown that the BAT may also take up the whole triglyceride-rich lipoprotein particle (Bartelt et al., 2011). There is evidence that the internalized FFAs are esterified and incorporated into triglycerides and stored in the small lipid droplets, from which they can be liberated again for mitochondrial β-oxidation (Labbé et al., 2015).

Clinical studies in humans have further shown that BAT is a very metabolically active tissue type, and cold exposure is its most potent activator. In lean men, oxidative metabolism is increased in BAT during cold exposure (Ouellet et al., 2012), being significantly higher in cold compared with baseline conditions (U Din et al., 2016). Cold also significantly increases perfusion and glucose extraction from the blood to the tissue (Orava et al., 2011). Importantly, perfusion of BAT correlates positively with whole-body energy expenditure (Orava et al., 2011; U Din et al., 2016), which reflects that increased BAT function contributes to total energy expenditure. Increased perfusion seems to provide more oxygen and nutrients to the brown adipocytes, and higher blood flow can also transfer heat from BAT to other areas of the body. Cold exposure in lean healthy men can increase glucose uptake in BAT up to 12-fold, whereas glucose uptake in subcutaneous WAT, visceral WAT or skeletal muscle do not change during cold exposure (Orava et al., 2011; Virtanen et al., 2009). Non-esterified fatty acids are also actively taken up into human BAT during cold exposure (Ouellet et al., 2012) and after eating a mixed meal (U Din et al., 2018). Cold exposure also increases the uptake of dietary fatty acids, even though the proportion of fatty acid clearance by BAT seems low compared to other tissues such as the liver, heart or skeletal muscle (Blondin et al., 2017b). Furthermore, there is evidence that prolonged cold exposure or cold acclimation by repeated cold exposure activates human BAT. Cold acclimation can increase BAT volume (van der Lans et al., 2013) and oxidative metabolism (Blondin et al., 2014). Prolonged cold exposure (of 3–8 hours) also increases resting energy expenditure by 15% in subjects with detectable BAT (Chondronikola et al., 2014).

2.2.3 Significance of BAT in Human Metabolism

Overweight and obesity are currently major health challenges, as obesity contributes to the pathogenesis of many chronic and metabolic diseases including diabetes, dyslipidemia, cardiovascular disease, osteoarthritis and cancer. Body weight categories are defined by body mass index (BMI), which is the weight of the subject in kilograms divided by the square of the height of the same individual in meters. The following BMI ranges are commonly used to evaluate nutritional status, body adiposity and risk for metabolic diseases: normal weight (BMI 18.5 ≤ 24.9 kg/m^2), overweight (BMI 25 ≤ 29.9 kg/m^2) and obesity (BMI ≥ 30 kg/m^2). (“WHO/Europe - Nutrition - Body Mass Index,” n.d.) In a cross-sectional study of the Finnish population in 2012, 65% of men and 46% of women were at least overweight and 20% of these were obese (Männistö et al., 2015). Moreover, the same study reported that 31% of Finns had abdominal obesity with a waist circumference of over 100 cm. On a global scale, the prevalence of overweight and

obesity in adults including both developed and developing countries, has increased by 27.5% during the past 30 years (between 1980 and 2013), which adds up to 2.1 billion overweight individuals worldwide. Prevalence of overweight and obesity has also risen by 47% in children. (Ng et al., 2014) Not only does obesity increase individual burden and morbidity (Flegal et al., 2013), the medical care costs of obesity are staggering. For example, these totaled to about $147 billion in the United States in 2008 (Jensen et al., 2014). In 2013, Member States of the World Health Organization introduced a target for stopping the rise in obesity by 2025, but new effective measures are needed to achieve this goal. Activating BAT in humans has emerged as one potential way for increasing whole-body energy expenditure and improving metabolic health.

There is evidence that obesity is linked with impaired BAT activity. For example, active BAT metabolism is associated with a leaner phenotype, lower BMI and lower visceral adiposity (Saito et al., 2009; Wang et al., 2015). The effects of both cold and insulin stimulation on BAT glucose uptake are severely blunted in overweight or obese subjects (Blondin et al., 2015a; Orava et al., 2013). However, it seems that cold acclimation can recruit BAT or increase its glucose uptake and improve insulin sensitivity in obese subjects (Hanssen et al., 2016) and subjects with originally low BAT activity (Yoneshiro et al., 2013). Interestingly, there is also evidence that weight loss in morbidly obese subjects could improve the metabolic activity of BAT (Orava et al., 2013; Vijgen et al., 2012) or cause the browning of WAT in supraclavicular depots (Dadson et al., 2018).

BAT also may have potential to ameliorate type 2 diabetes. Transplantation of BAT from healthy mice to the visceral cavity of obese mice or mice fed a high-fat diet resulted in improvements in metabolic parameters including glucose tolerance and whole-body insulin sensitivity (Liu et al., 2015, 2013; Stanford et al., 2013). Interestingly, BAT may be implicated in the mechanisms of the antidiabetic drug metformin. Metformin increased BAT mitochondrial content and activity and enhanced the clearance of VLDL-TG into BAT in a mouse model of human-like lipoprotein metabolism (Geerling et al., 2014). Active BAT may also enhance glucose disposal and insulin sensitivity in humans (Chondronikola et al., 2014; Hanssen et al., 2015b). One study found that the presence of cold-induced active BAT is one significant and independent determinant of glycosylated hemoglobin A1c (HbA1c) and blood glucose levels (Matsushita et al., 2014). Active BAT can also improve metabolism by increasing circulating levels of the insulin enhancer adiponectin, and by decreasing levels of leptin, a hormone that regulates food intake (Lee et al., 2014b). BAT is a very insulin-sensitive tissue, as the insulin-stimulated glucose uptake in human BAT increases 5-fold compared to basal rates, and this high level of response is similar to that found in skeletal muscle (Orava et al., 2011). It has been hypothesized that BAT partly reduces hyperglycemia by

acting as a "glucose sink" and internalizing glucose during its activation, but whether such a contribution is clinically significant is uncertain (Carpentier et al., 2018). Interestingly, patients with type 2 diabetes have lower glucose uptake in their BAT (measured with [^{18}F]FDG) and have a more white-like phenotype in their BAT regions (measured with CT radiodensity), although the fatty acid uptake and oxidative metabolism of BAT remain similar compared to healthy controls (Blondin et al., 2015a). Therefore, the true function and potential of BAT in type 2 diabetes patients requires further research.

Importantly, many studies show that activating BAT can improve overall metabolic parameters. A study in humans that used CT imaging has shown that higher radiodensity of adipose tissue (indicating active BAT) was associated with better measures of metabolic health, such as M-value, waist circumference and blood triglycerides (U Din et al., 2017). Evidence from pre-clinical studies also show that BAT activation could improve cardiometabolic risk factors by decreasing atherosclerotic plaque formation and by clearing triglycerides from the plasma (Bartelt et al., 2011; Berbeé et al., 2015; Chang et al., 2012). Interestingly, it has been found that perivascular adipose tissue in the thoracic area is morphologically and functionally similar to BAT (Fitzgibbons et al., 2011), and secretion of anti-inflammatory factors by this adipose tissue could possibly influence the progression of atherosclerosis (Hildebrand et al., 2018).

Although the amount of evidence of active BAT metabolism in humans has greatly increased in the past 10 years, there is still debate about whether BAT makes a significant contribution to human energy expenditure. Some studies have shown that the amount of energy expenditure from maximally activated cold-induced BAT thermogenesis amounts to about 10–20 kcal/day (Muzik et al., 2012; U Din et al., 2016). Other studies suggest a BAT thermogenesis of up to 100–125 kcal/day (Marlatt and Ravussin, 2017; Ouellet et al., 2012; Virtanen et al., 2009), which varies and depends on the mass of detected BAT. It has been well established that BAT can dissipate energy and increase the disposal of glucose and fatty acids. The proportion of energy expenditure caused by BAT activation, however, seems to be small due to its small mass in humans when compared to the contribution of the musculature (Blondin et al., 2015b). One strategy to treat obesity could thus be to increase the amount of BAT mass, which could then increase energy expenditure. It is noteworthy, however, that UCP1 does not increase respiratory activity of brown adipocytes under basal conditions, and therefore only expanding brown (or beige) adipose tissue without promoting activation may be inadequate for increasing energy expenditure. Nevertheless, a larger brown/beige depot could be activated by daily stimuli such as cold exposure to achieve therapeutic effects. (Harms and Seale, 2013) It is plausible that BAT could play a role in weight maintenance and improve systemic metabolic factors,

rather than cause substantial weight loss. More research is needed to develop strategies to utilize BAT for the treatment of metabolic disease in humans. The specific mechanisms and regulatory factors of BAT activation must still therefore be understood in order to develop suitable and effective therapies.

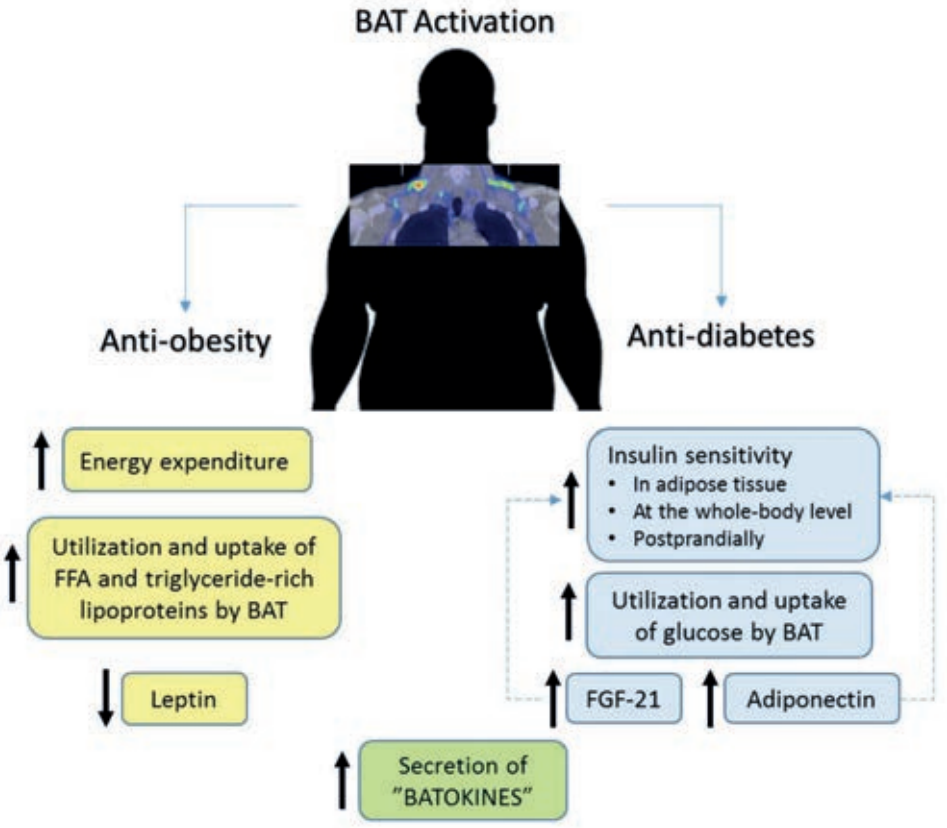

Figure 2. Potential mechanisms of how BAT activation may contribute to combating obesity and type 2 diabetes. "Batokines" refer to regulatory BAT-derived molecules that act in a paracrine or autocrine manner and influence metabolism.

2.3 Endogenous Regulation of Brown Adipose Tissue

Thermogenesis and activation of BAT is regulated by numerous endogenous factors and molecular pathways (Broeders et al., 2014). The SNS is an essential modulator of many of these regulatory mechanisms. For example, the ß3-ARs are essential for cold-induced BAT activation to occur. Interestingly, one study showed that a single-dose oral administration of the β3-AR agonist, mirabegron, increased glucose uptake in human BAT (Cypess et al., 2015). In line with this finding, previous [^{18}F]FDG-PET studies have shown that β-adrenergic blockers decrease BAT activity (Söderlund et al., 2007).

Exercise also increases SNS stimulus and catecholamine release, which cause lipolysis in both BAT and WAT, thus leading to increased thermogenesis (Virtanen, 2014). Furthermore, active skeletal muscle induces secretion of other molecules including natriuretic peptides and irisin, which may additively activate BAT (Sanchez-Delgado et al., 2015). Natriuretic peptides are secreted from the heart, with the classic physiological functions of diuresis, natriuresis and vasodilation. Excessive availability of natriuretic peptides decrease fat mass and promote browning of white adipocytes of mice, and enhance markers of mitochondrial biogenesis and cellular oxygen consumption in human adipocytes (Bordicchia et al., 2012). Indeed, obesity and diabetes in humans seem to be associated with lower levels of circulating natriuretic peptides (Wang et al., 2004). Irisin is a molecule that is released from the skeletal muscle into the blood circulation during both exercise and cold-induced shivering, and it has been shown to induce adipose tissue browning and thermogenesis in rodents (Boström et al., 2012; Lee et al., 2014a; Petrovic et al., 2010). In infants, the occurrence of BAT is strongly associated with early postnatal growth of skeletal muscle (Ponrartana et al., 2016). Additionally, some other systemic hormones that promote musculoskeletal development at puberty, including growth hormone, gonadal sex steroids, and insulin-like growth factor 1 (IGF-1), may also promote the growth of BAT (Rogers, 2015). Overall, the innumerable metabolic health benefits of exercise for humans are apparent, but whether some of these benefits are partly mediated by BAT activation is still unclear. A few human studies suggest that glucose uptake by the BAT may in fact decrease during endurance training (Vosselman et al., 2015) and also during short-term training (Motiani et al., 2017). This interesting skeletal muscle – BAT crosstalk still requires more studies for its elucidation (Dewal and Stanford, 2018).

Many other mechanisms have also been investigated, that demonstrate an interplay between different organ systems and BAT. Bile acids can increase energy expenditure in mice and humans by stimulating the transmembrane G protein-coupled receptor 5 (TGRF) on brown adipocytes and thus increasing D2-mediated

thyroid hormone thermogenesis in BAT (Broeders et al., 2015; Watanabe et al., 2006). Interestingly, cold-induced BAT activation in mice increases cholesterol metabolism and bile acid synthesis, which also alters the gut microbiome (Worthmann et al., 2017). Brown fat may also have a secretory role by producing molecules that act in a paracrine or autocrine fashion, and as messengers to other tissues. These numerous molecules have collectively been named brown adipokines or "batokines", and they may contribute to the systemic health benefits observed during BAT activation (Villarroya et al., 2017). For example, bone morphogenic proteins (BMPs) are extracellular signaling proteins that regulate tissue development and homeostasis, and BMP7 and BMP8b are especially necessary for beige adipogenesis, the expression of transcription factors PRDM16 and PGC1α, and other pathways significant for thermogenesis (Tseng et al., 2008; Whittle et al., 2012). BAT-mediated secretion of vascular endothelial growth factor A (VEGFA) can promote vascularization of BAT and upregulate UCP1 (Sun et al., 2014; Xue et al., 2009), whereas secretion of nerve growth factor (NGF) seems to enhance the sympathetic innervation in BAT (Nisoli et al., 1996). Fibroblast growth factor 21 (FGF21) promotes the action of glucose in adipose tissue and therefore moderates glycemia and lipidemia (Giralt et al., 2015). It is secreted mostly from the liver, but also from other tissues and organs including skeletal muscle and thermogenically activated human brown adipocytes (Lee et al., 2014a). Systemic plasma levels of FGF21 in humans are associated with the cold-induced metabolic activity of BAT (Hanssen et al., 2015). Furthermore, a preliminary clinical trial with exogenous administration of FGF21 in obese subjects with type 2 diabetes found improvements in lipid values and body weight, but not in glucose levels (Gaich et al., 2013). However, the specific mechanisms of action of FGF21 in humans still require further research (Lee et al., 2015).

These and other numerous studies present different mechanisms of how BAT is involved in the crosstalk with several organ systems, and understanding these complex regulatory pathways may provide novel ways by pharmacology, to increase human BAT activation. Several factors have been found and investigated in rodents, but species-specific differences in BAT regulation may also occur, which underlies the need for human studies. This thesis work focuses on investigating three endogenous aspects of BAT regulation, which have not previously been studied in humans, namely the thyroid hormones, the adenosinergic system, and the endocannabinoid system.

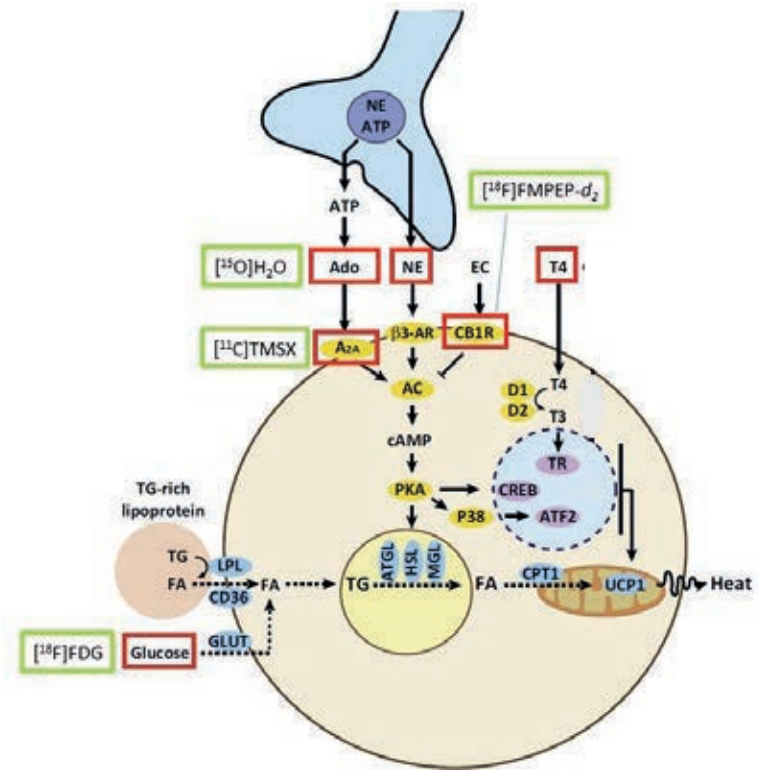

Figure 3. Activation mechanisms of the brown adipocyte. Red boxes represent the mechanisms that have been studied in this thesis. Green boxes show PET radioligands that were used for imaging BAT in this research. Abbreviations: noradrenaline (NE), adenosine triphosphate (ATP), adenosine (Ado), Adenosine A_{2A} receptor (A_{2A}), β3-adrenergic receptor (β3-AR), endocannabinoid (EC), Cannabinoid type 1 receptor (CB1R), thyroxine (T4), triiodothyronine (T3), thyroid hormone receptor (TR), type I iodothyronine deiodinase (D1), type II iodothyronine deiodinase (D2), adenylyl cyclase (AC), cyclic AMP (cAMP), protein kinase A (PKA), triglyceride (TG), fatty acids (FA), adipose triglyceride lipase (ATGL), hormone sensitive lipase (HSL), monoacylglycerol lipase (MGL), lipoprotein lipase (LPL), cluster of differentiation 36 (CD36), glucose transporters (GLUT), cAMP response element-binding protein (CREB), activating transcription factor 2 (ATF2), carnitine palmitoyltransferase I (CPT1), uncoupling protein 1 (UCP1). Modified from Kooijman et al., 2015.

2.3.1 Thyroid Hormones

Thyroid hormones are essential for normal metabolism and function of many tissues including BAT. The thyroid gland produces and releases thyroxine (T_4) and, to a minor extent, triiodothyronine (T_3) into the circulation, and systemic levels are controlled via a negative feedback system by the hypothalamus (which secretes Thyrotropin Releasing Hormone, TRH) and the pituitary gland (which secretes Thyroid Stimulating Hormone, TSH) (Yen, 2001). At the tissue level, BAT expresses the enzyme D2, which converts the prohormone T_4 into the biologically active metabolite T_3. These regulatory mechanisms ensure that BAT has a sufficient amount of thyroid hormone in order to function. (Cannon and Nedergaard, 2004; Weiner et al., 2017)

Normal thyroid status is required for cold-induced adaptive thermogenesis. T_3 actions are mediated by nuclear thyroid hormone T_3 receptors (TR), TRα and TRβ. Studies in mice have shown that TRβ is required for the induction of UCP1 and is essential for BAT function, whereas TRα regulates adrenergic sensitivity and body temperature. (Cioffi et al., 2018; Silva and Bianco, 2008) Mice with mutated TRβ receptors are unable to bind T_3, have reduced UCP1 expression, reduced adrenergic responsiveness and consequently the mutated mouse has defective adaptive thermogenesis (Ribeiro et al., 2010). Localized bioavailability of T_3 during embryogenesis is also crucial for the development of BAT (Hall et al., 2010). Furthermore, thyrotoxicosis in rats stimulates UCP1 expression and BAT heat production (Branco et al., 1999), whereas hypothyroid hibernating rodents develop severe hypothermia and death after cold exposure, largely due to the impaired BAT thermogenesis (Kates and Himms-Hagen, 1985).

The signaling pathways of thyroid hormones and the SNS are interconnected, and there is evidence that thyroid hormones regulate BAT function via the brain. Systemic hyperthyroidism or intracerebroventricular administration of T_3 in rats leads to activation of the SNS and the induction of BAT (López et al., 2010). Interestingly, central injection of T_3 in mice decreased weight independently of food intake, and caused browning of WAT when compared to control mice. Specifically the ventromedial hypothalamus and central AMPK are necessary for these effects to occur (Martínez-Sánchez et al., 2017). Furthermore, cold exposure increases expression and activity of D2 in BAT. Catecholamines and local T_3 act synergistically to stimulate UCP1 expression and consequently increase thermogenesis (Silva and Bianco, 2008). The thyroid receptor agonist GC-1 has been found to induce significant browning of subcutaneous WAT (but not epididymal WAT) in an obese mouse model. GC-1 treatment increased adaptive thermogenesis in a UCP1-dependent manner, improved glucose disposal rate, but interestingly, decreased activity of classic BAT. (Lin et al., 2015).

Although there is vast evidence from studies in rodents, the link between thyroid hormones and BAT activation in humans has not been thoroughly studied. A human study done in Greenland found that dwellers with most exposure to Arctic cold conditions had the highest serum thyroglobulin concentrations, low T_3 concentrations and high urinary iodine excretion, which indicates high thyroid turnover (Andersen et al., 2012). Human PET studies have shown slightly higher TSH levels under baseline room temperature conditions in "BAT-positive" individuals compared to individuals with no detectable BAT (Orava et al., 2013, 2011). Furthermore, cold exposure causes small decreases in plasma TSH values (Blondin et al., 2015a; Orava et al., 2011). Interestingly, TSH-receptors are also found in adipose tissue (Sorisky et al., 2008), and activation of TSH-receptors has been linked to increased UCP1 expression in preadipocytes (Zhang et al., 2006). Moreover, expression of *DIO2*, the gene that encodes D2, is higher in human BAT than in WAT (Virtanen et al., 2009). Cold exposure further induces the expression of *DIO2*, in addition to the expression of other factors essential for BAT thermogenesis, namely UCP1, β3-AR and PGC1α (Chondronikola et al., 2014). These findings together suggest a link between thyroid hormones and BAT function also occurs in adult humans.

Patients with hyperthyroidism are characterized by symptoms and signs of increased metabolism of tissues and activation of the SNS, such as unintentional weight loss, heat intolerance, tachycardia and tremor (Ross et al., 2016). Although most of the hyperthyroid symptoms can be explained by metabolic changes in other tissues, they may partly result from an over-activation of the signaling between thyroid hormones and BAT. Understanding the effects of thyroid hormones on human BAT function would provide insight into BAT regulation in addition to the disease mechanisms in hyperthyroidism.

2.3.2 Adenosine

Adenosine is a purine nucleoside, which functions as an important extracellular signaling molecule that exerts a range of responses in different tissues including adipose tissue. It is a short-lived molecule in the circulation, and it acts as a cytoprotective modulator in response to stress in a tissue or organ. The response restores homeostasis in the tissue by the action of one or more of the following: increasing blood supply, suppressing inflammation or by ischemic preconditioning. The effects of adenosine are mediated via four G protein-coupled receptor subtypes A_1, A_{2A}, A_{2B} and A_3. The subtypes A_1 and A_3 inhibit the production of intracellular cAMP, whereas A_{2A} and A_{2B} stimulate adenylate cyclase, therefore different receptors mediate different intracellular responses.

(Wilson and Mustafa, 2009) The release of adenosine is controlled by the SNS. During cold exposure, the SNS is activated thereby releasing noradrenaline and also ATP as a co-transmitter. ATP undergoes rapid enzymatic degradation into adenosine monophosphate (AMP), adenosine diphosphate (ADP) and adenosine, which further swiftly breaks down into inosine. (Abbracchio et al., 2009)

Studies with hamsters have shown that adenosine regulates BAT respiration by antagonizing lipolysis and respiration stimulated by the β-adrenoreceptor agonist isoproterenol (Schimmel and McCarthy, 1984; Szillat and Bukowiecki, 1983). However, more recently, adenosine in human brown adipocytes was found to increase lipolysis, and additively enhance lipolysis evoked by noradrenaline (Gnad et al., 2014). Adenosine also increased the expression of thermogenic markers in human brown and white adipocytes. The BAT of mice provides a better model for human BAT than that of hamsters, and electrical field stimulation of mice BAT induced the release of endogenous noradrenaline and ATP, with a simultaneous increase in adenosine concentration. Treatment of BAT and brown adipocytes with noradrenaline also increased adenosine concentrations, which were abolished by treatment with propranolol. (Gnad et al., 2014) These findings support the concept that adrenergic and purinergic signaling enhance BAT function concomitantly.

A_{2A} receptor (A2AR) signaling is required for the full activation of BAT, and selective A2AR agonism can also induce browning of white adipocytes (Gnad et al., 2014). There is also pre-clinical evidence that adenosine has a stimulatory effect on pancreatic β-cells via the A2AR, and A2AR agonism is significant in controlling the proliferation and survival of the cells (Antonioli et al., 2015). A2AR agonists have also been shown to improve adipose tissue inflammation and glucose homeostasis in obese mice (DeOliveira et al., 2017).

These data suggest that targeting the adenosine receptors in BAT could potentially provide a way to increase BAT activity. Despite the substantial pre-clinical evidence, the physiological significance of adenosine for BAT in humans is still unexplored.

2.3.3 Endocannabinoids

The endocannabinoid system (ECS) consists of a vast network of endogenous molecules, their receptors, and enzymes, which are significant for modulating processes including metabolism, inflammation, and intercellular signaling. Endogenous cannabinoids are produced on demand from phospholipid precursors, and they modulate and inhibit neurotransmission in a retrograde manner in the brain. The cannabinoid type 1 receptor (CB1R) is the most studied cannabinoid

receptor, and it is primarily found in the brain but also in various peripheral tissues including adipose tissue (Toczek and Malinowska, 2018).

CB1Rs participate in the control of lipid and glucose metabolism (Di Marzo, 2008). Agonism of CB1Rs promotes conservation of energy by increasing food intake and inhibiting energy expenditure and thermogenesis, which leads to an expansion of fat mass (Mazier et al., 2015). Physiologically, the ECS is activated in states of fasting or stress, which protects the organism from excessive energy expenditure or starvation, but in affluent lifestyles where food is abundant and easily accessible, the normal regulation of the system can become impaired. In fact, obese individuals have overactive endocannabinoid signaling, which manifests as higher circulating cannabinoid levels compared to those of lean individuals (Blüher et al., 2006; Engeli et al., 2005; Fanelli et al., 2018). Higher plasma endocannabinoid levels are also associated with increased abdominal adiposity, insulin resistance, dyslipidemia and cardiometabolic risk factors (Côté et al., 2007; Di Marzo et al., 2009; Fanelli et al., 2017). Furthermore, endocannabinoids are involved in the physiology of the gut, by modulating gastric emptying, gastrointestinal motility and inflammation. These effects of endocannabinoids on the gut may also be involved in the regulation of fat intake, postprandial glycemia, satiety and the gut microbiome. (Cani et al., 2016)

Blockade of CB1R decreases body weight and fat mass and improves glucose homeostasis and insulin sensitivity in humans and rodents, which is a finding that shows promise for using CB1R antagonists as potential drugs against obesity and diabetes. One CB1R inverse agonist, rimonabant, was previously in clinical use with good efficacy (Christopoulou and Kiortsis, 2011). Rimonabant treatment caused reductions in weight and waist circumference, and improvements in glucose and lipid homeostasis, fatty liver and insulin resistance (Christopoulou and Kiortsis, 2011). Some cardiometabolic risk factors were alleviated partly independently of weight loss, including improvements in adiponectin, HDL, triglycerides, and HbA1c in diabetic patients (Richey and Woolcott, 2017). Unfortunately, the drug caused severe psychiatric adverse effects and was withdrawn from the market (Christensen et al., 2007). Research is now focusing on developing neutral antagonists that would benefit metabolic health but which would not penetrate the blood-brain-barrier and cause harmful side-effects (Richey and Woolcott, 2017).

The weight loss effects due to rimonabant treatment were partly explained by blockade of the CB1R in the central nervous system, which decreased food intake and reduced appetite (Colombo et al., 1998; Sam et al., 2011). However, recent studies have also shown that rimonabant also functions in the peripheral tissues, including WAT, liver, skeletal muscle, the endocrine pancreas and macrophages

(Jbilo et al., 2005; Kunos and Tam, 2011). Interestingly, novel CB1R antagonists that act strictly peripherally, have been found to activate BAT in rodents, induce lipolysis and lipid oxidation, and improve metabolism (Hsiao et al., 2015; Takano et al., 2014).

A few studies have suggested that alternative activation of macrophages (M2 polarization) contributes to BAT activation and browning (Nguyen et al., 2011; Ruiz de Azua et al., 2017). Alternatively activated macrophages secrete catecholamines by stimulation from interleukin-4 (IL-4), increasing the thermogenic capacity of BAT and mobilizing fatty acids from WAT to fuel uncoupled respiration. Absence of these macrophages impaired the adaptations to cold, whereas IL-4 administration increased energy expenditure, thermogenic gene expression and fatty acid mobilization. (Nguyen et al., 2011) The selective adipocyte specific knock-out of CB1R in another study protected mice from diet-induced obesity, and the phenotype showed decreased body weight, reduced adiposity and improved insulin sensitivity (Ruiz de Azua et al., 2017). Adipocyte specific knock-out of CB1R resulted in the reprogramming of white adipocytes into a beige phenotype, increased the sympathetic outflow and increased the amount of alternatively activated macrophages. These data suggest a crosstalk between adipocytes, immune cells and the sympathetic nervous system for which the CB1R plays a regulatory role. Further proof of the link between the brain, the SNS and BAT has been provided by a PET imaging study with the noradrenaline analogue [^{11}C]-metahydroxyephedrine ([^{11}C]-MHED) (Quarta et al., 2013). This study presented accumulation of the radioligand in BAT of rodents, and reported that uptake was proportional to the level of SNS-induced BAT activity. Both acute and chronic changes in SNS-dependent BAT thermogenesis were observed, and in obese mice this SNS–BAT crosstalk was impaired. (Quarta et al., 2013)

Intriguingly, there is pre-clinical evidence that CB1Rs and endocannabinoids are upregulated in BAT following cold or stimulation of β3-AR (Krott et al., 2016). One human study also showed increased plasma endocannabinoid levels of healthy lean men after acute mild cold exposure (Kantae et al., 2017). The CB1Rs are expressed in BAT of rodents (Eriksson et al., 2015; Krott et al., 2016), but hitherto their function has not been studied in humans. Understanding the role of endocannabinoids for human BAT function could further facilitate the development of new treatment strategies for increasing BAT activity and improving metabolic health.

2.4 Positron Emission Tomography

Positron emission tomography (PET) is a non-invasive medical imaging technique, which *inter alia* has enabled the modern re-discovery of BAT in humans and has become a golden standard method for investigating BAT (Sun et al., 2017). PET utilizes medical radioactive compounds, which are administered to patients in trace amounts and mimic naturally occurring biological processes of the body. The radiation of the compound that accumulates in the organ or tissue is detected by a PET camera, after which the data are transformed into an image and can be further processed using mathematical models. Depending on the type of radioligand, the accumulation or turnover of the compound can represent the localization of the molecule into certain cells or the binding to specific receptors. In this way many molecular mechanisms can be visualized and quantified *in vivo*, and further combined with anatomical data from simultaneous CT or MR imaging. (Anand et al., 2009; Oikonen, n.d.).

2.4.1 Physical principles of PET

A PET radioligand is produced by incorporating a positron emitting radionuclide with a short half-life (e.g. ^{18}F, ^{11}C, ^{15}O) generated in a cyclotron into a biological molecule using different labeling methods. The radioligand is typically administered to the subject intravenously, but also oral administration or inhalation can be used. The radionuclide continues to undergo nuclear decay in the body and emits positrons. The positron collides with an electron, and annihilation occurs, which converts the mass of these particles into energy. This produces two gamma photons or rays that are emitted in opposite directions to each other. The photons are detected by the circular PET camera, which surrounds the patient. (van der Veldt et al., 2013) The scanner can calculate the point of annihilation based on the line of response from two simultaneous and opposite detections of gamma rays. The numerous annihilations detected by the PET scanner are processed and reconstructed by a computer to form a tomographic image. High accumulations of the radioligand are visualized as hotspots in the three-dimensional PET image, and the precise locations in the body can be determined by combining the image with an anatomical CT or MR image. (Turkington, 2001).

A.

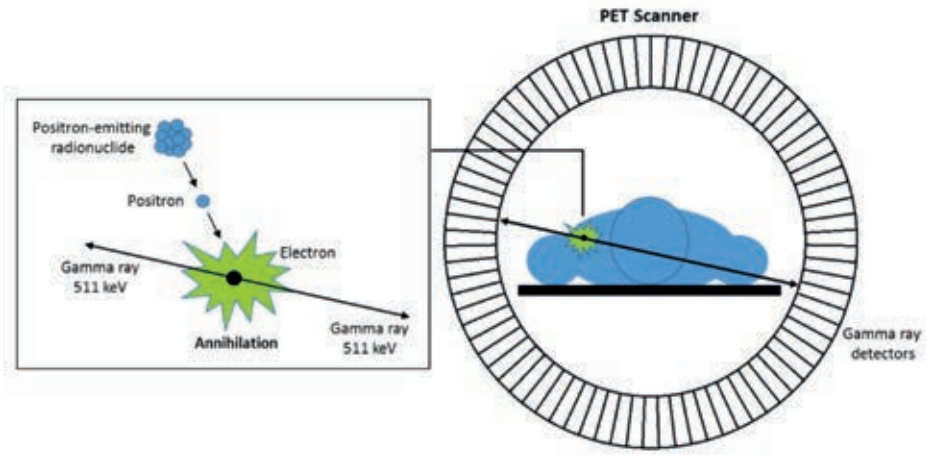

B.

Figure 4. A. Diagram depicting positron-electron annihilation and detection by the PET scanner. Modified from van der Veldt et al., 2013.

B. Study subject is lying in the supine position inside the PET/CT scanner (GE Healthcare), with only the covered legs in view, in the Turku PET Centre. Photo by Roni Lehti.

2.4.2 PET radioligands for Investigating BAT

Currently, the most widely used and available PET radioligand is ^{18}F-fluorodeoxyglucose ([^{18}F]FDG). The [^{18}F]FDG molecule is an analogue of glucose that mimics glucose metabolism in the body and it is transported into cells through the same transporters as glucose. In the cell [^{18}F]FDG is phosphorylated into ^{18}FDG-6-phosphate, but it does not undergo any further glycolysis and is trapped within the cell, until it decays. [^{18}F]FDG has been extensively used as an indicator of metabolically active BAT in humans since the first major BAT studies were published in 2009 (Cypess et al., 2009; Saito et al., 2009; van Marken Lichtenbelt et al., 2009; Virtanen et al., 2009).

Dynamic PET imaging is required to quantify the uptake rate of glucose into tissues. When dynamic PET data are combined with the [^{18}F]FDG concentration in plasma (i.e. the input function), the graphical Patlak method can be used to directly estimate the net uptake rate (K_i) for [^{18}F]FDG (Patlak and Blasberg, 1985). K_i is then used to calculate the metabolic rate of glucose, by multiplying K_i with the actual plasma glucose concentration of the subject during the scan, and dividing the product by the lumped constant (LC). The LC is a tissue-specific constant that accounts for differences in transport and phosphorylation rates between natural glucose and its tracer analogue [^{18}F]FDG (Sokoloff et al., 1977; Virtanen et al., 2001). This method provides an absolute, quantitative measure of glucose flux into tissue by taking into account the differences in biodistribution and plasma clearance of the tracer, such as uptake into other organs or excretion of [^{18}F]FDG. Semi-quantitative measurements, such as standardized uptake value (SUV), are widely used when dynamic imaging or blood sampling is not possible, and for clinical oncological studies to assess cancer treatment response. The SUV is calculated simply as the ratio of tissue radioactivity (kBq/ml) at one time point after injection of the tracer, and the administered dose at the time of the injection (MBq) divided by the body weight of the subject in kilograms (Cypess et al., 2014). However, SUV is vulnerable to major sources of variability, such as metabolic state (e.g. the fasting state vs. insulin stimulation) and any physiological changes in other tissues during the PET scan or any intervention (e.g. during exercise and muscle activation) (Oikonen, n.d.). The SUV and Patlak K_i values may in fact be discrepant, and can provide opposite conclusions regarding the progression of disease in cancer patients (Freedman et al., 2003). In scientific studies, therefore SUV values must be evaluated critically, and quantitative, dynamic PET imaging should currently be the methodology of choice whenever possible.

In addition to glucose, fatty acids are another essential substrate for BAT function (Townsend and Tseng, 2014). The long-chain fatty acid analogue, 14(R,S)-[^{18}F]fluoro-6-thia-heptadecanoic acid ([^{18}F]FTHA) is used to quantify the uptake

of circulatory non-esterified fatty acids into tissues. The radioligand enters the cells similar to the mechanism of natural fatty acids, and undergoes metabolism in the mitochondria, after which they are trapped. Accumulation of ^{18}F thus represents total fatty acid utilization of the tissue, including β-oxidation and storage in the cells (DeGrado et al., 1991; Oikonen, n.d.). This radioligand has been administered intravenously (Ouellet et al., 2012; U Din et al., 2017) and orally (Blondin et al., 2017b) in studies on BAT fatty acid metabolism.

There are also many radioligands, which enable the measurement of BAT function independent of substrate uptake. For example, by incorporating the radionuclide ^{15}O into the water molecule produces $[^{15}O]H_2O$, a diffusible and inert radiotracer, which can be administered intravenously. It is optimal for quantifying the perfusion of tissues, i.e. the volume of blood flowing through a specific quantity of tissue per unit of time. Radiowater has commonly been used in clinical studies to investigate cardiovascular function (Danad et al., 2014), and it has also been used to study the physiological changes in perfusion of skeletal muscle, BAT and WAT (Heinonen et al., 2014, 2010, Orava et al., 2013, 2011). Radiolabeled oxygen $[^{15}O]O_2$ has also been used to investigate BAT metabolism (Muzik et al., 2012; U Din et al., 2016). This radioligand is administered via inhalation and provides a direct measure of oxygen consumption of the tissues. It is especially suitable when the question of which substrate is used for oxygen consumption is irrelevant (U Din et al., 2016). However, because of its very short half-life (122.2 s), production of ^{15}O requires an on-site cyclotron in close special proximity to the PET camera, suitable infrastructure and facilities to administer the tracers.

Oxidative metabolism of BAT can also be estimated using [^{11}C]acetate (Blondin et al., 2017a; Ouellet et al., 2012). In living tissues acetate is metabolized into acetyl-CoA and enters Kreb's cycle. Consequently, retention of acetate and the ^{11}C radioactivity in tissue over time provides a measure of oxidative metabolism, and the peak ^{11}C radioactivity value can be used to estimate perfusion of a tissue. Interestingly, there is pre-clinical evidence in mice that a novel noradrenaline analogue [^{11}C]-meta-hydroxyephedrin ([^{11}C]HED) could be utilized to study the activity of the SNS in BAT. This radioligand could provide more insight into SNS-mediated BAT thermogenesis and even conversion of WAT to BAT. (Quarta et al., 2013)

Many other radioligands have been developed to quantify different receptors of tissues, but their use for human BAT imaging is still unexplored. [^{18}F]FMPEP-d_2 is an inverse agonist radioligand that binds to CB1 receptors of the endocannabinoid system. This tracer has previously been used to quantify the density of CB1R in the human brain and investigate changes in alcohol or cannabis abuse (Donohue et al., 2008; Hirvonen et al., 2013, 2012; Terry et al., 2010).

[^{18}F]FMPEP-d_2 has also recently been used to study CB1Rs of BAT in rats (Eriksson et al., 2015), although it has not yet been applied to humans. [^{11}C]TMSX is another receptor binding radioligand with specific affinity to adenosine A_{2A} receptors in the body. It has previously been used to quantify these receptors in the brain (Mishina et al., 2011, 2007; Rissanen et al., 2013) and skeletal or cardiac muscle tissues (Heinonen et al., 2008; Ishiwata et al., 2004; Mizuno et al., 2005) of humans and rodents, but has not previously been studied in adipose tissue. These radioligands provide potential tools to investigate the regulation of BAT further.

2.4.3 Strengths and Limitations of PET Imaging

The studies carried out in this thesis utilize four different PET radioligands and dynamic imaging to investigate several aspects of BAT function and regulation in humans. PET imaging provides an excellent non-invasive tool for investigating biological processes *in vivo*, and particularly when different imaging modalities are combined it offers new perspectives to physiological phenomena that occur in the BAT in humans. However, PET imaging also has its limitations. Administration of a radioligand causes exposure to ionizing radiation for the patient or subject, which limits the number of studies that can be done on one study subject. For example, administering 150 MBq of [^{18}F]FDG results in an effective dose of 2.85 mSv, whereas the mean annual background radiation dose in Finland is 3.2 mSv. Although the effects of such a dose on individual health are minimal, ethical guidelines and restrictions have been set to limit the radiation burden for healthy individuals and ensure their safety (Radiation and Nuclear Safety Authority (STUK), n.d.). PET imaging cannot investigate more than one function at a time, but depending on the radioligand, repeated measurements with various tracers can be done, as reported in this thesis. The field of view of the PET camera (usually 15–20 cm) also somewhat limits the ability to study simultaneous processes at the whole-body level with dynamic imaging. Furthermore, the resolution of PET images in this study is about 3.5 mm, which limits the visualization of smaller molecular processes. However, with highly specific radioligands and mathematical modeling in combination, PET can quantify many biological processes with high precision. PET data can also be combined with biopsy data and metabolic measures such as energy expenditure and blood values, which expand the understanding of biological phenomena.

3 AIMS OF THE STUDY

The purpose of this study was to investigate endogenous factors that regulate human brown adipose tissue function. Another aim was to assess the use of different PET radioligands for BAT imaging in humans.

The specific aims of the study were to:

1) Investigate whether hyperthyroidism increases the metabolism of BAT in humans, and whether the change is reversible after successful treatment of the condition.

2) Investigate the effects of adenosine on human BAT perfusion, and to study the significance of adenosine A_{2A} receptors for human BAT.

3) Study the cannabinoid type 1 receptors in human BAT and assess whether changes occur during cold-induced BAT activation.

4) Assess whether the CB1 receptor density varies in the BAT, the WAT, the brain and the skeletal muscle of lean and overweight men.

4 MATERIALS AND METHODS

4.1 Study subjects (I-III)

This study includes a total of 46 subjects who each participated in one of the three sub-studies. The study protocols were reviewed and approved by the Ethics committee of the Hospital District of Southwest Finland and were conducted according to the principles of the Declaration of Helsinki. All participants provided their written informed consent.

Study I included 10 patients (4 male, 6 female) with a novel diagnosis of hyperthyroidism, who had been recruited from Turku University Hospital and Helsinki University Hospital. Nine of the patients had Graves' disease with elevated TSH receptor antibodies, and one patient had toxic multinodular goiter. All patients had clinical symptoms and biochemically confirmed hyperthyroidism (plasma TSH <0.05 mU/L, and plasma free T_4 >19 pmol/L, and/or plasma free T_3 >6.0 pmol/L). Five of the hyperthyroid patients (1 male, 4 female) returned for follow-up studies after treatment of the disease with either total thyroidectomy combined with levothyroxine replacement therapy (n=2), or 18 months of carbimazole treatment (n=3). At the time of the follow-up studies, all 5 participants were clinically and biochemically euthyroid. Eight healthy, euthyroid individuals (2 males, 6 females) participated as control subjects in study I.

Study II included 10 healthy, lean men. Study III included 18 healthy men who were divided into a lean group or an overweight/obese group, based on the combined assessment of BMI (lean < 25 kg/m^2), waist circumference (lean < 100 cm) and body fat percentage (lean < 20%) (Table 1.). This combined assessment was used to estimate the individual's excess of adiposity, since BMI alone is not always accurate enough especially in men who have an excess of muscle mass, but a low waist circumference and a low fat percentage. Therefore, subjects with a BMI in the range of 25.1–26.9 were divided into the lean or overweight group based on their waist and body fat percentage values.

All 46 subjects and patients were screened for medical history, health and metabolic status. Apart from the hyperthyroid patients (10), all subjects had been determined healthy by means of clinical examination, blood tests and anthropometric measurements. Exclusion criteria applied to the healthy participants included:

1. Any significant disease (e.g. diabetes, asthma, thyroid dysfunction, blood pressure ≥160/100 mmHg, cardiovascular disease, psychiatric disorder, malignancies)
2. Regular use of medication
3. Smoking or use of nicotine products
4. Pregnancy or lactation
5. Presence of ferromagnetic objects in the body (contraindicating MRI)
6. Previous participation in PET studies

Table 1. Characteristics of study subjects.

Study	Characteristics	Number of subjects	Mean Age (years)	Sex (male/female)	Mean BMI (kg/m^2)	PET radioligand	Scan performed	Scanning conditions
I	Hyperthyroid	10	43 ± 10	4/6	25.0 ± 5.5	$[^{18}F]$FDG and $[^{15}O]H_2O$	PET/CT or PET/MR	Room temperature
	Euthyroid after treatment	5 (of 10)	43 ± 13	1/4	24.0 ± 2.7 (22.5 ± 2.4 in the hyperthyroid state)			
	Healthy	8	42 ± 10	2/6	22.8 ± 2.9			
II	Healthy, lean	10	26 ± 7	10/0	24.5 ± 1.7	$[^{15}O]H_2O$ and $[^{11}C]$TMSX	PET/CT	Room temperature and cold
III	Healthy, lean	9	32 ± 9	9/0	24.9 ± 1.7	$[^{18}F]$FDG and $[^{18}F]$FMPEP-d_2	PET/CT and PET/MR	Room temperature and cold
	Healthy, overweight/obese	9	34 ± 11	9/0	32.9 ± 4.6			

4.2 Study design

4.2.1 Study I (ThyBAT)

In study I, the activation of BAT and other tissues was measured in a group of hyperthyroid patients and a control group of healthy individuals. Additionally, five of the originally hyperthyroid patients who had become euthyroid after treatment for the disease participated in a follow-up study. All study participants had a PET scan of the cervicothoracic region after an overnight fast, in room temperature (RT) conditions. Glucose uptake and perfusion of BAT, WAT, the thyroid gland and skeletal muscle were quantified by using [^{18}F]FDG and [^{15}O]H_2O PET imaging, respectively. Anatomical reference was obtained by CT (n=5 from the hyperthyroid group) or MRI (n=18; including the control group, 5 hyperthyroid subjects and 5 re-studied subjects after treatment). Energy expenditure was measured using indirect calorimetry 30–40 minutes before the PET examination commenced.

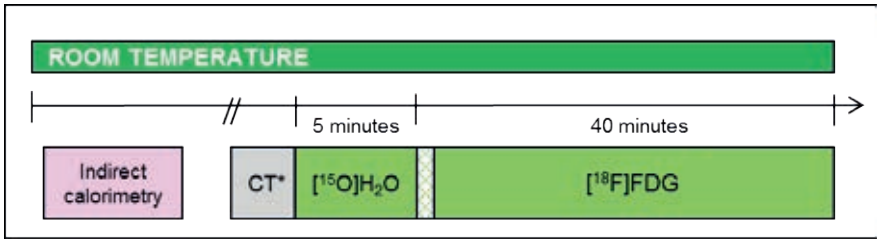

Figure 5. Clinical PET study design (I). *In (n=18) subjects MRI was used instead of CT for anatomical reference.

4.2.2 Study II (AdenoBAT)

In study II, the effects of adenosine on BAT perfusion, and the density of A2ARs in BAT were investigated in healthy, lean men. PET/CT imaging was performed on two separate days in random order, once in RT conditions and once during controlled cold exposure. Perfusion of BAT, WAT and skeletal muscle were measured with [^{15}O]H_2O-PET/CT at baseline, during intravenous infusion of adenosine, and during controlled cold exposure. A2ARs in BAT, WAT and muscle were quantified using [^{11}C]TMSX-PET/CT twice; at baseline under RT conditions and also during cold exposure. Before imaging, the study subjects fasted overnight

and avoided caffeine and strenuous exercise for a minimum of 24 hours. Energy expenditure was measured by using indirect calorimetry at baseline and during the cold exposure.

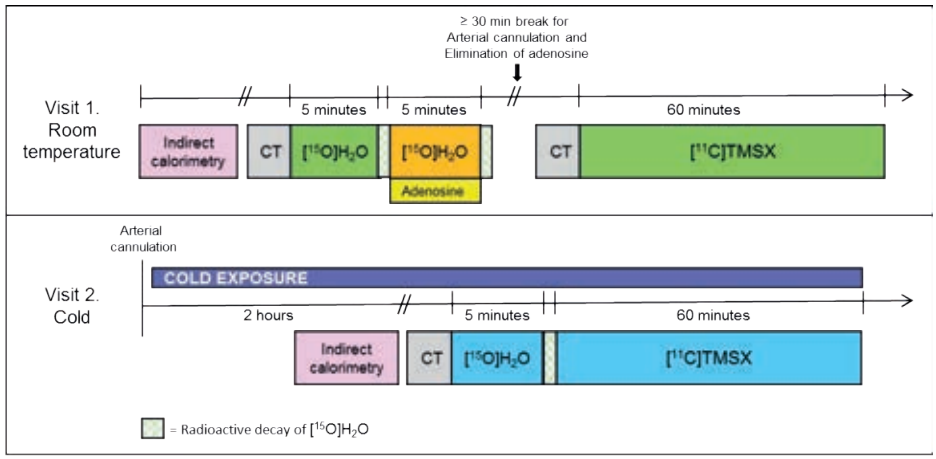

Figure 6. Clinical PET study design (II). Modified from Lahesmaa et al., 2018.

4.2.3 Study III (CANBAT)

In study III, the CB1Rs in human BAT and other tissues were studied in lean and overweight/obese men. Clinical data were complemented by PET studies with rats and *in vitro* cell experiments (see section 4.8). Each study subject (18 healthy men, 9 lean, 9 overweight/obese) took part in three study visits in the fasting state. CB1R density in BAT, WAT, skeletal muscle and brain was measured using [^{18}F]FMPEP-d_2 PET/CT imaging once in RT conditions and once during controlled cold exposure. The glucose uptake of BAT was quantified using [^{18}F]FDG PET/MR imaging of the cervicothoracic area during cold exposure. Energy expenditure was measured in RT and in cold conditions by indirect calorimetry. Tissue biopsies of the supraclavicular BAT were obtained from nine (5 lean, 4 overweight/obese) of the 18 study subjects, who had given their additional written informed consent.

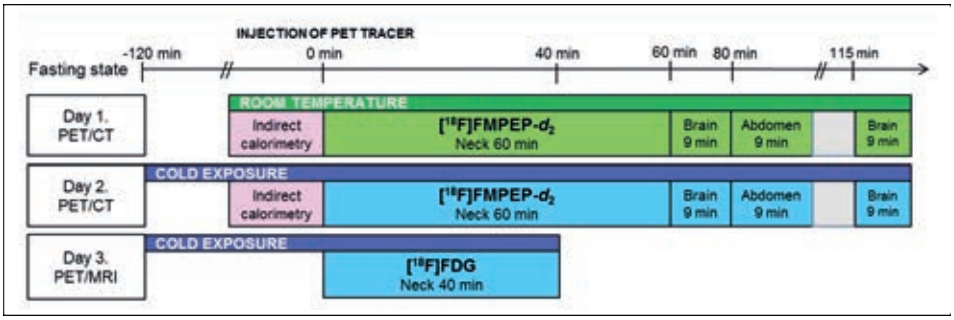

Figure 7. Clinical PET study design (III). Modified from Lahesmaa et al., 2018.

4.3 Cold Exposure (II-III)

A standardized cooling protocol was used in studies II and III. In study II, cold exposure was performed on one of the two study days. In study III, cold exposure was performed on two days, prior to the [^{18}F]FDG PET/MR scan, and also before one of the PET/CT scans with [^{18}F]FMPEP-d_2. The subject lay in the supine position between two cooling blankets (Blanketrol III, Cincinnati Sub-Zero, Cincinnati, OH, USA) with chilled flowing water for two hours prior to the PET scan. The temperature was gradually decreased from RT and adjusted individually to maintain a subjectively cold temperature but avoid muscle shivering (average temperatures: study II 16.2 ± 1.6 °C, study III 15.1 ± 2.6 °C). All subjects reported subjective cold sensation before and during the scans. Blood samples were acquired before and after cooling, and electrocardiography was monitored during the cooling protocol. Cooling was maintained by the cooling blankets during the PET/CT scans, whereas iced gel packs were placed on the legs and upper body during the PET/MR scans when needed. PET scans were performed over all seasons, as this could not be fully controlled due to the availability of PET scanners and scheduling issues. However, the cold exposure protocol was standardized for all subjects, thus the times and particularly seasonal variance between individual baselines and cold measurements were minimized.

Figure 8. A healthy subject during the cooling protocol prior to PET imaging. The temperature of the cooling blankets was decreased individually. Indirect calorimetry and ECG were recorded simultaneously. Photo by Minna Lahesmaa.

4.4 PET Imaging (I-III)

4.4.1 Production of Radioligands

PET scans were all performed at the Turku PET Centre, Finland. All radioligands in this study ([^{18}F]FDG, [^{15}O]H_2O, [^{18}F]FMPEP-d_2, and [^{11}C]TMSX) were produced in the Radiopharmaceutical Chemistry Laboratory of the Turku PET Centre as previously described (Donohue et al., 2008; Hamacher et al., 1986; Komar et al., 2012; Rissanen et al., 2013). Radiochemical purity exceeded 95% in every batch used.

4.4.2 PET Image Acquisition

Before each PET scan, two venous catheters (one for each arm) were inserted into the antecubital veins of the study subject, one catheter for the administration of PET radioligands and the other on the contralateral arm for obtaining blood samples. In study II, an arterial cannula placed in the radial artery was used for blood sampling, and in studies I and III arterialized venous blood samples were obtained. The subject was placed in a supine position in the PET scanner with primarily the cervicothoracic area in the axial field of view, including the supraclavicular BAT depots. Dynamic image acquisition was used in each study, which commenced immediately after injection of the radioligand. In addition to the cervicothoracic area, the abdomen and brain were scanned in study III.

To measure tissue perfusion in the cervical region, 900 MBq of [^{15}O]H_2O was injected intravenously and a dynamic scan was performed for 5 or 6 minutes (**I, II**). Glucose uptake measurements were performed by injecting 185 MBq of [^{18}F]FDG (**I**) or 150 MBq of [^{18}F]FDG (**III**) intravenously, followed by a 30 or 40 min dynamic scan, respectively. The CB1R density was quantified by injecting 150 MBq of [^{18}F]FMPEP-d_2 then dynamic scans of the cervicothoracic area (for 60 min), the abdomen (for 9 min) and the brain (for 9 min + 9 min) were conducted (**III**). The A2AR density was measured by injecting 500 MBq of [^{11}C]TMSX intravenously, followed by a dynamic scan of the cervicothoracic area for 60 minutes (**II**).

Study I was performed using PET or PET/CT scanners (PET GE Advance, PET/CT GE Discovery VCT, or Discovery PET/CT 690 scanner; General Electric Medical Systems), combined with anatomical reference using CT or MR imaging (Philips Gyroscan Intera CV Nova Dual 1.5 T MRI scanner). In study III, [^{18}F]FDG scans were performed using a 3T Philips Ingenuity TF PET/MR scanner (Philips Health Care), whereas studies II and III used the PET/CT GE Discovery VCT scanner (General Electric Medical Systems).

4.4.3 PET Image Analysis

Carimas software (versions 2.0 and 2.9, Turku PET Centre, Turku, Finland) were used for analyses of the PET images. Three-dimensional regions of interest (ROI) were manually drawn on the fused PET/CT or PET/MR images. BAT ROIs were drawn bilaterally on the supraclavicular adipose tissue depots, carefully avoiding blood vessels or other tissues. The ROIs of WAT were determined subcutaneously in the neck region (**I, II**) or both subcutaneously and intraperitoneally in the abdominal region (**III**). BAT and WAT ROIs included only voxels with CT

Hounsfield units (HU) within the adipose tissue range (-50 to -250 HU) (U Din et al., 2017). Study III additionally used MRI signal fat fraction maps for determining adipose tissue in the neck area. Skeletal muscle ROIs were drawn bilaterally on the trapezius or supraspinatus muscles, and in study I, ROIs were also drawn on the thyroid gland. Regional time-activity-curves (TAC) of the tissues were calculated from the dynamic images.

4.4.3.1 Modelling

Glucose uptake was quantified from [^{18}F]FDG scans (**I**, **III**), by using graphical analysis to calculate the fractional rate of tracer uptake (K_i) (Patlak and Blasberg, 1985). The input function for graphical analysis was derived from arterialized venous blood samples (**I**) or graphically from the aortic arch (**III**) (Liukko et al., 2007; Orava et al., 2011). The rate of glucose uptake (micromoles per gram per minute) was calculated by multiplying K_i by the plasma glucose concentration determined for the study subject and dividing this by the lumped constant of adipose tissue (Virtanen et al., 2001) or skeletal muscle (Peltoniemi et al., 2000). For thyroid tissue, the lumped constant value of 1 was used.

For perfusion assessment from [^{15}O]H_2O images (**I, II**), the standard 1-tissue compartment model was used, fitting K_1, k_2, and V_A. The input function was derived graphically from the aortic arch of the PET image, as previously described (U Din et al., 2016).

The density of receptors in a tissue can be quantified by calculating the distribution volume (V_T) of a radioligand, as was done in studies II and III. V_T is defined as the ratio of the concentration of the radioligand in tissue to the concentration of the radioligand in plasma of the subject, at equilibrium (Oikonen, n.d.). V_T of [^{18}F]FMPEP-d_2 images (**III**) were calculated from the supraclavicular BAT regions by applying the reversible one-tissue compartmental model, using the metabolite corrected plasma TAC as the model input. Model parameters K_1, k_2, and V_b represent the unidirectional transport of the tracer from plasma to tissue, transport back from tissue to plasma, and the vascular volume fraction in tissue, respectively. Equilibrium V_T is calculated as K_1/k_2 ratio. This method has been successfully used previously in rodents (Eriksson et al., 2015). For this analysis, the input function was formed by combining an image-derived TAC from the aortic arch (for the first 60 minutes) with the manual plasma samples from later time points. The image-derived blood curve was converted to a plasma curve using individual hematocrit values and an empirical function that describes the population-based red-blood-cell-to-plasma ratio as a function of time. The final plasma TAC was then corrected for the fraction of non-metabolized radioligand.

The [^{18}F]FMPEP-d_2 PET acquisition of the abdominal and brain areas did not start directly after radioligand injection, consequently V_T could not be calculated. Therefore, fractional uptake rate (FUR) was used to estimate and compare the CB1R density of BAT, abdominal subcutaneous WAT, intraperitoneal WAT and brain. The FUR of [^{18}F]FMPEP-d_2 was calculated for all of the analyzed tissues by dividing the tissue radioactivity concentration at X min by the $AUC_{0\text{-}X}$ of the metabolite corrected plasma curve. Values of BAT V_T correlated with BAT FUR in both RT and cold conditions (RT R=0.80, P<0.001, cold R=0.73, P=0.001), which indicates that FUR is indeed suitable for estimating the uptake of [^{18}F]FMPEP-d_2, when V_T is unavailable. FUR images of the brain were calculated with the same principles and analyzed using SPM12 software (www.fil.ion.ucl.ac.uk/spm/).

V_T for [^{11}C]TMSX (**II**) in the BAT, WAT, and muscle tissues was calculated using multiple-time graphical analysis for reversible tracer uptake, known as the Logan plot (Logan et al., 1990). Again, an image-derived TAC obtained from the aortic arch of the PET image (for the first 5 minutes) combined with manual arterial plasma samples from later time points were used to form an accurate input function. To do this, the image-derived blood curve was converted to plasma using individual hematocrit values, assuming that radioactivity concentration in the blood cells is zero. The plasma TAC was then corrected for the fraction of unchanged radioligand. The start time for the Logan plot line fit was set to 15 minutes. This analysis method was compared with the standard procedure of using only arterial blood samples as input, obtaining fully comparable results.

4.5 Indirect Calorimetry (I-III)

Energy expenditure (EE) was measured using indirect calorimetry (Deltatrac II; Datex-Ohmeda) under RT conditions (**I-III**) and during cold exposure (**II-III**). Data were collected before PET imaging, for 45–60 minutes. These collected data were cleaned when outlier measurements i.e. measurements that deviated more than 1.5 SD from the mean, vO_2, vCO_2, EE or respiratory quotient values (caused by irregular breathing) were excluded from the analyses. The first 15 min of the calorimetry data were also excluded, in order to measure the steady state. Whole-body EE, substrate utilization rates, and respiratory quotients were calculated according to the Weir equation (Weir, 1949) and the manufacturer's equations (Meriläinen, 1987) using Matlab (Version: R2011a). Protein oxidation was accounted for in the equations by assuming urinary nitrogen to be 13 g/24 h.

4.6 Biochemical Analyses (I-III)

Most biochemical analyses of blood samples were performed at the Turku University Hospital using standard assays as previously described (Orava et al., 2011; U Din et al., 2017). Plasma glucose concentration was determined by a glucose oxidase method (Analox GM9 Analyzer, Analox Instruments). Insulin, TSH, free T_4, and free T_3 plasma concentrations were measured using electrochemiluminescent immunoassay-based methods (Modular E170 automatic analyzer; Roche Diagnostics GmbH). Concentrations of serum TSH receptor antibodies were determined using the TRAK Human Radioimmunoassay method with human recombinant antigens (Multiskan EX 355 spectrophotometer; Thermo Fischer Scientific). Serum free fatty acid (FFA) and triglyceride values were measured using the enzymatic colorimetric method. The FFA were determined using the ACS-ACOD Method (Wako Chemicals GmbH, Neuss, Germany). A Cobas 8000 c502 Analyzer (Roche Diagnostics GmbH, Mannheim, Germany) was used for triglyceride analysis. Plasma concentrations of total cholesterol and high density lipoprotein (HDL) cholesterol, were measured photometrically (Modular P800, Roche Diagnostics GmbH). Concentration of low-density lipoprotein (LDL) was calculated using the Friedewald equation (Friedewald et al., 1972). Plasma noradrenaline values were measured in the laboratory of Eastern Finland (ISLAB, Kuopio, Finland) with high-performance liquid chromatography (HPLC).

4.7 Biopsy Procedures and Analysis (III)

Of the 18 study subjects recruited for study III, a total of 9 subjects additionally gave their written informed consent for acquiring BAT biopsies from the supraclavicular neck region. Biopsies of BAT were taken by a plastic surgeon through one small skin incision, using local anesthesia in sterile, operating room conditions and with an anesthesiologist monitoring the procedure. Anatomical location of BAT was pre-determined with [^{18}F]FDG PET/MR or [^{15}O]H_2O PET/CT images. After removal, samples were immediately snap-frozen into liquid nitrogen and stored at -70°C until analysis, or preserved in formalin for H&E staining. The presence of BAT or WAT in the samples was verified by a pathologist, in the Department of Pathology of the Turku University Hospital. The mRNA expression of human CB1R and CB2R, UCP1 and β3-AR in BAT were analyzed using polymerase chain reaction (PCR) methods in the University of Bonn, Germany.

4.8 Pre-clinical studies (III)

PET studies were performed on rats using the radioligands [^{18}F]FMPEP-d_2 and [^{18}F]FDG. All animal experiments were approved by the Regional State Administrative Agency for Southern Finland, and animal care complied with the principles of laboratory animal care and with guidelines of the International Council of Laboratory Animal Science. Sprague Dawley rats (n=39, male, 8–10 weeks old, 228 ± 28g) were bred at the animal facility of the University of Turku. The animals were housed at 21 ± 3°C, in an atmosphere of humidity 55 ± 15%, with a light period from 6.00 a.m. to 6.00 p.m. All animals had free access to RM1 (E) chow and tap water.

Rats were divided into three groups. Prior to PET scanning, each rat was administered 1) radioligand alone, or radioligand following 10 min intravenous pre-administration of 2) β3-AR agonist CL 316243 (2 mg/kg) or 3) CB1R antagonist rimonabant (2 mg/kg). Each rat was sedated and positioned in the PET/CT scanner with the interscapular BAT positioned in the center of the field of view.

The [^{18}F]FMPEP-d_2 PET scans were performed in 24 rats (n=8 from each treatment group). The radioligand was administered i.v. in the tail vein (9.7 ± 2.0 MBq) and a PET scan was performed for 120 min. V_T of [^{18}F]FMPEP-d_2 in BAT in each rat was calculated in the PMOD kinetic modeling module (PKIN, PMOD technologies, Zurich, Switzerland) using the one-tissue compartment model as previously described (Eriksson et al., 2015). The [^{18}F]FDG PET scans were performed in another group of rats (15 rats, n=5 from each treatment group). [^{18}F]FDG was administered i.v. via the tail vein (20.1 ± 1.6 MBq) and a PET scan was performed over 60 min. The glucose utilization in BAT was estimated by fitting the PET data to a [^{18}F]FDG two-tissue compartment model, using a lumped constant of 1.3.

Ex vivo organ distribution measurements were done after PET imaging. Each animal was sacrificed (120 min post [^{18}F]FMPEP-d_2 injection (n=24) or 60 min post [^{18}F]FDG injection (n=15)). Tissues were excised and measured in an automatic γ-counter (Wizard^2, PerkinElmer, Finland). Measured radioactivity was corrected for decay, weight of the organ, and background, and it was expressed as percentage of the injected dose/gram of tissue (%ID/g).

Additionally, *in vitro* cell experiments were performed using PCR methods in the University of Bonn, Germany. Human multipotent adipose-derived stem cells (hMADS) and human white adipocytes were differentiated as previously described (Rodriguez et al., 2005). mRNA expression of CB1Rs and CB2Rs cannabinoid

were measured in brown and white adipocytes with and without noradrenaline stimulation (incubation with 1 μM noradrenaline for 16 h). Further pharmacological experiments were also performed in brown adipocytes. Glucose uptake and glycerol release were measured after treatment with CB1R antagonist, CB1R agonist, CB2R antagonist or CB2R agonist. Cells were treated with 100 nM of each antagonist/inverse agonist (CB1R: SR141716A; CB2R: SR144528), each agonist (CB1R: ACEA; CB2R: JWH133), and/or 1 μM of noradrenaline. The glucose uptake assays (Abcam #136955) and lipolysis assays (Sigma-Aldrich) were then performed according to the manufacturer's instructions.

4.9 Statistical Analyses

The statistical analyses were performed using SAS software (version 9.2, SAS Institute Inc.) (**I**), JMP Pro 12.1 software (**II**), and IBM SPSS software (version 23.0) (**III**). All data are presented as means ± SD. T-tests were used to test the significance of differences between data of two different study groups (The Student's t-test for unpaired) or to compare changes within study subjects (The paired t-test). Natural logarithmic transformations were applied for data that were not normally distributed. Correlations were analyzed using the Pearson correlation test or the Spearman correlation test when applicable. P-values of <0.05 were considered significant.

5 RESULTS

5.1 Effect of Excess Thyroid Hormones on BAT, Skeletal Muscle and Whole-Body Metabolism (I)

The 10 hyperthyroid patients had a 3-fold glucose uptake (GU) in BAT, compared to healthy control subjects (2.7 ± 2.3 vs. 0.9 ± 0.1 μmol/100g/min, P=0.0013). However, perfusion of BAT was similar in both groups. The GU of BAT increased during hyperthyroidism, whereas the GU of WAT did not change. Plasma levels of thyroid hormones correlated with BAT GU (free T_4 R=0.53, P=0.03; free T_3 R=0.62, P=0.006; TSH R= -0.76, P<0.001). Five of the patients were followed-up after treatment of hyperthyroidism, and BAT GU was restored and decreased to similar levels to those of the control subjects in four of these five patients (2.1 ± 0.7 vs. 0.9 ± 0.3 μmol/100g/min, P=0.014, n=4).

Hyperthyroidism also increased GU of the skeletal muscle, but to a lesser extent. GU was 88% higher in hyperthyroid patients, compared to healthy controls (1.9 ± 0.6 vs. 1.0 ± 0.3 μmol/100g/min, P=0.0019). After treatment of the condition and the restoration of euthyroidism the same four individuals that had restored BAT GU, also had decreased GU of the skeletal muscles (2.3 ± 0.7 vs. 0.9 ± 0.2 μmol/100g/min, P=0.026, n=4). Thyroid hormone concentrations correlated positively with GU of skeletal muscle, whereas TSH correlated negatively (free T_4 R=0.64, P=0.010; free T_3 R=0.81, P<0.001; TSH R= -0.80, P<0.001).

Perfusion of skeletal muscle in the hyperthyroid state was twice as high compared to healthy controls (9.2 ± 5.3 vs. 4.4 ± 3.3 ml/100g/min, P=0.040), and again perfusion decreased back to a similar level as those of controls after restoration of euthyroidism (hyperthyroid 12.3 ± 5.5 vs. euthyroid 6.8 ± 2.6 ml/100g/min, P=0.057, n=4). Due to the large blood volume of the thyroid gland, the one-compartment model was not accurate enough to calculate and quantify thyroid gland perfusion, but qualitatively thyroid perfusion was distinctly increased.

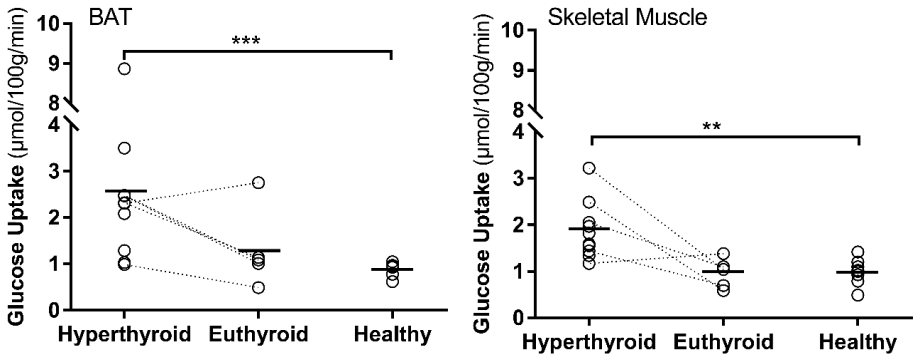

Figure 9. Glucose uptake of BAT and skeletal muscle in hyperthyroid patients, patients after treatment in the euthyroid state, and in healthy controls. ***P=0.0013, **P=0.0019. Modified from Lahesmaa et al., 2014 (I).

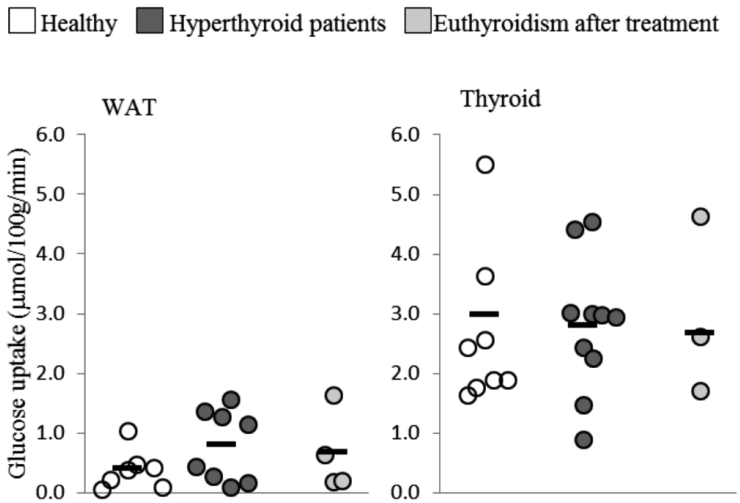

Figure 10. Glucose uptake from the WAT and the thyroid gland in healthy controls, hyperthyroid patients and in the patients after treatment in euthyroid state. Modified from Lahesmaa et al., 2014 (I).

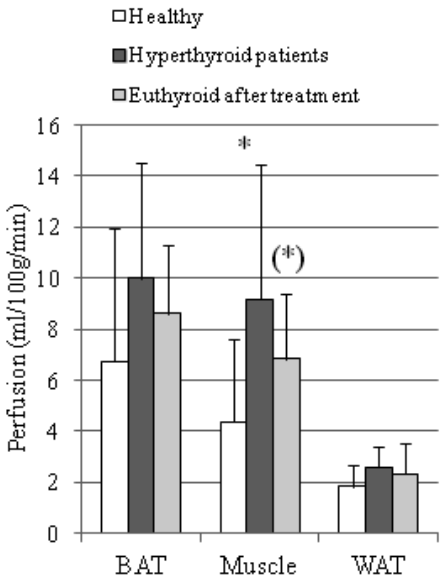

Figure 11. Perfusion of BAT, skeletal muscle and WAT in healthy controls, hyperthyroid patients and in the patients after treatment in the euthyroid state. Error bars are standard deviations. *P<0.05, hyperthyroid vs. healthy subjects; (*)P=0.057, pretreatment vs. posttreatment, n=4. Modified from Lahesmaa et al., 2014 (I).

Hyperthyroidism induced a significant increase in energy expenditure (8.2 ± 1.5 vs. 5.6 ± 0.7 MJ/24 h, P=0.005). The utilization of lipids as an energy substrate was significantly higher in hyperthyroid patients compared to healthy controls (5.0 ± 1.5 vs. 2.9 ± 0.8 MJ/24 h, P=0.001), and after restoration of euthyroidism it decreased on average by 1.7 MJ/24 h (P<0.001, n=5). Furthermore, plasma levels of free T_4, free T_3 and TSH correlated significantly with both EE and the utilization of lipids. There was no significant difference in use of carbohydrates between groups. After the restoration of euthyroidism, BMI increased in the patients who were followed-up (22.5 ± 2.4 vs. 24.0 ± 2.7, P<0.001, n=5).

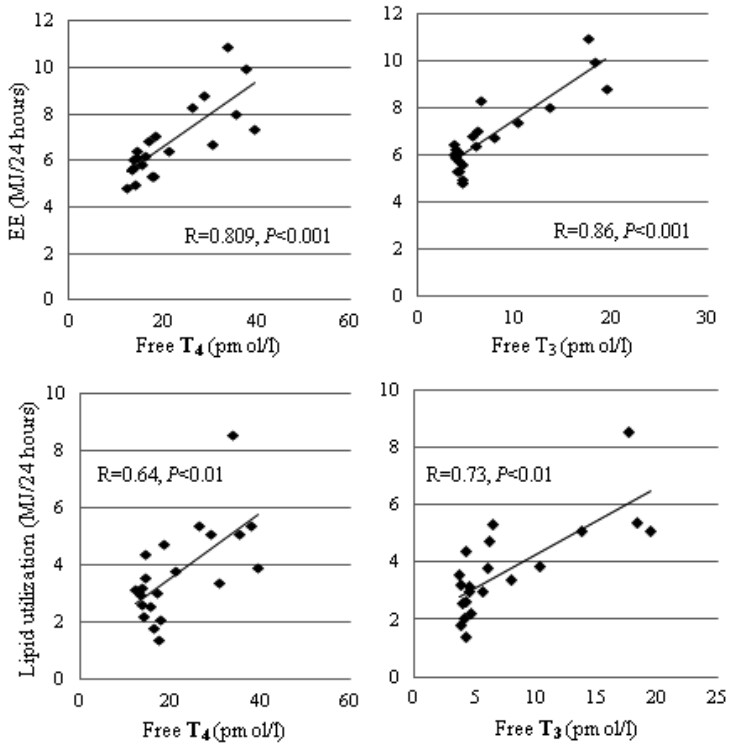

Figure 12. Correlations between thyroid hormones (T_4 = thyroxine, T_3 = triiodothyronine) and energy expenditure (EE) or lipid utilization. Modified from Lahesmaa et al., 2014 (I).

5.2 Perfusion of BAT, WAT and Skeletal Muscle during cold and adenosine stimulation (II)

Cold exposure in healthy lean men increased BAT perfusion 2.4-fold compared to baseline conditions (basal 8.3 ± 4.5 vs. cold 19.6 ± 9.3 ml/100g/min, P=0.006). Adenosine caused a maximal perfusion effect in BAT, which was even higher than during cold exposure (cold 19.6 ± 9.3 vs. adenosine 28.6 ± 7.9 ml/100g/min, P=0.003). No significant changes in perfusion were observed in WAT or in skeletal muscle during cold exposure. However, adenosine also increased perfusion in skeletal muscle (2.2 ± 1.1 vs. 19.4 ± 21.9, P=0.040) and WAT (2.1 ± 0.8 vs. 10.6 ± 7.4, P=0.004). During adenosine stimulation, perfusion of BAT was 2.7-fold compared to WAT.

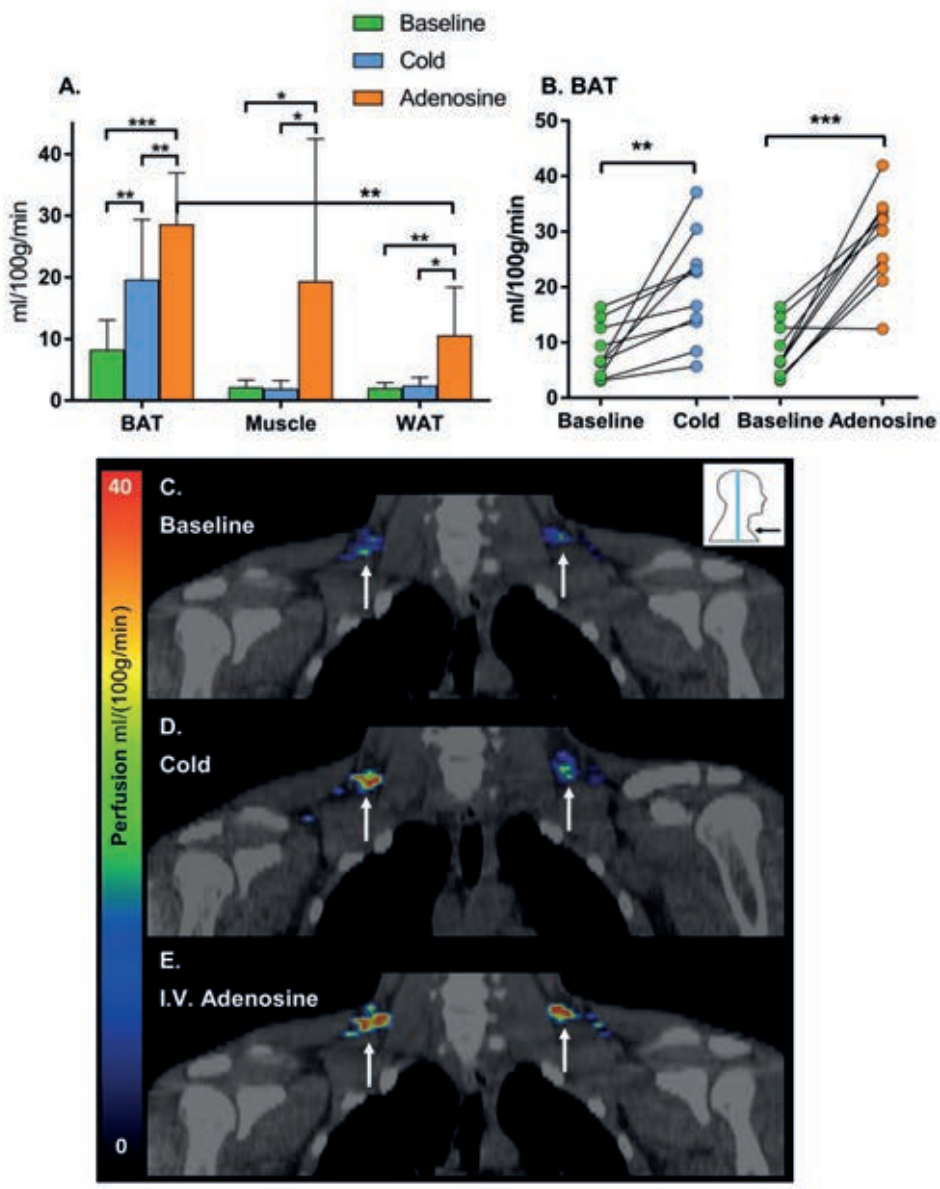

Figure 13. A. Perfusion of BAT, skeletal muscle and WAT (n=10) at baseline, during cold exposure and during i.v. adenosine administration. B. Perfusion in BAT, depicting individual change from baseline to cold, and from baseline to adenosine stimulation. Error bars are standard deviations. *P<0.05, **P<0.01 and ***P<0.001. C.–E. Coronal [^{15}O]H_2O-PET/CT images of BAT from one study subject in all three study conditions, arrows depict supraclavicular BAT. Modified from Lahesmaa et al., 2018 (II).

5.3 Adenosine A_{2A} Receptors in Human BAT (II)

To study the role of adenosine A_{2A} receptors in human BAT, volume distribution (V_T) of the radioligand [^{11}C]TMSX was calculated, to estimate the A2AR density of the tissue. V_T of [^{11}C]TMSX was significantly lower in BAT during cold exposure compared to baseline conditions (cold 0.90 ± 0.10 vs. baseline 1.24 ± 0.21, P=0.006). This indicates that the A2AR sites are predominantly occupied by endogenous ligand, hence fewer are available for radioligand binding during cold exposure. No significant changes in A2AR density were observed in WAT or skeletal muscle. Plasma noradrenaline values increased simultaneously with decreased A2AR radioligand binding in BAT.

Compared to RT conditions, cold exposure markedly increased plasma noradrenaline levels (2.06 ± 0.65 vs. 5.06 ± 1.42, P<0.0001). Similarly, during cold exposure plasma levels of FFAs and triglycerides as well as EE and utilization of lipids as an energy substrate increased. BAT perfusion was doubled concurrently with the increases in EE, consumption of lipids and plasma FFA levels, while [^{11}C]TMSX binding in BAT was simultaneously decreased.

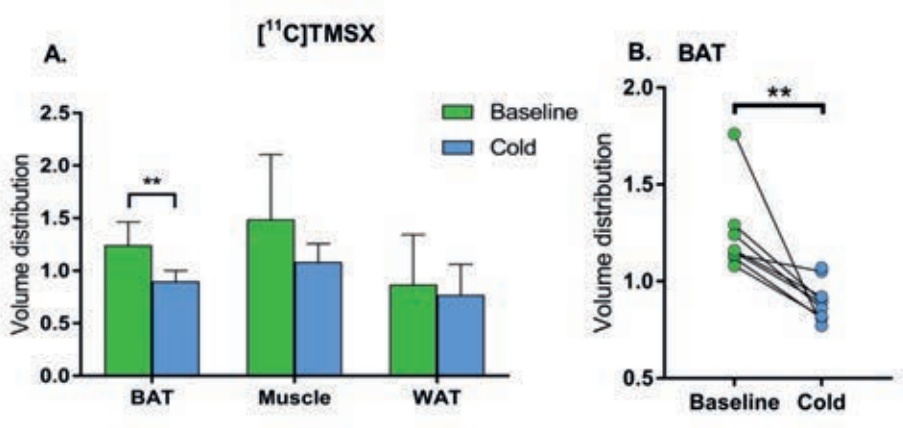

Figure 14. A. [^{11}C]TMSX volume distribution of BAT, skeletal muscle and WAT (n = 8) at baseline and during cold exposure. B. [^{11}C]TMSX volume distribution in BAT, depicting the individual change from baseline to cold. Error bars are standard deviations. **P < 0.01. Modified from Lahesmaa et al., 2018 (II).

5.4 Cannabinoid Type 1 Receptors in BAT during Acute Adrenergic Stimulus (III)

CB1 receptor density was quantified in human BAT and other tissues using the PET radioligand [^{18}F]FMPEP-d_2. Acute cold exposure in lean healthy men increased the fractional uptake rate (FUR) of the radioligand in BAT 3-fold, compared to baseline conditions. This indicates an increase in CB1R density in the tissue. CB1R density in overweight subjects at baseline was low, and the increase during cold exposure was markedly blunted, merely reaching the baseline levels of lean subjects. Furthermore, the uptake of [^{18}F]FMPEP-d_2 in BAT correlated strongly with the glucose uptake in cold (R=0.89, P<0.001).

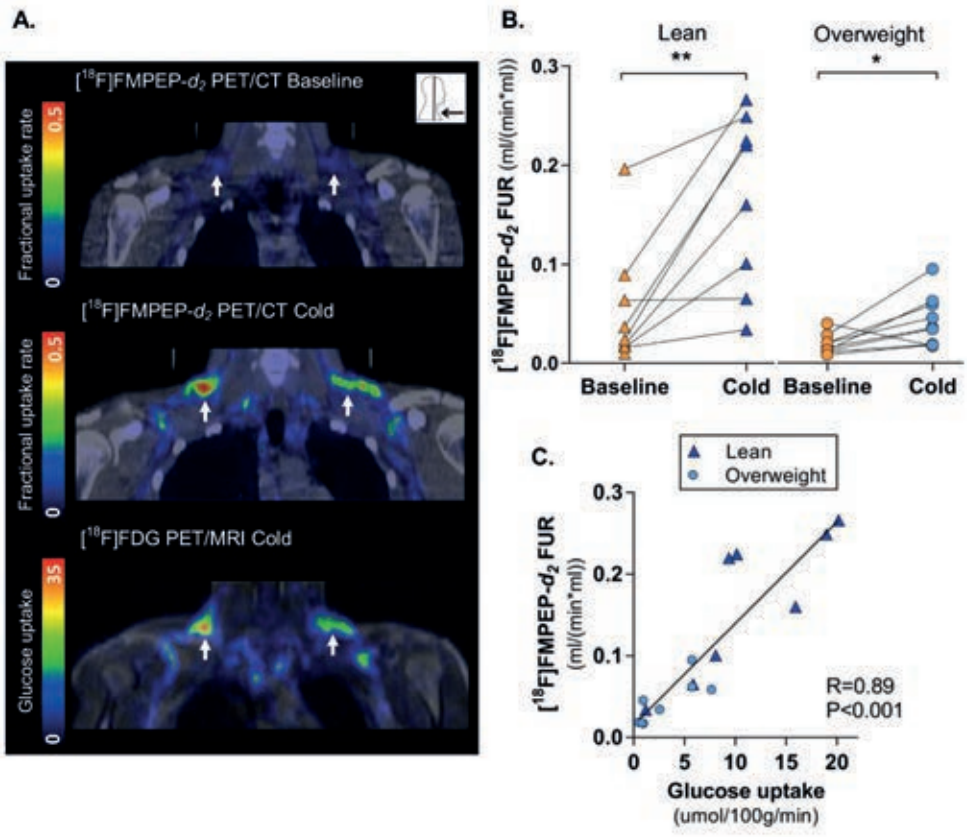

Figure 15. A. Coronal PET images of one lean study subject in all three PET scans, arrows depict supraclavicular BAT. B. Quantified uptake of [^{18}F]FMPEP-d_2 in BAT. C. BAT glucose uptake correlated with BAT [^{18}F]FMPEP-d_2 FUR in cold conditions. *P<0.05 and **P<0.01. Modified from Lahesmaa et al., 2018 (III).

Similarly, [^{18}F]FMPEP-d_2 uptake in rodents increased significantly in the interscapular BAT following an acute adrenergic stimulus, intravenous administration of β3-AR agonist. Similar to cold exposure in humans, β3-AR agonism increased glucose uptake in rodent BAT, which confirmed the *in vivo* activation of BAT. Pre-administration of the CB1R antagonist rimonabant to the rodents inhibited the [^{18}F]FMPEP-d_2 uptake in BAT and brain at basal conditions ($P<0.0001$), which indicated that the change in uptake was receptor mediated rather than non-specific.

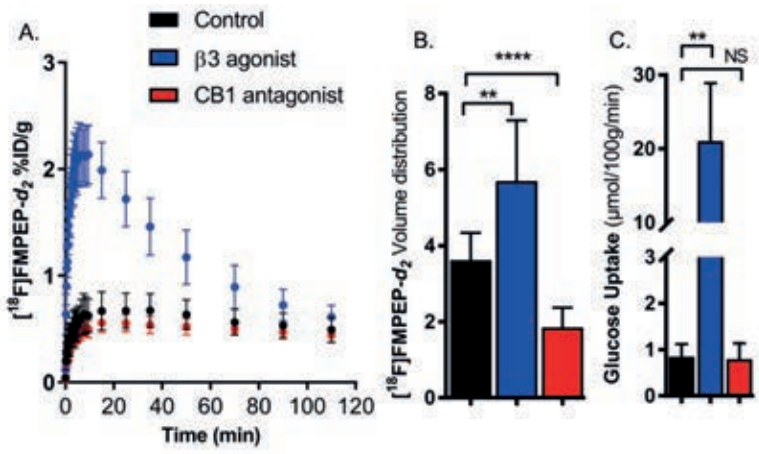

Figure 16. A. Uptake and B. volume distribution of [^{18}F]FMPEP-d_2 in rats and C. glucose uptake in rats, measured at baseline (black), with β3-agonism (blue) and CB1R-antagonism (red). Error bars are standard deviations. **P< 0.01 and ****P< 0.0001, NS=non-significant. Modified from Lahesmaa et al., 2018 (III).

Image-guided BAT biopsies were obtained from 9 out of the 18 study subjects (5 lean, 4 overweight/obese subjects) in RT conditions. CB1R mRNA expression was confirmed from these human samples, and mRNA expression of CB1R was significantly higher than the mRNA expression of CB2Rs. After pooling the biopsy data obtained from lean and overweight subjects, mRNA expression of UCP1 had a positive correlation with BAT [^{18}F]FMPEP-d_2 uptake ($R=0.73$, $P=0.027$).

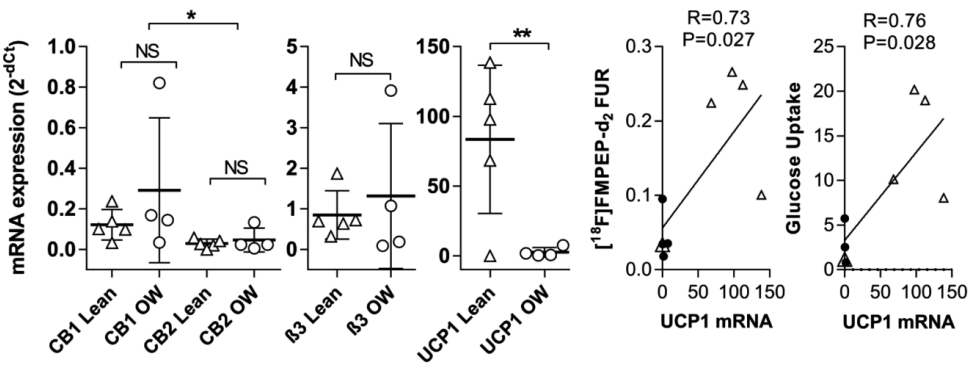

Figure 17. mRNA expression of cannabinoid receptors (CB1, CB2), β3-ARs and UCP1 in human supraclavicular BAT samples. Correlations between PET imaging data and UCP1 mRNA expression. Error bars represent standard deviations. *P<0.05 and **P<0.01. Modified from Lahesmaa et al., 2018 (III).

The CB1Rs were also studied *in vitro* in a human brown adipocyte cell line (hMADS) and primary human white adipocytes. CB1R mRNA expression was significantly higher in brown than in white adipocytes. Treatment with noradrenaline significantly increased CB1R mRNA expression in brown adipocytes but decreased the expression in white adipocytes. No changes were observed in CB2R mRNA expression during noradrenaline stimulation.

The function of human brown adipocytes *in vitro* was further studied during cannabinoid receptor agonism and antagonism. Blockade of CB1R (with rimonabant) increased glucose uptake and glycerol release of brown adipocytes. Activation of brown adipocytes with noradrenaline increased glucose uptake, and CB1R antagonism further enhanced this increase. However, CB1R stimulation, CB2R stimulation and CB2R blockade had no significant effect on glucose uptake or on lipolysis.

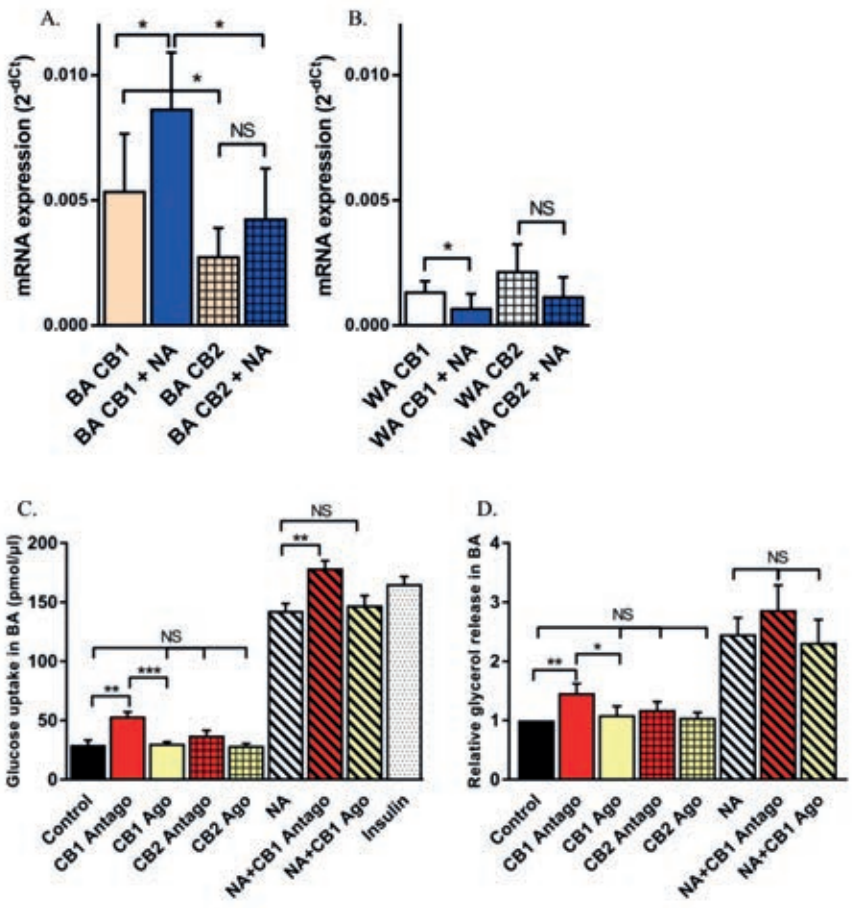

Figure 18. mRNA expression of type 1 (CB1) and type 2 (CB2) cannabinoid receptors in A. human brown adipocytes (BA) and B. white adipocytes (WA), with and without noradrenaline (NA) stimulation. C. Glucose uptake and D. glycerol release in rodent BA with pharmacological stimuli. Antagonist (Antago), agonist (Ago). Error bars indicate standard deviations. *P<0.05; **P<0.01 and ***P<0.001. Modified from Lahesmaa et al., 2018 (III).

5.5 Effect of Overweight on the CB1R Density of Tissues (III)

The CB1Rs were also quantified in other tissues of lean and overweight/obese men. The CB1R density of the brain under baseline conditions was 23% lower in the overweight subjects than in their lean counterparts. Cold exposure caused changes in the CB1R density of both lean and overweight subjects. In the pooled group of lean and overweight subjects, the CB1R density increased, (P=0.033) specifically in the anatomical areas of the midbrain, pons and parietal lobe. Furthermore, a positive correlation was found between [^{18}F]FMPEP-d_2 uptake in BAT and brain gray matter, in cold conditions (P<0.0005) but not at baseline. In addition to the changes in the brain, uptake of [^{18}F]FMPEP-d_2 was significantly lower in the subcutaneous and intraperitoneal WAT of overweight subjects, compared to lean subjects. However, uptake in skeletal muscle was similar in both groups. [^{18}F]FMPEP-d_2 uptake in BAT correlated negatively with BMI.

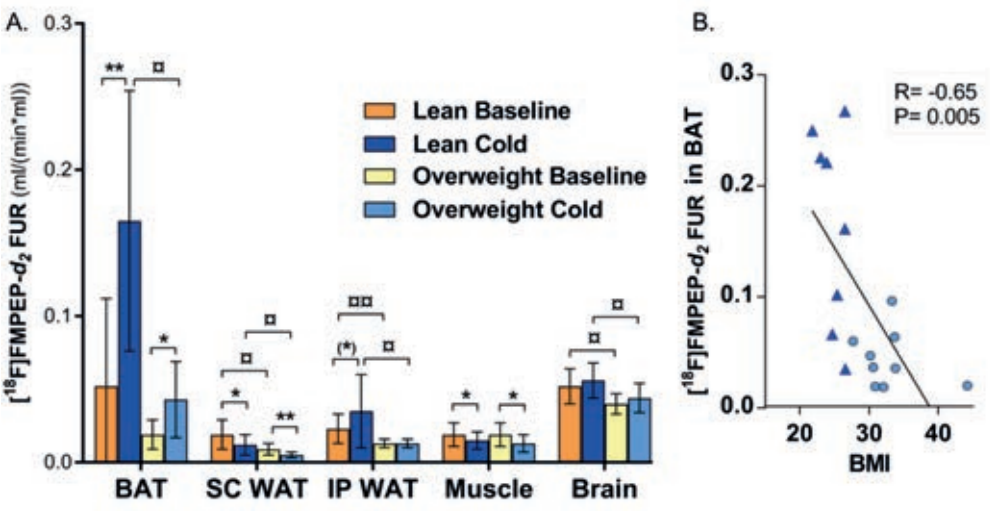

Figure 19. A. [^{18}F]FMPEP-d_2 uptake at baseline conditions and during cold exposure of lean and overweight subjects in brown adipose tissue (BAT), subcutaneous white adipose tissue (SC WAT), intraperitoneal white adipose tissue (IP WAT), skeletal muscle and brain gray matter. Error bars are standard deviations. *Paired t-test comparing the baseline and cold conditions, *P<0.050, **P<0.010, (*)P=0.070. ¤Independent t-test comparing the lean and overweight groups, ¤P<0.05, ¤¤P<0.01. B. Pearson's correlation between BMI and BAT [^{18}F]FMPEP-d_2 uptake in cold of lean (triangle) and overweight (circle) subjects.

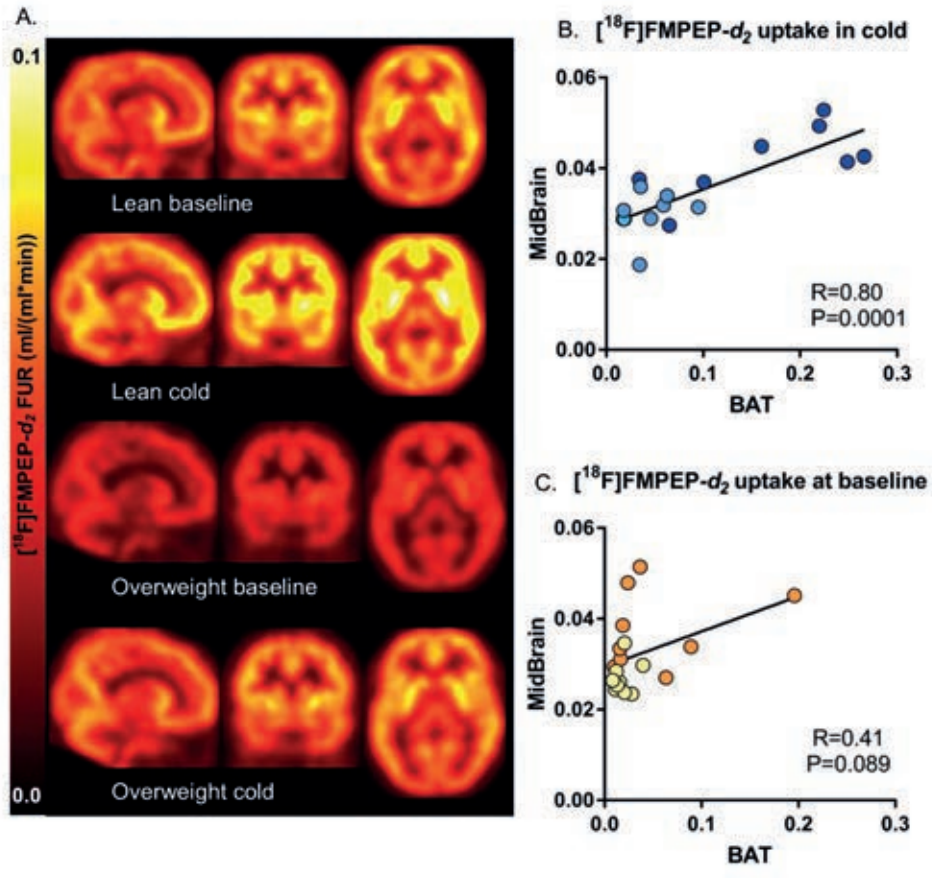

Figure 20. A. PET brain images of fractional uptake rate (FUR) of [^{18}F]FMPEP-d_2 in one lean and one obese subject at baseline and cold conditions. B-C. Pearson's correlation between [^{18}F]FMPEP-d_2 FUR values of BAT and the midbrain region of interest in cold and baseline conditions, pooled lean and overweight subjects. Dark blue=lean cold, light blue=overweight cold, orange=lean baseline, yellow=overweight baseline. Modified from Lahesmaa et al., 2018 (III).

6 DISCUSSION

Since the re-discovery of metabolically active BAT in humans, research has been aiming to understand the regulatory mechanisms of this tissue. There are many factors which fine-tune the metabolic response of BAT, which are still unexplored. Numerous studies have been published using rodent models that provide very important insight into BAT physiology and regulation. It is, however, also necessary to obtain data from humans, in order to translate novel findings into potential treatments that will improve human health and metabolism. The work in this thesis focused on studying the regulation of BAT in human cohorts, specifically investigating three endogenous regulatory factors, namely the thyroid hormones, the adenosinergic system, and the endocannabinoids.

6.1 Thyroid hormones

Thyroid hormones in humans seem to have direct metabolic effects on BAT. Glucose uptake in BAT of hyperthyroid patients was 3-fold compared to healthy controls (study **I**). After treatment of the disease, BAT glucose uptake of the patients in the euthyroid state declined back to a level comparable to those found in the healthy control subjects. Although the number of study subjects (N=18) is small, these results confirm earlier findings that BAT function is adaptable and sensitive to endogenous hormonal changes in the body.

The level of glucose uptake during hyperthyroidism in room temperature conditions was not as high as during cold exposure in healthy subjects, which can be up to 10–15 fold higher (study **III**, Orava et al., 2011; Virtanen et al., 2009). However, with the use of dynamic, quantitative [^{18}F]FDG imaging even small changes in glucose utilization can be detected. It was not possible in this study to investigate the combined effect of cold and hyperthyroidism, due to ethical reasons. A few recent studies have investigated this in cancer patients, both reporting higher [^{18}F]FDG uptake in BAT during cold exposure during thyrotoxicosis compared with cold exposure during hypothyroidism (Broeders et al., 2016; Gavrila et al., 2017). However, those studies used semi-quantitative SUV measures, and the subjects were a group of cancer patients who had undergone thyroidectomy and thyroid hormone treatment. Another human study used semi-quantitative [^{18}F]FDG imaging to study hyperthyroid subjects before and after treatment, but they obtained contradictory findings (Zhang et al., 2014). They also reported higher [^{18}F]FDG SUV in skeletal muscle during hyperthyroidism, but no accumulation in BAT. After treatment of hyperthyroidism, the muscle radioactivity of subjects decreased, and that of adipose tissue increased. (Zhang et

al., 2014) These variable results obtained from different human studies support the notion that quantitative PET imaging is necessary for the appropriate interpretation of [^{18}F]FDG data. The increased metabolism and activation of skeletal muscle in hyperthyroid patients can change the biodistribution of [^{18}F]FDG in the body, thus affecting the results. Therefore, when only relative SUV values are reported, misinterpretation of BAT physiology can occur.

Hyperthyroidism also induced a significant, 45% increase in energy expenditure, which doubled the use of lipids as an energy substrate. A similar magnitude of increase in EE in response to thyrotoxicosis was reported previously in human and rodent studies (Klieverik et al., 2009; Møller et al., 1996). Higher EE is expected, since the classic symptoms of hyperthyroidism include weight loss, tremor, and sweating. Hyperthyroidism also increased glucose uptake and perfusion of skeletal muscle. It seems therefore, that BAT activation and increased muscle metabolism are involved in hyperthyroidism. Interestingly, BAT glucose uptake increased independently of changes in BAT perfusion. Several previous studies have shown that thyroid vascularity and blood flow is increased in patients with hyperthyroidism, and this can be evaluated by Doppler ultrasound techniques (Bogazzi et al., 1999; Caruso et al., 2000; Fobbe et al., 1989). Indeed, visual assessment of the PET images distinctly showed high thyroid perfusion. Unfortunately, the rate of thyroid perfusion could not be accurately quantified in this study due to the large blood volume of the tissue, which disturbed the modeling of PET kinetics.

The mechanisms and synergy between thyroid hormones and BAT thermogenesis have been investigated in a multitude of studies that used rodent and cellular models. Thyroid hormones activate BAT and muscle metabolism, at least in part, by the direct stimulation of BAT UCP1 and muscle UCP3 gene transcription that is mediated through thyroid response elements located in their gene promoters (Rabelo et al., 1995; Solanes et al., 2005). Thyroxine also increases the expression of UCP1 and genes related to fatty acid oxidation and oxygen consumption in human multipotent adipose-derived stem cells (Lee et al., 2012). High thyroxine concentrations may modulate energy utilization in classic brown adipocytes and also in the beige cells (Wu et al., 2012), which are present in human BAT depots. The physiological link between BAT and thyroid hormones is regulated by the SNS. In rats, both systemic hyperthyroidism and central administration of T_3 is associated with a SNS-mediated activation of BAT (López et al., 2010). Additionally, both peripherally induced hyperthyroidism and central T_3 administration into the ventromedial hypothalamus of rats cause browning of WAT (Martínez-Sánchez et al., 2017). Sympathetic activation increases transcription of proteins critical for BAT thermogenesis, such as PGC-1α and D2 (Puigserver et al., 1998). Furthermore, thyroid hormones enhance the level of

proteins involved in the β-adrenergic pathway, thus amplifying intracellular signals of adrenergic stimulation (Silva and Bianco, 2008).

Hence, there is a growing body of evidence, which shows that BAT can be activated in direct response to thyroid hormones. During hyperthyroidism, the activation of BAT and skeletal muscle by excessive thyroid hormone secretion and synergistic SNS activation may partly explain the increased energy expenditure and higher use of lipids as an energy substrate. Potentially, thyroid hormone-based treatments could be developed in the future to activate BAT thermogenesis and increase energy expenditure. However, since thyroid hormones have multiple systemic effects on many organs, and since changes in systemic thyroid hormone levels can cause various and sometimes severe symptoms in humans, possible treatments would have to be BAT-specific and safe for therapeutic use. (Cannon and Nedergaard, 2010)

6.2 Adenosine system

Rodent and cell studies have shown that adenosine is a potent activator of BAT physiology, but this has not previously been investigated in humans. Adenosine administration to healthy study subjects stimulated BAT and caused a maximal perfusion effect in the tissue (study **II**). Adenosine also caused increased perfusion in skeletal muscle and WAT, but BAT perfusion was significantly higher compared to WAT perfusion. BAT is a densely vascularized tissue, and adenosine can bind to A2AR on the vascular smooth muscle cells, which results in relaxation and vasodilation (Sousa and Diniz, 2017), and this may partly explain the increased blood flow. Nevertheless, BAT perfusion is linearly associated with the metabolic rate of oxygen and the energy expenditure of the tissue (Muzik et al., 2013; Orava et al., 2011; U Din et al., 2016). Adenosine also enhances lipolysis and increases the expression of thermogenic markers in BAT (Gnad et al., 2014). Pre-clinical studies have shown that agonism and blockade of the A2AR increases and decreases oxygen consumption, respectively (Gnad et al., 2014). Therefore, the increased perfusion observed in this human cohort is likely a combination of vasodilation and BAT activation.

Rodent studies have shown that the adenosine A2AR are key in mediating the effects of adenosine in BAT. This thesis work measured A2AR density in human BAT for the first time, using the PET radioligand [^{11}C]TMSX, which binds specifically to A2AR with a very high affinity. Distribution volume (V_T) of the radioligand represents the density of A2AR available for radioligand binding in tissue (Leung, 2004; Naganawa et al., 2014). Interestingly, it was found that when BAT is physiologically activated during acute cold exposure, V_T of [^{11}C]TMSX

decreased, indicating fewer receptors available for binding (study **II**). These changes in receptor density were observed only in BAT, not in skeletal muscle or WAT.

It is known that during cold exposure the SNS is activated, and noradrenaline and its co-transmitter ATP are released at the efferent nerve endings in BAT. ATP is quickly degraded into adenosine, *inter alia*, which exerts its effects on BAT locally. (Abbracchio et al., 2009) This locally increased concentration of adenosine during SNS stimulation has previously been measured in the BAT of rodents (Gnad et al., 2014). In line with this, decreased binding of [^{11}C]TMSX in BAT was observed in human subjects, which signifies higher binding of endogenous adenosine that competes for the same receptors as the radioligand. Unfortunately adenosine could not be directly measured from blood samples in this study, because adenosine exerts its functions locally at a tissue level and is rapidly broken down to inosine (Chen et al., 2013; Zimmermann et al., 2012). There are, however, previous data that show increases in adenosine concentrations in BAT concomitant with increases in noradrenaline and ATP (Gnad et al., 2014). Systemic noradrenaline was therefore used in this study as an indirect measure of adenosine release. Increased noradrenaline levels were observed concurrently with lower [^{11}C]TMSX binding in BAT, signifying that the release of endogenous adenosine hindered the radioligand binding during cold exposure. Similar physiological changes in V_T of [^{11}C]TMSX have been reported in the skeletal muscle of mice, in which higher endogenous adenosine release during exercise caused a decrease in radioligand binding (Ishiwata et al., 2004). Exposure to the receptor agonist can also cause desensitization, internalization or downregulation of the A2AR (Mundell and Kelly, 2011), which may alternatively explain the observed lower V_T. Therefore, the specific molecular mechanisms should be studied further.

The findings of this study highlight that adenosine and A2AR are implicated in cold-induced BAT activation in humans. Targeting the adenosine A_{2A} receptors in BAT could provide another potential way to increase BAT function and improve metabolism.

6.3 BAT perfusion

There has recently been some speculation about whether glucose uptake and perfusion are optimal measures for BAT thermogenesis (Blondin and Carpentier, 2016). A recent study using [^{11}C]acetate as an index of perfusion showed that perfusion in BAT may be increased without higher oxidative metabolism of the tissue (Blondin et al., 2017a). Cold exposure of lean healthy men has been shown to increase BAT perfusion, glucose uptake and thermogenesis (Orava et al., 2011;

U Din et al., 2016; Virtanen et al., 2009), but in overweight individuals with or without type 2 diabetes, cold-stimulated BAT perfusion and glucose uptake were impaired (Orava et al., 2013), whereas oxidative metabolism as measured by [^{11}C]acetate was not (Blondin et al., 2015b). This apparent paradox could suggest that BAT glucose uptake, perfusion and thermogenesis may sometimes be dissociated. One study in mice with high-resolution laser-Doppler imaging showed an increase in BAT blood flow during noradrenaline stimulation or a glucose injection, in mice without UCP1. The authors concluded that BAT blood flow may increase without actual thermogenesis, and yet, enhanced thermogenesis cannot occur without increased blood flow (Abreu-Vieira et al., 2015). Intravenous and oral glucose administration in humans also causes increased perfusion in other organs, such as the pancreas and the small intestine (Koffert et al., 2017). Furthermore, eating a mixed meal, i.e. increasing circulating glucose and insulin levels, increases perfusion and oxygen consumption in the BAT of healthy subjects (U Din et al., 2018). Nevertheless, human studies with [^{15}O]-labeled water and oxygen have shown that BAT perfusion correlates positively with BAT tissue-specific energy expenditure under both room temperature and cold conditions (U Din et al., 2016), and the metabolic rate of oxygen correlates strongly with tissue perfusion, which indicates that perfusion is a major determinant of oxidative metabolism in BAT (Muzik et al., 2012).

It is noteworthy that different modalities of measuring perfusion (e.g. [^{11}C]acetate and [^{15}O]H_2O PET imaging) may lead to discrepant interpretations of results, as every PET radioligand has its own strengths and limitations. Similarly, measuring glucose uptake by PET imaging provides only one measure of BAT metabolism, thus neglecting possible fatty acid or cholesterol uptake, which may be more important for BAT function. It is important to understand the properties and kinetics of the radioligand used, as well as the limitations. Future studies in humans that combine different PET radioligands will be valuable for the understanding of the different phenomena in BAT physiology and regulation.

Interestingly, insulin stimulation with euglycemic-hyperinsulinemic clamp in lean individuals, caused increased BAT glucose extraction, whereas perfusion did not increase (Orava et al., 2011). Similarly, BAT glucose uptake in hyperthyroid patients was elevated, without increasing perfusion (study **I**). It may be that an increase of perfusion in tissues is a rapid physiological response, and perfusion may change acutely in accordance to different stimuli (e.g. glucose load, cold exposure, adrenergic stimulus). It is unclear how long the perfusion remains increased. Perhaps prolonged high perfusion in chronic conditions, such as hyperthyroidism, could be physiologically harmful, and therefore perfusion levels decrease to a stable level with time. Furthermore, an increased perfusion in BAT may be significant for providing nutrients and oxygen to the cells, for distributing

produced heat from BAT to other areas of the body, and also possibly for currently unknown purposes such as humoral or hormonal messaging between BAT and other organs.

6.4 Endocannabinoid system

The endocannabinoid system seems to play a role in regulating human BAT function. Acute adrenergic stimulation of BAT by cold exposure in humans or β3-AR stimulus in rats caused a physiological increase in CB1R density in BAT (study **III**). This was confirmed *in vitro* in brown adipocytes, where noradrenaline administration increased the expression of CB1R mRNA (study **III**). Similar results have been found previously in a study with mice, which showed that the stimulation of BAT by cold and β3-AR agonism increased endocannabinoid levels in BAT (Krott et al., 2016). That same study also reported that the activation of primary brown adipocytes induced transcription of *Cnr1*, the gene that encodes CB1R. In a recent human study, mild cold exposure was shown to increase plasma endocannabinoid levels in healthy lean men (Kantae et al., 2017).

CB1R agonism promotes a positive energy balance (Mazier et al., 2015). The up-regulation seen in this study during cold exposure and BAT activation may be a negative feedback response of the ECS, where endocannabinoids, their enzymes and receptors are up-regulated as a potential auto-regulatory loop to inhibit thermogenesis (Krott et al., 2016). An acute cold stress may stimulate the ECS to provide more CB1Rs for endocannabinoid binding in BAT, in order to limit excess energy expenditure and return homeostasis towards a positive energy balance, thus restoring homeostasis in the body. The response is likely mediated via the central nervous system.

During cold exposure, CB1Rs were also upregulated in the brain areas that are closely related to the sympathetic control of BAT function, namely the midbrain, pons and parietal lobe. Additionally, CB1R density in BAT correlated positively with CB1R density in the midbrain during cold exposure, but not under warm conditions (study **III**). These results indicate a relationship between the ECS, SNS and BAT function. Endocannabinoids are produced on demand and act primarily in the brain, however**,** they also exert important regulatory effects on metabolism in adipose tissue (Cani et al., 2016). The region of the midbrain includes the hypothalamus, which is one key site for controlling homeostasis and energy expenditure, and where endocannabinoids play a major regulatory role (Silvestri and Di Marzo, 2013). The parietal lobe receives and processes sensory input, including temperature, whereas the pons is a significant signaling route that *inter alia* controls autonomic functions (Jacobson and Marcus, 2008). Ambient

temperature is sensed in peripheral tissues and information is received and processed in these areas of the central nervous system, after which efferent sympathetic outflow is enhanced in the form of increased noradrenaline secretion to the BAT, which results in increased thermogenesis (Cannon and Nedergaard, 2004). Endocannabinoid signaling in the brain and in the BAT seem to be up-regulated acutely in a cold stimulus and this may inhibit an excessive thermogenic response.

Endocannabinoid tone changes in states of obesity, and this may also affect BAT regulation. Many studies have shown that obesity is associated with excessive activation of the ECS (Mazier et al., 2015). In overweight subjects, CB1R density in BAT, WAT and the brain was significantly lower compared to lean subjects (study **III**), which reflects the impairment of the endogenous cannabinoid system in obesity. A negative association between CB1R density in the brain and BMI has been reported previously (Hirvonen et al., 2013, 2012). Obese subjects also have increased circulating endogenous cannabinoid levels, and mRNA expression of CB1R is lower in the WAT of obese subjects compared to lean subjects (Blüher et al., 2006; Engeli et al., 2005). Higher plasma endocannabinoid levels are also associated with increased abdominal adiposity and cardiometabolic risk factors (Côté et al., 2007; Di Marzo et al., 2009; Fanelli et al., 2018). These findings exhibit the negative feedback loop of the ECS; thus, chronically high amounts of circulating endocannabinoids in obesity are associated with fewer CB1R in brain and adipose tissue. Interestingly, BMI is also inversely related to CB1R availability specifically in the homeostatic and mesolimbic brain regions of normal weight individuals and patients with eating disorders such as anorexia nervosa and bulimia nervosa (Ceccarini et al., 2016). The mesolimbic reward system and eating behavior is partly regulated by the endogenous opioid system, and obesity is also associated with lower availability of μ-opioid receptors, which can be normalized after weight loss by bariatric surgery (Karlsson et al., 2016). Weight loss in obese subjects also seems to increase and normalize 2-AG levels and CB1R expression in WAT (Bennetzen et al., 2011), but whether losing weight can normalize CB1R in the brain has not yet been determined.

It is noteworthy that CB1Rs are also present in other tissues involved in metabolic regulation including the liver, the intestine and the pancreas. For example, hepatic CB1Rs play a major role in the obesity-related development of insulin resistance and fatty liver disease (Tam et al., 2011). Unfortunately changes in the liver CB1Rs could not be investigated in this study, because the radioligand [^{18}F]FMPEP-d_2 is partly metabolized and excreted into bile (Terry et al., 2010). This causes high radioactivity and a strong PET signal in the images of the liver and the gallbladder of the subjects, which would have caused false results.

The phenomenon of increased endocannabinoid tone in obesity could be utilized for improving health. The CB1R antagonist, rimonabant, was previously on the market as a weight-loss drug, with good efficacy in obese patients. Rimonabant administration demonstrated that blocking the ECS can enhance the following metabolic factors: a decrease in waist circumference, improve systemic glucose levels and improve systemic lipid values (Christopoulou and Kiortsis, 2011). Due to its psychiatric adverse effects, rimonabant had to be removed from clinical use. However, pre-clinical studies on rimonabant have continued, with the aim of understanding the mechanisms of weight loss and improved metabolism caused by the drug. Intriguingly, blocking CB1Rs seems to regulate BAT function in a SNS-dependent manner. In mice, CB1R antagonism blocks the inhibition of β3-AR, which leads to the increased activation in BAT, lipolysis, and uptake of FFAs from the plasma (Boon et al., 2014). Deletion of adipocyte specific CB1R results in the browning of WAT, the promotion of a thermogenic program and an increase in alternatively activated macrophages, which increase local noradrenaline levels (Ruiz de Azua et al., 2017). In this thesis work CB1R antagonism increased glucose uptake and lipolysis of brown adipocytes, but CB1R agonism, CB2R antagonism or CB2R agonism did not have any effect (study **III**). During increased availability of noradrenaline the expression of CB1R mRNA was increased in brown but not in white adipocytes (study **III**).

This study adds to the existing evidence that CB1Rs are significant in regulating brown adipocyte function in a SNS-dependent manner. Endocannabinoid signaling via the CB1Rs is significant in the activation and regulation of human BAT, and targeting CB1Rs could provide a prospective way to treat obesity and metabolism. Ongoing research aims to develop specific CB1R antagonists, which could act strictly in peripheral tissues such as adipose tissue and improve metabolism, but would not cross the blood-brain barrier and cause harmful adverse effects.

6.5 Strengths, Limitations and Future Aspects of Research

This thesis work provides novel data about BAT regulation, and importantly, it examines selected physiological phenomena in humans for the first time. The dynamic PET imaging used in this study provides quantitative and high-quality data, and by combining different radioligands, several regulatory aspects can be investigated concurrently. Furthermore, the imaging data of different tissues in this study including BAT, WAT, skeletal muscle and brain have been combined with tissue biopsies, systemic blood values, and energy expenditure measurements, to understand physiological events as a whole.

However, this study also has its limitations. The number of study subjects in each sub-study was relatively small, and also only male subjects were recruited in studies II and III. PET imaging requires many resources and causes a radiation burden for the study subjects, and these issues together limited the possibilities for studying larger cohorts with a prospective study design. Future studies could be done that combine PET with MRI instead of CT, to decrease the radiation dose, and further assess BAT in humans (Holstila et al., 2017). Furthermore, more female subjects should also be included, to apply the findings to a broader population.

In studies II and III, cold exposure was used to activate BAT thermogenesis in the subjects. The aim was to induce non-shivering thermogenesis in BAT using an individualized cooling protocol, irrespective of body adiposity. The protocol was standardized and therefore repeatable, and subjects were monitored for shivering and the sensation of cold was repeatedly evaluated during the study. However, measurements using electromyography to detect muscle shivering and more detailed measurements of core and skin temperature could have improved the accuracy of the cooling protocol. For example, liquid conditioned suits perfused with chilled water, combined with a temperature- and flow-controlled circulation bath, as reported in other studies (Blondin et al., 2017b), could be used in future studies to ensure the appropriate stimulation of BAT thermogenesis. Furthermore, the studies were carried out over all the seasons, which may affect BAT activity. Although the aim was to perform individual baseline and cold measurements within the shortest time possible and within one season, this could not always be achieved due to PET scanner availability and scheduling issues. Although the standardized cooling protocol and dynamic image analysis minimized the effect of outdoor temperature on the results in these studies, there is some evidence that seasonal variation may influence BAT activity (Au-Yong et al., 2009; Yoneshiro et al., 2016), and this should be noted and controlled for when planning future studies.

The importance of thyroid hormones on BAT function has become clear over the years, but data from humans is still limited, and only a few high-quality prospective human studies have been done. Study I was a follow-up study that investigated BAT metabolism in hyperthyroid patients before and after treatment. It would be intriguing to perform similar studies with hypothyroid patients. Moreover, studying the connection between thyroid hormones, BAT and the brain could further elucidate the pathophysiologies in patients with hyper- and hypothyroidism.

Studies II and III are pilot studies that show proof-of-concept that the PET radioligands [^{11}C]TMSX and [^{18}F]FMPEP-d_2 can be used for BAT imaging in

humans, and that physiological changes occur in adenosine and cannabinoid receptors during cold activation of BAT. It is noteworthy, however, that the specific molecular mechanisms could not be fully investigated with these human *in vivo* imaging methods. Additional pre-clinical experiments would therefore be required to understand the detailed changes in A2AR kinetics during BAT activation. Furthermore, in study III, the density of CB1R in BAT was measured *in vivo*, combined with CB1R mRNA expression *in vitro*, but CB1R protein measurements were lacking. It would also be interesting to measure CB1R protein expression in human BAT using immunohistochemistry or a targeted proteomics approach to confirm the changes observed with PET imaging. However, a study investigating the change caused by cold would require repeated BAT biopsies, which may not be feasible in humans for ethical reasons. Determining the CB1R protein expression in a pre-clinical setting would provide additional evidence to elucidate the mechanisms and CB1R kinetics during cold exposure at the cellular level.

Such experiments would be valuable and warranted, because A_{2A} and CB1 receptors may provide potential drug targets for activating human BAT. Currently, many novel compounds that target the cannabinoid receptors are being investigated and developed for pharmaceutical use (Shrestha et al., 2018). In this thesis work, the effect of CB1R antagonism in humans unfortunately could not be investigated due to ethical restrictions. No CB1R antagonist is currently in clinical use for humans, and the subjects in this study had already received the maximal acceptable annual radiation dose considered safe for healthy volunteers. Future studies with novel pharmaceutical compounds are therefore warranted. Importantly, [^{18}F]FMPEP-d_2 could be further utilized to investigate the binding of such CB1R drugs in peripheral tissues, including BAT. Similarly, [^{11}C]TMSX has potential for future pharmaceutical studies of the A2ARs in BAT.

Overall, the studies in this thesis provide new information about important molecular mechanisms involved in endogenous BAT regulation. Future pharmacological studies and clinical trials will reveal whether the targeting of these mechanisms is feasible for the enhancement of energy expenditure, the improvement of metabolic health and the management of obesity in humans.

7 CONCLUSIONS

1. Hyperthyroidism increases the glucose uptake of BAT in humans, even without cold exposure. Excess systemic thyroid hormones also increase glucose uptake and perfusion of skeletal muscle. These changes in metabolism are reversible and return to the level of healthy controls after restoration of euthyroidism. Hyperthyroidism is further characterized by augmented energy expenditure and an increased use of lipids as an energy substrate.

2. Adenosine administration causes maximal perfusion in BAT of humans. Physiological activation of BAT during cold exposure decreases A_{2A} receptor density of the tissue, which indicates that endogenous adenosine is involved in the regulation of BAT function.

3. Cannabinoid type 1 receptors are upregulated during cold exposure in human BAT. This indicates an auto-regulatory loop of the endocannabinoid system, which contributes to the control of BAT metabolism and energy expenditure. This negative feedback response is likely controlled by the brain via the sympathetic nervous system.

4. Compared to lean subjects, overweight subjects with reduced BAT activity exhibit decreased CB1 receptor density in BAT, WAT, and the brain. This may manifest in impaired regulation of the endocannabinoid system in obesity.

5. BAT function is modulated by thyroid hormones, adenosinergic signaling, and the endocannabinoid system, in synergy with the sympathetic nervous system. These mechanisms provide potential pharmaceutical targets for specifically activating BAT and improving metabolic health.

ACKNOWLEDGEMENTS

This study was carried out at the Turku PET Centre and conducted within the Finnish Centre of Excellence in Cardiovascular and Metabolic Diseases supported by the Academy of Finland, University of Turku, Turku University Hospital and Åbo Akademi University.

Financially the study was supported by the Academy of Finland, the University of Turku Graduate School, the Turku University Hospital Research Funds, the EU DIABAT project, the Instrumentarium Foundation, the Paulo Foundation, and the Emil Aaltonen Foundation.

I wish to sincerely thank my supervisors Docent Kirsi Virtanen and Professor Pirjo Nuutila for the opportunity to conduct my doctoral thesis work under their guidance. Thank you for teaching me how to perform high quality research and for encouraging me along every step of the way. I have learned so much from each of you during these years, and I admire your experience and ways of thinking. I am very grateful for your mentorship and support, which have inspired me to work hard and grow as a scientist.

I express my gratitude to the reviewers of this thesis, Docent Niina Matikainen and Professor Uberto Pagotto. Your perspectives and constructive comments improved this thesis considerably. I would further like to thank Niina Matikainen and Docent Eriika Savontaus for their encouragement and guidance as members of my Ph.D. follow-up committee. I am also grateful to Professor Patrick Schrauwen for accepting the invitation to act as my opponent in the dissertation defense.

I wish to thank all of my collaborators and co-authors who have played a key role in the work presented in this thesis. I warmly acknowledge Camilla Schalin-Jäntti in Helsinki University Central Hospital and Minna Soinio in Turku University Hospital for their clinical expertise and valuable contribution to my first research article as a young medical student. Thank you to Olof Eriksson in Uppsala University for his vital work and input regarding the pre-clinical PET imaging studies, as well as his assistance and support with the clinical studies. I am very grateful to the excellent biopsy team Tarja Niemi, Markku Taittonen and Jukka Laine in Turku University Hospital for providing their valuable expertise in obtaining the human brown adipose tissue samples. Thank you to Professor Alexander Pfeifer and Thorsten Gnad in the Institute of Pharmacology and Toxicology in the University of Bonn for their essential contribution to the pre-clinical work and biopsy analyses.

I am thankful for the opportunity to have worked in the Turku PET Centre, which provides a terrific community of experts and scientists from different fields. Thank you to Professor Juhani Knuuti, director of the PET Centre, for providing the excellent facilities for research. I express my utmost gratitude to Vesa Oikonen for his significant work with the challenging PET image analyses in this thesis, and for always having the patience to answer my questions about radioligand kinetics. Marco Bucci and Jussi Hirvonen are warmly acknowledged for their expertise and assistance with the analyses of brain images.

I want to express my thanks to the radiochemists, physicists, radiographers, laboratory technicians, study nurses, coordinators and other staff members of the Turku PET Centre, these studies would not have been possible without your know-how, skills and hard work. Thank you for your positive attitude, the friendly and helpful atmosphere, and for making the long, hectic days of clinical imaging fun! A special thank you to study nurse Mia Koutu for her friendship and assistance with the clinical studies. A great deal of thanks go to my co-authors Kalle Koskensalo, Jarmo Teuho, Merja Haaparanta-Solin, Pauliina Luoto, Tommi Noponen, Semi Helin, Salla Lahdenpohja, Anna Kirjavainen, Hidehiro Iida and Nobuyuki Kudomi for their important input to the original publications. Alisdair Mclean is greatly acknowledged for the language revision of this thesis. I especially wish to express my gratitude to all of the volunteers who participated as study subjects in these studies!

I am privileged to have worked as part of an excellent research group with wonderful colleagues. Thank you to Jarna Hannukainen for all of the assistance and advice from the very beginning of my studies at the PET Centre. I owe my sincere thanks to Janne Orava, who introduced me to the fundamentals of BAT image analysis. I would like to warmly thank Mueez U Din, it has been great working on our doctoral theses side by side, thank you for the inspiring discussions, the peer support, and your friendship. I am also grateful to Sanna Laurila, my colleague and friend, for sharing thoughts, experiences, and not to mention many laughs during the clinical studies. A heartfelt thank you to all of my colleagues, especially Eleni Rebelos, Prince Dadson, Miikka Honka, Aino Latva-Rasku, Piryanka Motiani, Mia Ståhle, Simona Malaspina, Luis Juárez-Orozco, Kirsi Mikkola, Juho Raiko and Teemu Saari for the friendly and encouraging atmosphere, and for all of the great times we've shared in and outside of the workplace.

I want to thank all of my friends outside of science, near and far, for their support during these years and for cheering me on. A special thank you to my friends from medical school Jaana, Emma, Anna-Kaisa, Marie, Essi and Anna K. for encouraging me from the very beginning and through the collectively challenging

times of the "Syvärit". Sonja, thank you for your friendship, support and perspective, which have been essential for me during these years. I would also like to thank my friends and teachers from dance for helping me leave any stress or worries behind whenever stepping onto the dance floor!

I wish to sincerely thank my parents, Riitta & Timo and Arto & Pirkko, for their continuous encouragement, love and guidance. I am especially grateful to my mother, who is my role model and has always believed in me. I also wish to acknowledge my wonderful grandmother Pirkko and grandparents Terttu & Pekka for their support. Thank you to my sister Anna-Maria, to whom I have always looked up to, for her constant support, and to her wonderful family for bringing joy and sunshine to my daily life. Finally, I wish to thank Benjamin for always being there for me. Thank you for your love and endless support throughout this journey, and for always making me smile.

Turku, October 2018

Minna Lahesmaa

REFERENCES

Abbracchio, M., Burnstock, G., Verkhratsky, A., Zimmermann, H., 2009. Purinergic signalling in the nervous system: an overview. Trends Neurosci. 32, 19–29.

Abreu-Vieira, G., Hagberg, C.E., Spalding, K.L., Cannon, B., Nedergaard, J., 2015. Adrenergically stimulated blood flow in brown adipose tissue is not dependent on thermogenesis. Am. J. Physiol. Metab. 308, E822–E829.

Anand, S.S., Singh, H., Dash, A.K., 2009. Clinical Applications of PET and PET-CT. Med. journal, Armed Forces India 65, 353–8.

Andersen, S., Kleinschmidt, K., Hvingel, B., Laurberg, P., 2012. Thyroid hyperactivity with high thyroglobulin in serum despite sufficient iodine intake in chronic cold adaptation in an Arctic Inuit hunter population. Eur. J. Endocrinol. 166, 433–440.

Antonioli, L., Blandizzi, C., Csóka, B., Pacher, P., Haskó, G., 2015. Adenosine signalling in diabetes mellitus--pathophysiology and therapeutic considerations. Nat. Rev. Endocrinol. 11, 228–241.

Au-Yong, I.T.H., Thorn, N., Ganatra, R., Perkins, A.C., Symonds, M.E., 2009. Brown adipose tissue and seasonal variation in humans. Diabetes 58, 2583–2587.

Bartelt, A., Bruns, O.T., Reimer, R., Hohenberg, H., Ittrich, H., Peldschus, K., Kaul, M.G., Tromsdorf, U.I., Weller, H., Waurisch, C., Eychmüller, A., Gordts, P.L.S.M., Rinninger, F., Bruegelmann, K., Freund, B., Nielsen, P., Merkel, M., Heeren, J., 2011. Brown adipose tissue activity controls triglyceride clearance. Nat. Med. 17, 200–205.

Bennetzen, M.F., Wellner, N., Ahmed, S.S., Ahmed, S.M., Diep, T.A., Hansen, H.S., Richelsen, B., Pedersen, S.B., 2011. Investigations of the human endocannabinoid system in two subcutaneous adipose tissue depots in lean subjects and in obese subjects before and after weight loss. Int. J. Obes. 35, 1377–1384.

Berbeé, J.F.P., Boon, M.R., Khedoe, P.P.S.J., Bartelt, A., Schlein, C., Worthmann, A., Kooijman, S., Hoeke, G., Mol, I.M., John, C., Jung, C., Vazirpanah, N., Brouwers, L.P.J., Gordts, P.L.S.M., Esko, J.D., Hiemstra, P.S., Havekes, L.M., Scheja, L., Heeren, J., Rensen, P.C.N., 2015. Brown fat activation reduces hypercholesterolaemia and protects from atherosclerosis development. Nat. Commun. 6, 6356.

Bhatt, P.S., Dhillo, W.S., Salem, V., 2017. Human brown adipose tissue-function and therapeutic potential in metabolic disease. Curr. Opin. Pharmacol. 37, 1–9.

Blondin, D., Carpentier, A.C., 2016. The role of BAT in cardiometabolic disorders and aging. Best Pract. Res. Clin. Endocrinol. Metab. 30, 497–513.

Blondin, D., Frisch, F., Phoenix, S., Gurin, B., Turcotte, ric E., Haman, F., Richard, D., Carpentier, A., 2017a. Inhibition of Intracellular Triglyceride Lipolysis Suppresses Cold-Induced Brown Adipose Tissue Metabolism and Increases Shivering in Humans. Cell Metab. 25, 438–447.

Blondin, D., Labbé, S.M., Noll, C., Kunach, M., Phoenix, S., Guérin, B., Turcotte, É.E., Haman, F., Richard, D., Carpentier, A.C., 2015a. Selective impairment of glucose but not fatty acid or oxidative metabolism in brown adipose tissue of subjects with type 2 diabetes. Diabetes 64, 2388–2397.

Blondin, D., Labbé, S.M., Phoenix, S., Guérin, B., Turcotte, É.E., Richard, D., Carpentier, A.C., Haman, F., 2015b. Contributions of white and brown adipose tissues and skeletal muscles to acute cold-induced metabolic responses in healthy men. J. Physiol. 593, 701–714.

Blondin, D., Labbé, S.M., Tingelstad, H.C., Noll, C., Kunach, M., Phoenix, S., Guérin, B., Turcotte, É.E., Carpentier, A.C., Richard, D., Haman, F., 2014. Increased Brown Adipose Tissue Oxidative Capacity in Cold-Acclimated Humans. J. Clin. Endocrinol. Metab. 99, E438–E446.

Blondin, D., Tingelstad, H., Noll, C., Frisch, F., Phoenix, S., Gurin, B., Turcotte, ric E., Richard, D., Haman, F., Carpentier, A., 2017b. Dietary fatty acid metabolism of brown adipose tissue in cold-acclimated men. Nat. Commun. 8, 14146.

Blüher, M., Engeli, S., Klöting, N., Berndt, J., Fasshauer, M., Bátkai, S., Pacher, P., Schön, M.R., Jordan, J., Stumvoll, M., 2006. Dysregulation of the peripheral and adipose tissue endocannabinoid system in human abdominal obesity. Diabetes 55, 3053–3060.

Bogazzi, F., Bartalena, L., Brogioni, S., Burelli, A., Manetti, L., Tanda, M.L., Gasperi, M., Martino, E., 1999. Thyroid vascularity and blood flow are not dependent on serum thyroid hormone levels: studies in vivo by color flow doppler sonography. Eur. J. Endocrinol. 140, 452–6.

Bonnot, E., 1908. The Interscapular Gland. J. Anat. Physiol. 43, 43–58.

Boon, M.R., Kooijman, S., van Dam, A.D., Pelgrom, L.R., Berbee, J.F.P., Visseren, C.A.R., van Aggele, R.C., van den Hoek, A.M., Sips, H.C.M., Lombes, M., Havekes, L.M., Tamsma, J.T., Guigas, B., Meijer, O.C., Jukema, Jw., Rensen, P.C.N., 2014. Peripheral cannabinoid 1 receptor blockade activates brown adipose tissue and diminishes dyslipidemia and obesity. FASEB J. 28, 5361–5375.

Bordicchia, M., Liu, D., Amri, E.Z., Ailhaud, G., Dessì-Fulgheri, P., Zhang, C., Takahashi, N., Sarzani, R., Collins, S., 2012. Cardiac natriuretic peptides act via p38 MAPK to induce the brown fat thermogenic program in mouse and human adipocytes. J. Clin. Invest. 122, 1022–1036.

Boström, P., Wu, J., Jedrychowski, M.P., Korde, A., Ye, L., Lo, J.C., Rasbach, K.A., Boström, E.A., Choi, J.H., Long, J.Z., Kajimura, S., Zingaretti, M.C., Vind, B.F., Tu, H., Cinti, S., Højlund, K., Gygi, S.P., Spiegelman, B.M., 2012. A PGC1-α-dependent myokine that drives brown-fat-like development of white fat and thermogenesis. Nature 481, 463–468.

Branco, M., Ribeiro, M., Negrão, N., Bianco, A.C., 1999. 3,5,3'-Triiodothyronine actively stimulates UCP in brown fat under minimal sympathetic activity. Am. J. Physiol. 276, E179-87.

Broeders, E., Bouvy, N.D., van Marken Lichtenbelt, W.D., 2014. Endogenous ways to stimulate brown adipose tissue in humans. Ann. Med. 3890, 1–10.

Broeders, E.P., Vijgen, G.H., Havekes, B., Bouvy, N.D., Mottaghy, F.M., Kars, M., Schaper, N.C., Schrauwen, P., Brans, B., van Marken Lichtenbelt, W.D., 2016. Thyroid Hormone Activates Brown Adipose Tissue and Increases Non-Shivering Thermogenesis--A Cohort Study in a Group of Thyroid Carcinoma Patients. PLoS One 11, e0145049.

Broeders, E.P.M., Nascimento, E.B.M., Havekes, B., Brans, B., Roumans, K.H.M., Tailleux, A., Schaart, G., Kouach, M., Charton, J., Deprez, B., Bouvy, N.D.,

Mottaghy, F., Staels, B., Van Marken Lichtenbelt, W.D., Schrauwen, P., 2015. The bile acid chenodeoxycholic acid increases human brown adipose tissue activity. Cell Metab. 22, 418–426.

Cani, P.D., Plovier, H., Hul, M. Van, Geurts, L., Delzenne, N.M., Druart, C., Everard, A., 2016. Endocannabinoids--at the crossroads between the gut microbiota and host metabolism. Nat. Rev. Endocrinol. 12, 133–143.

Cannon, B., Nedergaard, J., 2010. Thyroid hormones: igniting brown fat via the brain. Nat. Med. 16, 965–967.

Cannon, B., Nedergaard, J., 2004. Brown Adipose Tissue: Function and Physiological Significance. Physiol. Rev. 84, 277–359.

Carpentier, A.C., Blondin, D.P., Virtanen, K.A., Richard, D., Haman, F., Turcotte, É.E., 2018. Brown Adipose Tissue Energy Metabolism in Humans. Front. Endocrinol. (Lausanne). 9, 1–21.

Caruso, G., Attard, M., Caronia, A., Lagalla, R., 2000. Color Doppler measurement of blood flow in the inferior thyroid artery in patients with autoimmune thyroid diseases. Eur. J. Radiol. 36, 5–10.

Ceccarini, J., Weltens, N., Ly, H.G., Tack, J., Van Oudenhove, L., Van Laere, K., 2016. Association between cerebral cannabinoid 1 receptor availability and body mass index in patients with food intake disorders and healthy subjects: a [(18)F]MK-9470 PET study. Transl. Psychiatry 6, e853.

Chang, L., Villacorta, L., Li, R., Hamblin, M., Xu, W., Dou, C., Zhang, J., Wu, J., Zeng, R., Chen, Y.E., 2012. Loss of perivascular adipose tissue on peroxisome proliferator-activated receptor-γ deletion in smooth muscle cells impairs intravascular thermoregulation and enhances atherosclerosis. Circulation 126, 1067–78.

Chen, J.-F., Eltzschig, H.K., Fredholm, B.B., 2013. Adenosine receptors as drug targets — what are the challenges? Nat. Rev. Drug Discov. 12, 265–286.

Chondronikola, M., Volpi, E., Børsheim, E., Porter, C., Annamalai, P., Enerbäck, S., Lidell, M.E., Saraf, M.K., Labbe, S.M., Hurren, N.M., Yfanti, C., Chao, T., Andersen, C.R., Cesani, F., Hawkins, H., Sidossis, L.S., 2014. Brown adipose tissue improves whole-body glucose homeostasis and insulin sensitivity in humans. Diabetes 63, 4089–4099.

Christensen, R., Kristensen, P.K., Bartels, E.M., Bliddal, H., Astrup, A., 2007. Efficacy and safety of the weight-loss drug rimonabant: a meta-analysis of randomised trials. Lancet 370, 1706–1713.

Christopoulou, F.D., Kiortsis, D.N., 2011. An overview of the metabolic effects of rimonabant in randomized controlled trials: potential for other cannabinoid 1 receptor blockers in obesity. J. Clin. Pharm. Ther. 36, 10–18.

Cioffi, F., Gentile, A., Silvestri, E., Goglia, F., Lombardi, A., 2018. Effect of Iodothyronines on Thermogenesis: Focus on Brown Adipose Tissue. Front. Endocrinol. (Lausanne). 9, 254.

Cohade, C., Mourtzikos, K.A., Wahl, R.L., 2003a. “USA-Fat”: prevalence is related to ambient outdoor temperature-evaluation with 18F-FDG PET/CT. J. Nucl. Med. 44, 1267–70.

Cohade, C., Osman, M., Pannu, H.K., Wahl, R.L., 2003b. Uptake in supraclavicular

area fat ("USA-Fat"): description on 18F-FDG PET/CT. J. Nucl. Med. 44, 170–6.

Colombo, G., Agabio, R., Diaz, G., Lobina, C., Reali, R., Gessa, G.L., 1998. Appetite suppression and weight loss after the cannabinoid antagonist SR 141716. Life Sci. 63, PL113-7.

Contreras, C., Gonzalez, F., Fernø, J., Diéguez, C., Rahmouni, K., Nogueiras, R., López, M., 2015. The brain and brown fat. Ann. Med. 47, 150–168.

Côté, M., Matias, I., Lemieux, I., Petrosino, S., Alméras, N., Després, J.-P., Marzo, V. Di, 2007. Circulating endocannabinoid levels, abdominal adiposity and related cardiometabolic risk factors in obese men. Int. J. Obes. 31, 692–699.

Cramer, W., 1920. On Glandular Adipose Tissue, and its Relation to other Endocrine Organs and to the Vitamine Problem. Br. J. Exp. Pathol. 1, 184.

Cypess, A., Haft, C., Laughlin, M., Hu, H., 2014. Brown Fat in Humans: Consensus Points and Experimental Guidelines. Cell Metab. 20, 408–415.

Cypess, A.M., Lehman, S., Williams, G., Tal, I., Rodman, D., Goldfine, A.B., Kuo, F.C., Palmer, E.L., Tseng, Y.-H., Doria, A., Kolodny, G.M., Kahn, C.R., 2009. Identification and Importance of Brown Adipose Tissue in Adult Humans. N. Engl. J. Med. 360, 1509–1517.

Cypess, A.M., Weiner, L.S., Roberts-Toler, C., Elía, E.F., Kessler, S.H., Kahn, P.A., English, J., Chatman, K., Trauger, S.A., Doria, A., Kolodny, G.M., 2015. Activation of human brown adipose tissue by a β3-adrenergic receptor agonist. Cell Metab. 21, 33–38.

Dadson, P., Hannukainen, J.C., Din, M.U., Lahesmaa, M., Kalliokoski, K.K., Iozzo, P., Pihlajamäki, J., Karlsson, H.K., Parkkola, R., Salminen, P., Virtanen, K.A., Nuutila, P., 2018. Brown adipose tissue lipid metabolism in morbid obesity: Effect of bariatric surgery-induced weight loss. Diabetes, Obes. Metab. 20, 1280–1288.

Danad, I., Raijmakers, P.G., Harms, H.J., Heymans, M.W., van Royen, N., Lubberink, M., Boellaard, R., van Rossum, A.C., Lammertsma, A.A., Knaapen, P., 2014. Impact of anatomical and functional severity of coronary atherosclerotic plaques on the transmural perfusion gradient: a [15O]H2O PET study. Eur. Heart J. 35, 2094–2105.

DeGrado, T.R., Coenen, H.H., Stocklin, G., 1991. 14(R,S)-[18F]fluoro-6-thia-heptadecanoic acid (FTHA): evaluation in mouse of a new probe of myocardial utilization of long chain fatty acids. J. Nucl. Med. 32, 1888–1896.

DeOliveira, C.C., Paiva Caria, C.R.E., Gotardo, E.M.F., Ribeiro, M.L., Gambero, A., 2017. Role of A1 and A2A adenosine receptor agonists in adipose tissue inflammation induced by obesity in mice. Eur. J. Pharmacol. 799, 154–159.

Dewal, R.S., Stanford, K.I., 2018. Effects of exercise on brown and beige adipocytes. Biochim. Biophys. Acta - Mol. Cell Biol. Lipids. doi: 0.1016/j.bbalip.2018.04.013. [Epub ahead of print]

Di Marzo, V., 2008. The endocannabinoid system in obesity and type 2 diabetes. Diabetologia 51, 1356–1367.

Di Marzo, V., Côté, M., Matias, I., Lemieux, I., Arsenault, B.J., Cartier, A., Piscitelli, F., Petrosino, S., Alméras, N., Després, J.P., 2009. Changes in plasma endocannabinoid levels in viscerally obese men following a 1 year lifestyle modification programme and waist circumference reduction: Associations with

changes in metabolic risk factors. Diabetologia 52, 213–217.

Donohue, S.R., Krushinski, J.H., Pike, V.W., Chernet, E., Lee, P., Chesterfield, A.K., Felder, C.C., Halldin, C., Schaus, J.M., Phebus, L., Chesterfield, A.K., Felder, C.C., Halldin, C., Schaus, J.M., 2008. Synthesis, Ex Vivo Evaluation and Radiolabeling of Potent 1,5-Diphenyl-pyrrolidin-2-one Cannabinoid Subtype-1 (CB(1)) Receptor Ligands as Candidates for In Vivo Imaging. J. Med. Chem. 51, 5833–5842.

Engeli, S., Böhnke, J., Feldpausch, M., Gorzelniak, K., Janke, J., Bátkai, S., Pacher, P., Harvey-White, J., Luft, F.C., Sharma, A.M., Jordan, J., 2005. Activation of the peripheral endocannabinoid system in human obesity. Diabetes 54, 2838–2843.

Eriksson, O., Mikkola, K., Espes, D., Tuominen, L., Virtanen, K., Forsback, S., Haaparanta-Solin, M., Hietala, J., Solin, O., Nuutila, P., 2015. The Cannabinoid Receptor-1 Is an Imaging Biomarker of Brown Adipose Tissue. J. Nucl. Med. 56, 1937–1941.

Fanelli, F., Mezzullo, M., Belluomo, I., Di Lallo, V.D., Baccini, M., Ibarra Gasparini, D., Casadio, E., Mastroroberto, M., Vicennati, V., Gambineri, A., Morselli-Labate, A.M., Pasquali, R., Pagotto, U., 2017. Plasma 2-arachidonoylglycerol is a biomarker of age and menopause related insulin resistance and dyslipidemia in lean but not in obese men and women. Mol. Metab. 6, 406–415.

Fanelli, F., Mezzullo, M., Repaci, A., Belluomo, I., Ibarra Gasparini, D., Di Dalmazi, G., Mastroroberto, M., Vicennati, V., Gambineri, A., Morselli-Labate, A.M., Pasquali, R., Pagotto, U., 2018. Profiling plasma N-Acylethanolamine levels and their ratios as a biomarker of obesity and dysmetabolism. Mol. Metab. 14, 82–94.

Festuccia, W.T., Blanchard, P.-G., Deshaies, Y., 2011. Control of Brown Adipose Tissue Glucose and Lipid Metabolism by PPARγ. Front. Endocrinol. (Lausanne). 2, 84.

Fitzgibbons, T.P., Kogan, S., Aouadi, M., Hendricks, G.M., Straubhaar, J., Czech, M.P., 2011. Similarity of mouse perivascular and brown adipose tissues and their resistance to diet-induced inflammation. Am. J. Physiol. Heart Circ. Physiol. 301, H1425-37.

Flegal, K.M., Kit, B.K., Orpana, H., Graubard, B.I., 2013. Association of all-cause mortality with overweight and obesity using standard body mass index categories a systematic review and meta-analysis. JAMA - J. Am. Med. Assoc. 309, 71–82.

Fobbe, F., Finke, R., Reichenstein, E., Schleusener, H., Wolf, K.J., 1989. Appearance of thyroid diseases using colour-coded duplex sonography. Eur. J. Radiol. 9, 29–31.

Forner, F., Kumar, C., Luber, C.A., Fromme, T., Klingenspor, M., Mann, M., 2009. Proteome differences between brown and white fat mitochondria reveal specialized metabolic functions. Cell Metab. 10, 324–35.

Freedman, N., Sundaram, S., Kurdziel, K., Carrasquillo, J., Whatley, M., Carson, J., Sellers, D., Libutti, S., Yang, J., Bacharach, S., 2003. Comparison of SUV and Patlak slope for monitoring of cancer therapy using serial PET scans. Eur. J. Nucl. Med. Mol. Imaging 30, 46–53.

Friedewald, W.T., Levy, R.I., Fredrickson, D.S., 1972. Estimation of the concentration of low-density lipoprotein cholesterol in plasma, without use of the preparative ultracentrifuge. Clin. Chem. 18, 499–502.

Gaich, G., Chien, J.Y., Fu, H., Glass, L.C., Deeg, M.A., Holland, W.L., Kharitonenkov, A., Bumol, T., Schilske, H.K., Moller, D.E., 2013. The Effects of LY2405319, an FGF21 Analog, in Obese Human Subjects with Type 2 Diabetes. Cell Metab. 18, 333–340.

Gavrila, A., Hasselgren, P.-O., Glasgow, A., Doyle, A.N., Lee, A.J., Fox, P., Gautam, S., Hennessey, J. V., Kolodny, G.M., Cypess, A.M., 2017. Variable Cold-Induced Brown Adipose Tissue Response to Thyroid Hormone Status. Thyroid 27, 1–10.

Geerling, J.J., Boon, M.R., van der Zon, G.C., van den Berg, S.A.A., van den Hoek, A.M., Lombès, M., Princen, H.M.G., Havekes, L.M., Rensen, P.C.N., Guigas, B., 2014. Metformin lowers plasma triglycerides by promoting VLDL-triglyceride clearance by brown adipose tissue in mice. Diabetes 63, 880–91.

Giralt, M., Gavaldà-Navarro, A., Villarroya, F., 2015. Fibroblast growth factor-21, energy balance and obesity. Mol. Cell. Endocrinol. 418, 66–73.

Gnad, T., Scheibler, S., von Kugelgen, I., Scheele, C., Kilic, A., Glode, A., Hoffmann, L.S., Reverte-Salisa, L., Horn, P., Mutlu, S., El-Tayeb, A., Kranz, M., Deuther-Conrad, W., Brust, P., Lidell, M., Betz, M.J., Enerbäck, S., Schrader, J., Yegutkin, G.G., Muller, C.E., Pfeifer, A., 2014. Adenosine activates brown adipose tissue and recruits beige adipocytes via A(2A) receptors. Nature 516, 395–399.

Hall, J., Ribich, S., Christoffolete, M., Simovic, G., Correa-Medina, M., Patti, M., Bianco, A., 2010. Absence of thyroid hormone activation during development underlies a permanent defect in adaptive thermogenesis. Endocrinology 151, 4573–4582.

Hamacher, K., Coenen, H.H., Stöcklin, G., 1986. Efficient stereospecific synthesis of no-carrier-added 2-[18F]-fluoro-2-deoxy-D-glucose using aminopolyether supported nucleophilic substitution. J Nucl Med 27, 235–8.

Hanssen, M.J., van der Lans, A.A., Brans, B., Hoeks, J., Jardon, K.M., Schaart, G., Mottaghy, F.M., Schrauwen, P., van Marken Lichtenbelt, W.D., 2016. Short-term Cold Acclimation Recruits Brown Adipose Tissue in Obese Humans. Diabetes 65, 1179–1189.

Hanssen, M.J.W., Broeders, E., Samms, R.J., Vosselman, M.J., van der Lans, A.A.J.J., Cheng, C.C., Adams, A.C., van Marken Lichtenbelt, W.D., Schrauwen, P., 2015a. Serum FGF21 levels are associated with brown adipose tissue activity in humans. Sci. Rep. 5, 10275.

Hanssen, M.J.W., Hoeks, J., Brans, B., van der Lans, A.A., Schaart, G., van den Driessche, J.J., Jorgensen, J.A., Boekschoten, M. V, Hesselink, M.K., Havekes, B., Kersten, S., Mottaghy, F.M., van Marken Lichtenbelt, W.D., Schrauwen, P., 2015b. Short-term cold acclimation improves insulin sensitivity in patients with type 2 diabetes mellitus. Nat. Med. 21, 863–865.

Hany, T.F., Gharehpapagh, E., Kamel, E.M., Buck, A., Himms-Hagen, J., Von Schulthess, G.K., 2002. Brown adipose tissue: A factor to consider in symmetrical tracer uptake in the neck and upper chest region. Eur. J. Nucl. Med. 29, 1393–1398.

Harms, M., Seale, P., 2013. Brown and beige fat: development, function and therapeutic potential. Nat. Med. 19, 1252–1263.

Heaton, J.M., 1972. The distribution of brown adipose tissue in the human. J. Anat. 112, 35–39.

Heinonen, I., Kemppainen, J., Kaskinoro, K., Knuuti, J., Boushel, R., Kalliokoski, K.K., 2014. Capacity and Hypoxic Response of Subcutaneous Adipose Tissue Blood Flow in Humans. Circ. J. 78, 1501–1506.

Heinonen, I., Kemppainen, J., Kaskinoro, K., Peltonen, J.E., Borra, R., Lindroos, M.M., Oikonen, V., Nuutila, P., Knuuti, J., Hellsten, Y., Boushel, R., Kalliokoski, K.K., 2010. Comparison of exogenous adenosine and voluntary exercise on human skeletal muscle perfusion and perfusion heterogeneity. J. Appl. Physiol. 108, 378–386.

Heinonen, I., Nesterov, S. V, Liukko, K., Kemppainen, J., NÃ¥gren, K., Luotolahti, M., Virsu, P., Oikonen, V., Nuutila, P., Kujala, U.M., Kainulainen, H., Boushel, R., Knuuti, J., Kalliokoski, K.K., 2008. Myocardial blood flow and adenosine A2A receptor density in endurance athletes and untrained men. J. Physiol. 586, 5193–5202.

Hildebrand, S., Stümer, J., Pfeifer, A., 2018. PVAT and its relation to brown, beige, and white adipose tissue in development and function. Front. Physiol. 9, 70.

Hirvonen, J., Goodwin, R.S., Li, C.-T., Terry, G.E., Zoghbi, S.S., Morse, C., Pike, V.W., Volkow, N.D., Huestis, M.A., Innis, R.B., 2012. Reversible and regionally selective downregulation of brain cannabinoid CB1 receptors in chronic daily cannabis smokers. Mol. Psychiatry 17, 642–649.

Hirvonen, J., Zanotti-Fregonara, P., Umhau, J.C., George, D.T., Rallis-Frutos, D., Lyoo, C.H., Li, C.-T., Hines, C.S., Sun, H., Terry, G.E., Morse, C., Zoghbi, S.S., Pike, V.W., Innis, R.B., Heilig, M., 2013. Reduced cannabinoid CB1 receptor binding in alcohol dependence measured with positron emission tomography. Mol. Psychiatry 18, 916–921.

Hoeke, G., Kooijman, S., Boon, M.R., Rensen, P.C.N., Berbée, J.F.P., 2016. Role of Brown Fat in Lipoprotein Metabolism and Atherosclerosis. Circ. Res. 118, 173–82.

Holstila, M., Pesola, M., Saari, T., Koskensalo, K., Raiko, J., Borra, R.J.H., Nuutila, P., Parkkola, R., Virtanen, K.A., 2017. MR signal-fat-fraction analysis and T2* weighted imaging measure BAT reliably on humans without cold exposure. Metabolism. 70, 23–30.

Hsiao, W.C., Shia, K.S., Wang, Y.T., Yeh, Y.N., Chang, C.P., Lin, Y., Chen, P.H., Wu, C.H., Chao, Y.S., Hung, M.S., 2015. A novel peripheral cannabinoid receptor 1 antagonist, BPR0912, reduces weight independently of food intake and modulates thermogenesis. Diabetes, Obes. Metab. 17, 495–504.

Huttunen, P., Hirvonen, J., Kinnula, V., 1981. The occurrence of brown adipose tissue in outdoor workers. Eur. J. Appl. Physiol. Occup. Physiol. 46, 339–45.

Ishiwata, K., Mizuno, M., Kimura, Y., Kawamura, K., Oda, K., Sasaki, T., Nakamura, Y., Muraoka, I., Ishii, K., 2004. Potential of [11C]TMSX for the evaluation of adenosine A2A receptors in the skeletal muscle by positron emission tomography. Nucl. Med. Biol. 31, 949–956.

Jacobson, S., Marcus, E.M., 2008. Neuroanatomy for the neuroscientist, Neuroanatomy for the Neuroscientist. Springer US, Boston, MA.

Jakus, P.B., Sandor, A., Janaky, T., Farkas, V., 2008. Cooperation between BAT and WAT of rats in thermogenesis in response to cold, and the mechanism of glycogen accumulation in BAT during reacclimation. J. Lipid Res. 49, 332–9.

Jbilo, O., Ravinet-Trillou, C., Arnone, M., Buisson, I., Bribes, E., Péleraux, A., Pénarier, G., Soubrié, P., Le Fur, G., Galiègue, S., Casellas, P., 2005. The CB1 receptor antagonist rimonabant reverses the diet-induced obesity phenotype through the regulation of lipolysis and energy balance. FASEB J. 19, 1567–1569.

Jensen, M.D., Ryan, D.H., Donato, K.A., Apovian, C.M., Ard, J.D., Comuzzie, A.G., Hu, F.B., Hubbard, V.S., Jakicic, J.M., Kushner, R.F., Loria, C.M., Millen, B.E., Nonas, C.A., Pi-Sunyer, F.X., Stevens, J., Stevens, V.J., Wadden, T.A., Wolfe, B.M., Yanovski, S.Z., 2014. Executive summary: Guidelines (2013) for the management of overweight and obesity in adults. Obesity 22, S5–S39.

Kantae, V., Nahon, K.J., Straat, M.E., Bakker, L.E.H., Harms, A.C., van der Stelt, M., Hankemeier, T., Jazet, I.M., Boon, M.R., Rensen, P.C.N., 2017. Endocannabinoid tone is higher in healthy lean South Asian than white Caucasian men. Sci. Rep. 7, 7558.

Karlsson, H.K., Tuulari, J.J., Tuominen, L., Hirvonen, J., Honka, H., Parkkola, R., Helin, S., Salminen, P., Nuutila, P., Nummenmaa, L., 2016. Weight loss after bariatric surgery normalizes brain opioid receptors in morbid obesity. Mol. Psychiatry 21, 1057–1062.

Kates, A.-L., Himms-Hagen, J., 1985. Defective cold-induced stimulation of thyroxine 5′-deiodinase in brown adipose tissue of the genetically obese (obob) mouse. Biochem. Biophys. Res. Commun. 130, 188–193.

Klieverik, L., Coomans, C., Endert, E., Sauerwein, H., Havekes, L., Voshol, P., Rensen, P.C.N., Romijn, J., Kalsbeek, A., Fliers, E., 2009. Thyroid hormone effects on whole-body energy homeostasis and tissue-specific fatty acid uptake in vivo. Endocrinology 150, 5639–5648.

Koffert, J., Honka, H., Teuho, J., Kauhanen, S., Hurme, S., Parkkola, R., Oikonen, V., Mari, A., Lindqvist, A., Wierup, N., Groop, L., Nuutila, P., 2017. Effects of meal and incretins in the regulation of splanchnic blood flow. Endocr. Connect. 6, 179–187.

Komar, G., Oikonen, V., Sipilä, H., Seppänen, M., Minn, H., 2012. Noninvasive parametric blood flow imaging of head and neck tumours using [15O]H2O and PET/CT. Nucl. Med. Commun. 33, 1169–1178.

Krott, L.M., Piscitelli, F., Heine, M., Borrino, S., Scheja, L., Silvestri, C., Heeren, J., Marzo, V. Di, 2016. Endocannabinoid regulation in white and brown adipose tissue following thermogenic activation. J. Lipid Res. 57, 464–473.

Kunos, G., Tam, J., 2011. The case for peripheral CB(1) receptor blockade in the treatment of visceral obesity and its cardiometabolic complications. Br. J. Pharmacol. 163, 1423–1431.

Labbé, S.M., Caron, A., Bakan, I., Laplante, M., Carpentier, A.C., Lecomte, R., Richard, D., 2015. In vivo measurement of energy substrate contribution to cold-induced brown adipose tissue thermogenesis. FASEB J. 29, 2046–58.

Lee, J.-Y., Takahashi, N., Yasubuchi, M., Kim, Y.-I., Hashizaki, H., Kim, M.-J., Sakamoto, T., Goto, T., Kawada, T., 2012. Triiodothyronine induces UCP-1 expression and mitochondrial biogenesis in human adipocytes. Am. J. Physiol. Physiol. 302, C472.

Lee, P., Linderman, J.D., Smith, S., Brychta, R.J., Wang, J., Idelson, C., Perron, R.M., Werner, C.D., Phan, G.Q., Kammula, U.S., Kebebew, E., Pacak, K., Chen, K.Y.,

Celi, F.S., 2014a. Irisin and FGF21 are cold-induced endocrine activators of brown fat function in humans. Cell Metab. 19, 302–9.

Lee, P., Smith, S., Linderman, J., Courville, A.B., Brychta, R.J., Dieckmann, W., Werner, C.D., Chen, K.Y., Celi, F.S., 2014b. Temperature-acclimated brown adipose tissue modulates insulin sensitivity in humans. Diabetes 63, 3686–98.

Lee, P., Swarbrick, M.M., Greenfield, J.R., 2015. The Sum of All Browning in FGF21 Therapeutics. Cell Metab. 21, 795–796.

Leung, K., 2004. [7-methyl-11C]-(E)-8-(3,4,5-Trimethoxystyryl)-1,3,7-trimethylxanthine, in: Molecular Imaging and Contrast Agent Database (MICAD). National Center for Biotechnology Information (US).

Lidell, M., Betz, M., Leinhard, O., Heglind, M., Elander, L., Slawik, M., Mussack, T., Nilsson, D., Romu, T., Nuutila, P., Virtanen, K., Beuschlein, F., Persson, A., Borga, M., Enerbäck, S., 2013. Evidence for two types of brown adipose tissue in humans. Nat. Med. 19, 631–634.

Lin, J.Z., Martagón, A.J., Cimini, S.L., Gonzalez, D.D., Tinkey, D.W., Biter, A., Baxter, J.D., Webb, P., Gustafsson, J.Å., Hartig, S.M., Phillips, K.J., 2015. Pharmacological Activation of Thyroid Hormone Receptors Elicits a Functional Conversion of White to Brown Fat. Cell Rep. 13, 1528–1537.

Liu, X., Wang, S., You, Y., Meng, M., Zheng, Z., Dong, M., Lin, J., Zhao, Q., Zhang, C., Yuan, X., Hu, T., Liu, L., Huang, Y., Zhang, L., Wang, D., Zhan, J., Lee, H.J., Speakman, J.R., Jin, W., 2015. Brown adipose tissue transplantation reverses obesity in Ob/Ob mice. Endocrinology 156, 2461–2469.

Liu, X., Zheng, Z., Zhu, X., Meng, M., Li, L., Shen, Y., Chi, Q., Wang, D., Zhang, Z., Li, C., Li, Y., Xue, Y., Speakman, J.R., Jin, W., 2013. Brown adipose tissue transplantation improves whole-body energy metabolism. Cell Res. 23, 851–4.

Liukko, K., Oikonen, V., Tolvanen, T., Virtanen, K., Viljanen, A., Sipilä, H., Nuutila, P., Iozzo, P., 2007. Non-invasive estimation of subcutaneous and visceral adipose tissue blood flow by using H2O PET with image derived input functions. Open Med Imaging J 1, 7–13.

Logan, J., Fowler, J.S., Volkow, N.D., Wolf, A.P., Dewey, S.L., Schlyer, D.J., MacGregor, R.R., Hitzemann, R., Bendriem, B., Gatley, S.J., Christman, D.R., 1990. Graphical Analysis of Reversible Radioligand Binding from Time—Activity Measurements Applied to [*N* - ^{11} C-Methyl]-(−)-Cocaine PET Studies in Human Subjects. J. Cereb. Blood Flow Metab. 10, 740–747.

López, M., Varela, L., Vázquez, M.J., Rodríguez-Cuenca, S., González, C.R., Velagapudi, V.R., Morgan, D.A., Schoenmakers, E., Agassandian, K., Lage, R., de Morentin, P.B.M., Tovar, S., Nogueiras, R., Carling, D., Lelliott, C., Gallego, R., Orešič, M., Chatterjee, K., Saha, A.K., Rahmouni, K., Diéguez, C., Vidal-Puig, A., 2010. Hypothalamic AMPK and fatty acid metabolism mediate thyroid regulation of energy balance. Nat. Med. 16, 1001–1008.

Männistö, S., Laatikainen, T., Harald, K., Borodulin, K., Jousilahti, P., Kanerva, N., Peltonen, M., Vartiainen, E., 2015. Työikäisten ylipainon ja lihavuuden kasvu näyttää hidastuneen. Suom. Lääkäril. 14–15, 969–976.

Marlatt, K.L., Ravussin, E., 2017. Brown Adipose Tissue: an Update on Recent Findings. Curr. Obes. Rep. 6, 389–396.

Martínez-Sánchez, N., Moreno-Navarrete, J.M., Contreras, C., Rial-Pensado, E., Fernø, J., Nogueiras, R., Diéguez, C., Fernández-Real, J.-M., López, M., 2017. Thyroid hormones induce browning of white fat. J. Endocrinol. 232, 351–362.

Matsushita, M., Yoneshiro, T., Aita, S., Kameya, T., Sugie, H., Saito, M., 2014. Impact of brown adipose tissue on body fatness and glucose metabolism in healthy humans. Int. J. Obes. 38, 812–817.

Mazier, W., Saucisse, N., Gatta-Cherifi, B., Cota, D., 2015. The Endocannabinoid System: Pivotal Orchestrator of Obesity and Metabolic Disease. Trends Endocrinol. Metab. 26, 524–537.

Meriläinen, P.T., 1987. Metabolic monitor. Int. J. Clin. Monit. Comput. 4, 167–177.

Merklin, R.J., 1974. Growth and distribution of human fetal brown fat. Anat. Rec. 178, 637–645.

Mishina, M., Ishiwata, K., Kimura, Y., Naganawa, M., Oda, K., Kobayashi, S., Katayama, Y., Ishii, K., 2007. Evaluation of distribution of adenosine A2A receptors in normal human brain measured with [11C]TMSX PET. Synapse 61, 778–784.

Mishina, M., Ishiwata, K., Naganawa, M., Kimura, Y., Kitamura, S., Suzuki, M., Hashimoto, M., Ishibashi, K., Oda, K., Sakata, M., Hamamoto, M., Kobayashi, S., Katayama, Y., Ishii, K., 2011. Adenosine A2A Receptors Measured with [11C]TMSX PET in the Striata of Parkinson's Disease Patients. PLoS One 6, e17338.

Mizuno, M., Kimura, Y., Tokizawa, K., Ishii, K., Oda, K., Sasaki, T., Nakamura, Y., Muraoka, I., Ishiwata, K., 2005. Greater adenosine A2A receptor densities in cardiac and skeletal muscle in endurance-trained men: a [11C]TMSX PET study. Nucl. Med. Biol. 32, 831–836.

Møller, N., Nielsen, S., Nyholm, B., Pørksen, N., Alberti, K.G.M.M., Weeke, J., 1996. Glucose turnover, fuel oxidation and forearm substrate exchange in patients with thyrotoxicosis before and after medical treatment. Clin. Endocrinol. (Oxf). 44, 453–459.

Morrison, S.F., Madden, C.J., Tupone, D., 2012. Central Control of Brown Adipose Tissue Thermogenesis. Front. Endocrinol. (Lausanne). 3, 5.

Motiani, P., Virtanen, K.A., Motiani, K.K., Eskelinen, J.J., Middelbeek, R.J., Goodyear, L.J., Savolainen, A.M., Kemppainen, J., Jensen, J., Din, M.U., Saunavaara, V., Parkkola, R., Löyttyniemi, E., Knuuti, J., Nuutila, P., Kalliokoski, K.K., Hannukainen, J.C., 2017. Decreased insulin-stimulated brown adipose tissue glucose uptake after short-term exercise training in healthy middle-aged men. Diabetes, Obes. Metab. 19, 1379–1388.

Mundell, S., Kelly, E., 2011. Adenosine receptor desensitization and trafficking. Biochim. Biophys. Acta 1808, 1319–1328.

Muzik, O., Mangner, T., Leonard, W., Kumar, A., Janisse, J., Granneman, J., 2013. 15O PET measurement of blood flow and oxygen consumption in cold-activated human brown fat. J. Nucl. Med. 54, 523–531.

Muzik, O., Mangner, T.J., Granneman, J.G., 2012. Assessment of oxidative metabolism in brown fat using PET imaging. Front. Endocrinol. (Lausanne). 3, 15.

Naganawa, M., Mishina, M., Sakata, M., Oda, K., Hiura, M., Ishii, K., Ishiwata, K.,

2014. Test-retest variability of adenosine A2A binding in the human brain with 11C-TMSX and PET. EJNMMI Res. 4, 76.

Ng, M., Fleming, T., Robinson, M., Thomson, B., Graetz, N., Margono, C., Mullany, E.C., Biryukov, S., Abbafati, C., Abera, S.F., Abraham, J.P., Abu-Rmeileh, N.M.E., Achoki, T., Albuhairan, F.S., Alemu, Z.A., Alfonso, R., Ali, M.K., Ali, R., Guzman, N.A., Ammar, W., Anwari, P., Banerjee, A., Barquera, S., Basu, S., Bennett, D.A., Bhutta, Z., Blore, J., Cabral, N., Nonato, I.C., Chang, J.C., Chowdhury, R., Courville, K.J., Criqui, M.H., Cundiff, D.K., Dabhadkar, K.C., Dandona, L., Davis, A., Dayama, A., Dharmaratne, S.D., Ding, E.L., Durrani, A.M., Esteghamati, A., Farzadfar, F., Fay, D.F.J., Feigin, V.L., Flaxman, A., Forouzanfar, M.H., Goto, A., Green, M.A., Gupta, R., Hafezi-Nejad, N., Hankey, G.J., Harewood, H.C., Havmoeller, R., Hay, S., Hernandez, L., Husseini, A., Idrisov, B.T., Ikeda, N., Islami, F., Jahangir, E., Jassal, S.K., Jee, S.H., Jeffreys, M., Jonas, J.B., Kabagambe, E.K., Khalifa, S.E.A.H., Kengne, A.P., Khader, Y.S., Khang, Y.H., Kim, D., Kimokoti, R.W., Kinge, J.M., Kokubo, Y., Kosen, S., Kwan, G., Lai, T., Leinsalu, M., Li, Y., Liang, X., Liu, S., Logroscino, G., Lotufo, P.A., Lu, Y., Ma, J., Mainoo, N.K., Mensah, G.A., Merriman, T.R., Mokdad, A.H., Moschandreas, J., Naghavi, M., Naheed, A., Nand, D., Narayan, K.M.V., Nelson, E.L., Neuhouser, M.L., Nisar, M.I., Ohkubo, T., Oti, S.O., Pedroza, A., Prabhakaran, D., Roy, N., Sampson, U., Seo, H., Sepanlou, S.G., Shibuya, K., Shiri, R., Shiue, I., Singh, G.M., Singh, J.A., Skirbekk, V., Stapelberg, N.J.C., Sturua, L., Sykes, B.L., Tobias, M., Tran, B.X., Trasande, L., Toyoshima, H., Van De Vijver, S., Vasankari, T.J., Veerman, J.L., Velasquez-Melendez, G., Vlassov, V.V., Vollset, S.E., Vos, T., Wang, C., Wang, X., Weiderpass, E., Werdecker, A., Wright, J.L., Yang, Y.C., Yatsuya, H., Yoon, J., Yoon, S.J., Zhao, Y., Zhou, M., Zhu, S., Lopez, A.D., Murray, C.J.L., Gakidou, E., 2014. Global, regional, and national prevalence of overweight and obesity in children and adults during 1980-2013: A systematic analysis for the Global Burden of Disease Study 2013. Lancet 384, 766–781.

Nguyen, K.D., Qiu, Y., Cui, X., Goh, Y.P.S., Mwangi, J., David, T., Mukundan, L., Brombacher, F., Locksley, R.M., Chawla, A., 2011. Alternatively activated macrophages produce catecholamines to sustain adaptive thermogenesis. Nature 480, 104–108.

Nisoli, E., Tonello, C., Benarese, M., Liberini, P., Carruba, M.O., 1996. Expression of nerve growth factor in brown adipose tissue: implications for thermogenesis and obesity. Endocrinology 137, 495–503.

Oikonen, V., n.d. PET data analysis and modelling [WWW Document]. URL http://www.turkupetcentre.net/petanalysis/ (accessed 3.29.18).

Orava, J., Nuutila, P., Lidell, M., Oikonen, V., Noponen, T., Viljanen, T., Scheinin, M., Taittonen, M., Niemi, T., Enerbäck, S., Virtanen, K., 2011. Different metabolic responses of human brown adipose tissue to activation by cold and insulin. Cell Metab. 14, 272–279.

Orava, J., Nuutila, P., Noponen, T., Parkkola, R., Viljanen, T., Enerbäck, S., Rissanen, A., Pietiläinen, K.H., Virtanen, K.A., 2013. Blunted metabolic responses to cold and insulin stimulation in brown adipose tissue of obese humans. Obesity 21, 2279–2287.

Ouellet, V., Labb, S., Blondin, D., Phoenix, S., Gurin, B., Haman, F., Turcotte, E., Richard, D., Carpentier, A., 2012. Brown adipose tissue oxidative metabolism

contributes to energy expenditure during acute cold exposure in humans. J. Clin. Invest. 122, 545–552.

Patlak, C.S., Blasberg, R.G., 1985. Graphical Evaluation of Blood-to-Brain Transfer Constants from Multiple-Time Uptake Data. Generalizations. J. Cereb. Blood Flow Metab. 5, 584–590.

Peltoniemi, P., Lönnroth, P., Laine, H., Oikonen, V., Tolvanen, T., Grönroos, T., Strindberg, L., Knuuti, J., Nuutila, P., 2000. Lumped constant for [(18)F]fluorodeoxyglucose in skeletal muscles of obese and nonobese humans. Am. J. Physiol. Endocrinol. Metab. 279, E1122-30.

Petrovic, N., Walden, T.B., Shabalina, I.G., Timmons, J.A., Cannon, B., Nedergaard, J., 2010. Chronic peroxisome proliferator-activated receptor gamma (PPARgamma) activation of epididymally derived white adipocyte cultures reveals a population of thermogenically competent, UCP1-containing adipocytes molecularly distinct from classic brown adipocytes. J. Biol. Chem. 285, 7153–64.

Pfannenberg, C., Werner, M.K., Ripkens, S., Stef, I., Deckert, A., Schmadl, M., Reimold, M., Häring, H.-U., Claussen, C.D., Stefan, N., 2010. Impact of age on the relationships of brown adipose tissue with sex and adiposity in humans. Diabetes 59, 1789–93.

Pfeifer, A., Hoffmann, L., 2015. Brown, beige, and white: the new color code of fat and its pharmacological implications. Annu. Rev. Pharmacol. Toxicol. 55, 207–227.

Ponrartana, S., Aggabao, P.C., Chavez, T.A., Dharmavaram, N.L., Gilsanz, V., 2016. Changes in Brown Adipose Tissue and Muscle Development during Infancy. J Pediatr 173, 116–21.

Puigserver, P., Wu, Z., Park, C.W., Graves, R., Wright, M., Spiegelman, B.M., 1998. A cold-inducible coactivator of nuclear receptors linked to adaptive thermogenesis. Cell 92, 829–839.

Quarta, C., Lodi, F., Mazza, R., Giannone, F., Boschi, L., Nanni, C., Nisoli, E., Boschi, S., Pasquali, R., Fanti, S., Iozzo, P., Pagotto, U., 2013. 11C-meta-hydroxyephedrine PET/CT imaging allows in vivo study of adaptive thermogenesis and white-to-brown fat conversion. Mol. Metab. 2, 153–160.

Rabelo, R., Schifman, A., Rubio, A., Sheng, X., Silva, J.E., 1995. Delineation of thyroid hormone-responsive sequences within a critical enhancer in the rat uncoupling protein gene. Endocrinology 136, 1003–1013.

Radiation and Nuclear Safety Authority (STUK), n.d. Mitä säteily on? [WWW Document]. URL http://www.stuk.fi/aiheet/mita-sateily-on (accessed 4.18.18).

Ribeiro, M., Bianco, S.D.C., Kaneshige, M., Schultz, J., Cheng, S., Bianco, A., Brent, G., 2010. Expression of uncoupling protein 1 in mouse brown adipose tissue is thyroid hormone receptor-beta isoform specific and required for adaptive thermogenesis. Endocrinology 151, 432–440.

Richey, J.M., Woolcott, O., 2017. Re-visiting the Endocannabinoid System and Its Therapeutic Potential in Obesity and Associated Diseases. Curr. Diab. Rep. 17, 99.

Rissanen, E., Virta, J.R., Paavilainen, T., Tuisku, J., Helin, S., Luoto, P., Parkkola, R., Rinne, J.O., Airas, L., 2013. Adenosine A2A Receptors in Secondary Progressive Multiple Sclerosis: A [11C]TMSX Brain PET Study. J. Cereb. Blood Flow Metab. 33, 1394–1401.

Rodriguez, A.M., Pisani, D., Dechesne, C.A., Turc-Carel, C., Kurzenne, J.Y., Wdziekonski, B., Villageois, A., Bagnis, C., Breittmayer, J.P., Groux, H., Ailhaud, G., Dani, C., 2005. Transplantation of a multipotent cell population from human adipose tissue induces dystrophin expression in the immunocompetent mdx mouse. J. Exp. Med. 201, 1397–1405.

Rogers, N.H., 2015. Brown adipose tissue during puberty and with aging. Ann. Med. 47, 142–149.

Ross, D.S., Burch, H.B., Cooper, D.S., Greenlee, M.C., Laurberg, P., Maia, A.L., Rivkees, S.A., Samuels, M., Sosa, J.A., Stan, M.N., Walter, M.A., 2016. 2016 American Thyroid Association Guidelines for Diagnosis and Management of Hyperthyroidism and Other Causes of Thyrotoxicosis. Thyroid 26, 1343–1421.

Ruiz de Azua, I., Mancini, G., Srivastava, R.K., Rey, A.A., Cardinal, P., Tedesco, L., Zingaretti, C.M., Sassmann, A., Quarta, C., Schwitter, C., Conrad, A., Wettschureck, N., Vemuri, V.K., Makriyannis, A., Hartwig, J., Mendez-Lago, M., Bindila, L., Monory, K., Giordano, A., Cinti, S., Marsicano, G., Offermanns, S., Nisoli, E., Pagotto, U., Cota, D., Lutz, B., 2017. Adipocyte cannabinoid receptor CB1 regulates energy homeostasis and alternatively activated macrophages. J. Clin. Invest. 127, 4148–4162.

Saito, M., Okamatsu-Ogura, Y., Matsushita, M., Watanabe, K., Yoneshiro, T., Nio-Kobayashi, J., Iwanaga, T., Miyagawa, M., Kameya, T., Nakada, K., Kawai, Y., Tsujisaki, M., 2009. High incidence of metabolically active brown adipose tissue in healthy adult humans: Effects of cold exposure and adiposity. Diabetes 58, 1526–1531.

Sam, A.H., Salem, V., Ghatei, M.A., 2011. Rimonabant: From RIO to Ban. J. Obes. 2011, 432607.

Sanchez-Delgado, G., Martinez-Tellez, B., Olza, J., Aguilera, C.M., Gil, Á., Ruiz, J.R., 2015. Role of exercise in the activation of brown adipose tissue. Ann. Nutr. Metab. 67, 21–32.

Schimmel, R.J., McCarthy, L., 1984. Role of adenosine as an endogenous regulator of respiration in hamster brown adipocytes. Am. J. Physiol. 246, C301–C307.

Schreiber, R., Diwoky, C., Schoiswohl, G., Feiler, U., Wongsiriroj, N., Abdellatif, M., Kolb, D., Hoeks, J., Kershaw, E.E., Sedej, S., Schrauwen, P., Haemmerle, G., Zechner, R., 2017. Cold-Induced Thermogenesis Depends on ATGL-Mediated Lipolysis in Cardiac Muscle, but Not Brown Adipose Tissue. Cell Metab. 26, 753–763.e7.

Sepa-Kishi, D.M., Ceddia, R.B., 2018. White and beige adipocytes: Are they metabolically distinct? Horm. Mol. Biol. Clin. Investig. 33, 1–10.

Shin, H., Ma, Y., Chanturiya, T., Cao, Q., Wang, Y., Kadegowda, A.K.G., Jackson, R., Rumore, D., Xue, B., Shi, H., Gavrilova, O., Yu, L., 2017. Lipolysis in Brown Adipocytes Is Not Essential for Cold-Induced Thermogenesis in Mice. Cell Metab. 26, 764–777.e5.

Shrestha, N., Cuffe, J.S.M., Hutchinson, D.S., Headrick, J.P., Perkins, A. V., McAinch, A.J., Hryciw, D.H., 2018. Peripheral modulation of the endocannabinoid system in metabolic disease. Drug Discov. Today 23, 592–604.

Silva, J.E., Bianco, S.D.C., 2008. Thyroid–Adrenergic Interactions: Physiological and Clinical Implications. Thyroid 18, 157–165.

Silvestri, C., Di Marzo, V., 2013. The endocannabinoid system in energy homeostasis and the etiopathology of metabolic disorders. Cell Metab. 17, 475–90.

Söderlund, V., Larsson, S.A., Jacobsson, H., 2007. Reduction of FDG uptake in brown adipose tissue in clinical patients by a single dose of propranolol. Eur. J. Nucl. Med. Mol. Imaging 34, 1018–1022.

Sokoloff, L., Reivich, M., Kennedy, C., Des Rosiers, M.H., Patlak, C.S., Pettigrew, K.D., Sakurada, O., Shinohara, M., 1977. The [14C]deoxyglucose method for the measurement of local cerebral glucose utilization: theory, procedure, and normal values in the conscious and anesthetized albino rat. J. Neurochem. 28, 897–916.

Solanes, G., Pedraza, N., Calvo, V., Puig, A.V., Lowell, B., Villarroya, F., 2005. Thyroid hormones directly activate the expression of the human and mouse uncoupling protein-3 genes through a thyroid response element in the proximal promoter region. Biochem. J. 386, 505–513.

Sorisky, A., Antunes, T.T., Gagnon, A., 2008. The Adipocyte as a novel TSH target. Mini Rev. Med. Chem. 8, 91–6.

Sousa, J.B., Diniz, C., 2017. The adenosinergic system as a therapeutic target in the vasculature: New ligands and challenges. Molecules.

Stanford, K.I., Middelbeek, R.J.W., Townsend, K.L., An, D., Nygaard, E.B., Hitchcox, K.M., Markan, K.R., Nakano, K., Hirshman, M.F., Tseng, Y.-H., Goodyear, L.J., 2013. Brown adipose tissue regulates glucose homeostasis and insulin sensitivity. J. Clin. Invest. 123, 215–23.

Sun, K., Kusminski, C.M., Luby-Phelps, K., Spurgin, S.B., An, Y.A., Wang, Q.A., Holland, W.L., Scherer, P.E., 2014. Brown adipose tissue derived VEGF-A modulates cold tolerance and energy expenditure. Mol. Metab. 3, 474–483.

Sun, L., Yan, J., Sun, L., Velan, S.S., Leow, M.K.S., 2017. A synopsis of brown adipose tissue imaging modalities for clinical research. Diabetes Metab. 43, 401–410.

Szillat, D., Bukowiecki, L.J., 1983. Control of brown adipose tissue lipolysis and respiration by adenosine. Am. J. Physiol. 245, E555–E559.

Takano, A., Gulyás, B., Varnäs, K., Little, P.B., Noerregaard, P.K., Jensen, N.O., Elling, C.E., Halldin, C., 2014. Low brain CB1 receptor occupancy by a second generation CB1 receptor antagonist TM38837 in comparison with rimonabant in nonhuman primates: a PET study. Synapse 68, 89–97.

Tam, J., Liu, J., Mukhopadhyay, B., Cinar, R., Godlewski, G., Kunos, G., 2011. Endocannabinoids in liver disease. Hepatology 53, 346–355.

Terry, G.E., Hirvonen, J., Liow, J.-S., Seneca, N., Tauscher, J.T., Schaus, J.M., Phebus, L., Felder, C.C., Morse, C.L., Pike, V.W., Halldin, C., Innis, R.B., 2010. Biodistribution and dosimetry in humans of two inverse agonists to image cannabinoid CB1 receptors using positron emission tomography. Eur. J. Nucl. Med. Mol. Imaging 37, 1499–1506.

Toczek, M., Malinowska, B., 2018. Enhanced endocannabinoid tone as a potential target of pharmacotherapy. Life Sci. 204, 20–45.

Townsend, K.L., Tseng, Y.H., 2014. Brown fat fuel utilization and thermogenesis. Trends Endocrinol. Metab. 25, 168–177.

Tseng, Y.-H., Kokkotou, E., Schulz, T.J., Huang, T.L., Winnay, J.N., Taniguchi, C.M.,

Tran, T.T., Suzuki, R., Espinoza, D.O., Yamamoto, Y., Ahrens, M.J., Dudley, A.T., Norris, A.W., Kulkarni, R.N., Kahn, C.R., 2008. New role of bone morphogenetic protein 7 in brown adipogenesis and energy expenditure. Nature 454, 1000–1004.

Turkington, T.G., 2001. Introduction to PET instrumentation. J. Nucl. Med. Technol. 29, 4–11.

U Din, M., Raiko, J., Saari, T., Kudomi, N., Tolvanen, T., Oikonen, V., Teuho, J., Sipilä, H., Savisto, N., Parkkola, R., Nuutila, P., Virtanen, K., 2016. Human brown adipose tissue [15O]O2 PET imaging in the presence and absence of cold stimulus. Eur. J. Nucl. Med. Mol. Imaging 43, 1878–1886.

U Din, M., Raiko, J., Saari, T., Saunavaara, V., Kudomi, N., Solin, O., Parkkola, R., Nuutila, P., Virtanen, K.A., 2017. Human Brown Fat Radiodensity Indicates Underlying Tissue Composition and Systemic Metabolic Health. J. Clin. Endocrinol. Metab. 102, 2258–2267.

U Din, M., Saari, T., Raiko, J., Kudomi, N., Maurer, S.F., Lahesmaa, M., Fromme, T., Amri, E.Z., Klingenspor, M., Solin, O., Nuutila, P., Virtanen, K.A., 2018. Postprandial Oxidative Metabolism of Human Brown Fat Indicates Thermogenesis. Cell Metab. 28, 207–216.e3.

van der Lans, A.A.J.J., Hoeks, J., Brans, B., Vijgen, G.H.E.J., Visser, M.G.W., Vosselman, M., Hansen, J., Jrgensen, J., Wu, J., Mottaghy, F., Schrauwen, P., van Marken Lichtenbelt, W.D., 2013. Cold acclimation recruits human brown fat and increases nonshivering thermogenesis. J. Clin. Invest. 123, 3395–3403.

van der Veldt, A.A.M., Smit, E.F., Lammertsma, A.A., 2013. Positron Emission Tomography as a Method for Measuring Drug Delivery to Tumors in vivo: The Example of [11C]docetaxel. Front. Oncol. 3, 208.

van Marken Lichtenbelt, W.D., Vanhommerig, J., Smulders, N., Drossaerts, J.M.A.F.L., Kemerink, G., Bouvy, N., Schrauwen, P., Teule, G.J.J., 2009. Cold-activated brown adipose tissue in healthy men. N. Engl. J. Med. 360, 1500–1508.

Verty, A.N.A., Allen, A.M., Oldfield, B.J., 2009. The Effects of Rimonabant on Brown Adipose Tissue in Rat: Implications for Energy Expenditure. Obesity 17, 254–261.

Vijgen, G.H.E.J., Bouvy, N.D., Teule, G.J.J., Brans, B., Hoeks, J., Schrauwen, P., Van Marken Lichtenbelt, W.D., 2012. Increase in brown adipose tissue activity after weight loss in morbidly obese subjects. J. Clin. Endocrinol. Metab. 97, E1229–E1233.

Villarroya, F., Cereijo, R., Villarroya, J., Giralt, M., 2017. Brown adipose tissue as a secretory organ. Nat. Rev. Endocrinol. 13, 26–35.

Virtanen, K., 2014. BAT thermogenesis: Linking shivering to exercise. Cell Metab. 19, 352–354.

Virtanen, K.A., Lidell, M.E., Orava, J., Heglind, M., Westergren, R., Niemi, T., Taittonen, M., Laine, J., Savisto, N.-J., Enerback, S., Nuutila, P., 2009. Functional Brown Adipose Tissue in Healthy Adults. N. Engl. J. Med. 360, 1518–1525.

Virtanen, K.A., Peltoniemi, P., Marjamäki, P., Asola, M., Strindberg, L., Parkkola, R., Huupponen, R., Knuuti, J., Lönnroth, P., Nuutila, P., 2001. Human adipose tissue glucose uptake determined using [18F]-fluoro-deoxy-glucose ([18F]FDG) and PET in combination with microdialysis. Diabetologia 44, 2171–2179.

Vosselman, M.J., Hoeks, J., Brans, B., Pallubinsky, H., Nascimento, E.B.M., Van Der Lans, A.A.J.J., Broeders, E.P.M., Mottaghy, F.M., Schrauwen, P., Van Marken Lichtenbelt, W.D., 2015. Low brown adipose tissue activity in endurance-trained compared with lean sedentary men. Int. J. Obes. 39, 1696–1702.

Wang, Q., Zhang, M., Xu, M., Gu, W., Xi, Y., Qi, L., Li, B., Wang, W., 2015. Brown adipose tissue activation is inversely related to central obesity and metabolic parameters in adult human. PLoS One 10, e0123795.

Wang, T.J., Larson, M.G., Levy, D., Benjamin, E.J., Leip, E.P., Wilson, P.W.F., Vasan, R.S., 2004. Impact of Obesity on Plasma Natriuretic Peptide Levels. Circulation 109, 594–600.

Wang, W., Seale, P., 2016. Control of brown and beige fat development. Nat. Rev. Mol. Cell Biol. 17, 691–702.

Watanabe, M., Houten, S.M., Mataki, C., Christoffolete, M.A., Kim, B.W., Sato, H., Messaddeq, N., Harney, J.W., Ezaki, O., Kodama, T., Schoonjans, K., Bianco, A.C., Auwerx, J., 2006. Bile acids induce energy expenditure by promoting intracellular thyroid hormone activation. Nature 439, 484–489.

Weiner, J., Hankir, M., Heiker, J.T., Fenske, W., Krause, K., 2017. Thyroid hormones and browning of adipose tissue. Mol. Cell. Endocrinol. 458, 156–159.

Weir, J.B. de V, 1949. New methods for calculating metabolic rate with special reference to protein metabolism. J. Physiol. 109, 1–9.

Whittle, A.J., Carobbio, S., Martins, L., Slawik, M., Hondares, E., Vázquez, M.J., Morgan, D., Csikasz, R.I., Gallego, R., Rodriguez-Cuenca, S., Dale, M., Virtue, S., Villarroya, F., Cannon, B., Rahmouni, K., López, M., Vidal-Puig, A., 2012. BMP8B increases brown adipose tissue thermogenesis through both central and peripheral actions. Cell 149, 871–85.

WHO/Europe - Nutrition - Body Mass Index [WWW Document], n.d. URL http://www.euro.who.int/en/health-topics/disease-prevention/nutrition/a-healthy-lifestyle/body-mass-index-bmi (accessed 8.25.18).

Wilson, C.N., Mustafa, S.J. (Eds.), 2009. Adenosine Receptors in Health and Disease, Handbook of Experimental Pharmacology. Springer Berlin Heidelberg, Berlin, Heidelberg.

Worthmann, A., John, C., Rühlemann, M.C., Baguhl, M., Heinsen, F.A., Schaltenberg, N., Heine, M., Schlein, C., Evangelakos, I., Mineo, C., Fischer, M., Dandri, M., Kremoser, C., Scheja, L., Franke, A., Shaul, P.W., Heeren, J., 2017. Cold-induced conversion of cholesterol to bile acids in mice shapes the gut microbiome and promotes adaptive thermogenesis. Nat. Med. 23, 839–849.

Wu, J., Bostrom, P., Sparks, L.M., Ye, L., Choi, J.H., Giang, A.-H., Khandekar, M., Virtanen, K.A., Nuutila, P., Schaart, G., Huang, K., Tu, H., Lichtenbelt, W.D. van M., Hoeks, J., Enerbaeck, S., Schrauwen, P., Spiegelman, B.M., 2012. Beige Adipocytes Are a Distinct Type of Thermogenic Fat Cell in Mouse and Human. Cell 150, 366–376.

Xue, Y., Petrovic, N., Cao, R., Larsson, O., Lim, S., Chen, S., Feldmann, H.M., Liang, Z., Zhu, Z., Nedergaard, J., Cannon, B., Cao, Y., 2009. Hypoxia-Independent Angiogenesis in Adipose Tissues during Cold Acclimation. Cell Metab. 9, 99–109.

Yen, P.M., 2001. Physiological and Molecular Basis of Thyroid Hormone Action.

Physiol. Rev. 81, 1097–1143.

Yoneshiro, T., Aita, S., Matsushita, M., Kayahara, T., Kameya, T., Kawai, Y., Iwanaga, T., Saito, M., 2013. Recruited brown adipose tissue as an antiobesity agent in humans. J. Clin. Invest. 123, 3404–3408.

Yoneshiro, T., Aita, S., Matsushita, M., Ogura, Y.O., Kameya, T., Kawai, Y., Miyagawa, M., Tsujisaki, M., Saito, M., 2011. Age-related decrease in cold-activated brown adipose tissue and accumulation of body fat in healthy humans. Obesity 19, 1755–1760.

Yoneshiro, T., Matsushita, M., Nakae, S., Kameya, T., Sugie, H., Tanaka, S., Saito, M., 2016. Brown adipose tissue is involved in the seasonal variation of cold-induced thermogenesis in humans. Am. J. Physiol. Integr. Comp. Physiol. 310, R999–R1009.

Zhang, L., Baker, G., Janus, D., Paddon, C.A., Fuhrer, D., Ludgate, M., 2006. Biological Effects of Thyrotropin Receptor Activation on Human Orbital Preadipocytes. Investig. Opthalmology Vis. Sci. 47, 5197-5203.

Zhang, Q., Miao, Q., Ye, H., Zhang, Z., Zuo, C., Hua, F., Guan, Y., Li, Y., 2014. The effects of thyroid hormones on brown adipose tissue in humans: a PET-CT study. Diabetes. Metab. Res. Rev. 30, 513–520.

Zimmermann, H., Zebisch, M., Strter, N., 2012. Cellular function and molecular structure of ecto-nucleotidases. Purinergic Signal. 8, 437–502.

Annales Universitatis Turkuensis

UNIVERSITY OF TURKU

ISBN 978-951-29-7430-6 (PRINT)
ISBN 978-951-29-7431-3 (PDF)
ISSN 0355-9483 (Print) ISSN 2343-3213 (Online)

Grano Oy, Turku, Finland 2018